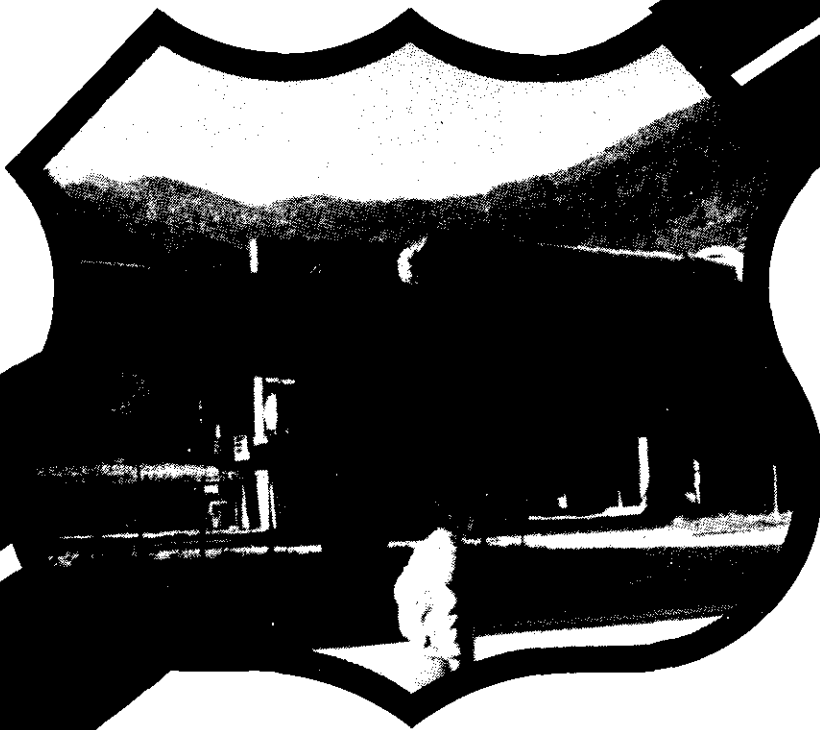


DEVELOPMENT OF STRENGTH IN CEMENTS

April 1981
Interim Report



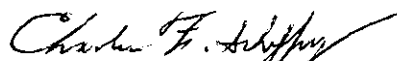
Document is available to the public through the National Technical Information Service, Springfield, Virginia 22161



Prepared for
FEDERAL HIGHWAY ADMINISTRATION
Offices of Research & Development
Materials Division
Washington, D.C. 20590

FOREWORD

In these energy saving and inflation fighting times, the U. S. Department of Transportation is constantly in search of any means related to highway materials or construction for furthering the attainment of economy and energy conservation, however great or small. In this quest the U. S. Department of Transportation concluded Agreement No. 4(PL. 480) with the Yugoslav Joint Board of Scientific and Technological Cooperation for a laboratory study by Yugoslav researchers of the fabrication of Portland and Sorel cements with objectives toward furthering economical and energy savings in cement manufacture and hopefully with attendant increases in strength of the cements. The requested research was carried out by a team of researchers headed by principal investigator Dr. B. Matkovic from the Rudjer Boskovic Institute in Zagreb. His chief collaborators were Engineer T. Gacesa, head of the research department of JUCEMA, Association of the Yugoslav Cement Producers and Professor Z. Kostrencic from the Institute for Civil Engineering, Zagreb. Other research associates contributing to the program were Dr. M. Paljevic, Dr. S. Popovic, Engineers M. Luic and T. Zunic from the Rudjer Boskovic; Dr. I. Jelenic, Dr. K. Popovic, Engineers V. Carin, I. Gerek, R. Halle, S. Mehmedagic and M. Mikoc from JUCEMA; Drs. V. Korac and I. Halavanja from the Institute for Civil Engineering. The researchers also had the cooperation of Professor J. F. Young, Department of Civil Engineering at the University of Illinois, Urbana, Illinois, who conceived the project in cooperation with Dr. Matovic. Scanning electron microscope (SEM) studies and microprobe measurements were made at the University of Illinois and Dr. S. Chromy of the Research Institute of Building Materials, Brno, Czechoslovakia contributed crystallo-optical examinations of various specimens to the study.


Charles F. Scheffey

NOTICE

This document is disseminated under the sponsorship of the Department of Transportation in the interest of information exchange. The United States Government assumes no liability for its contents or use thereof.

The contents of this report reflect the views of the authors who are responsible for the facts and the accuracy of the data presented herein. The contents do not necessarily reflect the official views or policy of the Department of Transportation.

The report does not constitute a standard, specification, or regulation.

The United States Government does not endorse products or manufacturers. Trademarks or manufacturers' names appear herein only because they are considered essential to the object of this document.



U.S. Department
of Transportation

**Federal Highway
Administration**

Memorandum

Subject: Transmittal of Research Report No. FHWA-RD-80-128 Date: **MAR 13 1981**
"Development of Strength in Cements"

From: Director, Office of Research
Washington, D.C. 20590

Reply to
Attn. of: **HRS-23**

To: Individual Researchers

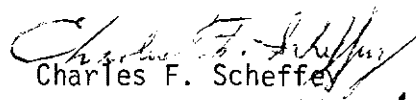
Distributed with this memorandum is the subject report intended primarily for highway material research and development personnel and manufacturers of Portland or Sorel cements.

The report is a product of the labors of a team of Yugoslav researchers under Dr. Boris Matkovic in response to the U. S. Department of Transportation's Agreement No. 4 (PL 480) with the Yugoslav Joint Board on Scientific and Technological Cooperation.

In this report are to be found some research findings of considerable interest. Among these with respect to Portland cement the researchers report that the production of doped belite (dicalcium silicate) clinkers can be a prospective means for saving energy in cement production. This is accomplished by small additions of either barium sulfate (BaSO_4), calcium tribasic phosphate ($\text{Ca}_5(\text{PO}_4)_3\text{OH}$), or vanadium oxide (V_2O_5) to belite (Ca_2SiO_4) clinker. In addition to conserving energy, doping the belite with barium sulfate imparts greater strength to the resulting modified belite.

Also, the report supplies an interesting and informative treatment of reactants, additives and factors contributing to the fabrication of Sorel cement.

This report is being distributed to materials and pavement researchers and technologists who have either requested copies or have previously indicated an interest in related reports. Additional copies are available from the National Technical Information Service (NTIS), Department of Commerce, 5285 Port Royal Road, Springfield, Virginia 22161. A small charge is imposed for copies provided by NTIS.


Charles F. Scheffey

Attachment

1. Report No. FHWA/RD-80/128		2. Government Accession No.		3. Recipient's Catalog No. PB82 10397 9	
4. Title and Subtitle Development of Strength in Cements				5. Report Date April 1981	
				6. Performing Organization Code	
7. Author(s) Dr. B. Matkovic et al.				8. Performing Organization Report No.	
9. Performing Organization Name and Address Institute "Rudjer Boskovic" Zagreb, Yugoslavia				10. Work Unit No. (TRAIS)	
				11. Contract or Grant No. Agreement No. 4(PI 480)	
12. Sponsoring Agency Name and Address U. S. Department of Transportation Washington, D. C. Yugoslav Joint Board on Scientific and Technological Cooperation, Belgrade, Yugoslavia				13. Type of Report and Period Covered INTERIM REPORT (September 1977-September 1978)	
				14. Sponsoring Agency Code M/ 0722	
15. Supplementary Notes DOT Project Officer; Charles F. Scheffey (HRS-1) FHWA Contract Manager: W. C. Ormsby, (HRS-23) Editors: J. A. Zenewitz; L. M. Smith (HRS-23)					
16. Abstract This report is divided into two parts: Portland and Sorel Cements. <u>Portland Cement:</u> The production of doped belite (dicalcium silicate) clinkers can be a prospective way of saving energy in cement production. Barium sulfate ($BaSO_4$), calcium tribasic phosphate ($Ca_5(PO_4)_3(OH)$), and vanadium oxide (V_2O_5) stabilize β -, α' - and α modifications of belite (C_2S). The α' modification shows better strength development than the β - C_2S . Strength develops more slowly in $Ca_5(PO_4)_3 OH$ than in $BaSO_4$, stabilized belites. Also, belite clinkers doped with $BaSO_4$ attain greater strength than belites without $BaSO_4$. <u>Sorel Cement:</u> The reaction products are dependent on the proportion of reactants (MgO , $MgCl_2$, and H_2O) and on MgO activity. Hardened cements achieve the best strength development and stability when phase 5 ($5Mg(OH)_2 \cdot MgCl_2 \cdot 8H_2O$) is the main reaction product. Phosphate addition, especially soluble phosphates, which are more effective, improves the cement's resistance to the effects of water. <u>Cover Photo:</u> "Salonit Anhovo" - cement plant in Anhovo, Yugoslavia.					
17. Key Words Portland cement, belite doping, belite stabilization Sorel cement, MgO activity, phosphate addition, water resistance.			18. Distribution Statement No restrictions. This document is available to the public through the National Technical Information Service, Springfield, Virginia 22161.		
19. Security Classif. (of this report) UNCLASSIFIED		20. Security Classif. (of this page) UNCLASSIFIED		21. No. of Pages 149	22. Price

TABLE OF CONTENTS

	<u>Page</u>
I. INTRODUCTION	1
PORTLAND CEMENT	1
SOREL CEMENT	4
II. PORTLAND CEMENT	4
1. STABILIZERS AND CLINKER ACTIVITY	4
A. LITERATURE SURVEY	4
B. EXPERIMENTAL DATA	5
Materials	6
Preparation of specimens	6
Investigative methods	8
C. RESULTS AND DISCUSSION	13
Effects of BaSO ₄ on C ₂ S activity	13
Reactivity of BaSO ₄ -stabilized belites	16
Effect of BaSO ₄ on the reactivity of belite cements	16
Effects OF CaSO ₄ on the reactivity of belite clinker	23
C ₂ S doped with BaCO ₃ , MnO ₂ , CaSO ₄ and CaO	26
Reactivity of C ₂ S and belite stabilized by Ca ₅ (PO ₄) ₃ (OH)	26
Effects of V ₂ O ₅ on C ₂ S activity	32
Additional data on polymorphs and stabilizer distribution	35
Differential thermal analyses	35
Selective extraction method	46
Optical microscopy	49
Scanning electron microscopy	56
D. CONCLUSIONS	66

TABLE OF CONTENTS (cont'd)

	<u>Page</u>
2. HYDRATION PROCESS ACCELERATED BY CARBONATION ...	67
Materials.....	67
Preparation of specimens	67
Results.....	70
3. CEMENT WITH LIMESTONE	72
A. LITERATURE SURVEY	72
B. EXPERIMENTAL DATA	73
Materials	73
Preparation of specimens	73
Investigative methods	77
C. RESULTS AND DISCUSSION	81
D. CONCLUSIONS	89
III. SOREL CEMENT	93
A. LITERATURE SURVEY	93
MgO activity and paste composition	93
Strength development in phases 5 and 3	93
Effectiveness of phosphates on water resistance of hardened cement	94
B. EXPERIMENTAL DATA	95
Materials	95
Preparation of specimens	96
Investigative methods	97
C. RESULTS AND DISCUSSION	99
MgO activity and paste composition	99
Strength development in phases 5 and 3	103
Effects of phosphates on water resistance of hardened cement	111
D. CONCLUSIONS	121

TABLE OF CONTENTS (cont'd)

	<u>Page</u>
IV. CONCLUSIONS	122
PORTLAND CEMENT	122
SOREL CEMENT	124
V. RECOMMENDATIONS	124
FIGURES	VI
TABLES	XI
REFERENCES	126

LIST OF ILLUSTRATIONS

<u>Figure</u>	<u>Caption</u>	<u>Page</u>
1.	Microstructure of C_2S -forms	12
2.	C_2S stabilized by $BaSO_4$: Compressive strengths of paste specimens.....	15
3.	Belites (high grade limestone and quartz) stabilized by $BaSO_4$: Compressive strengths of mortar specimens.....	18
4.	Clinkers (marlaceous limestone and marl) stabilized by $BaSO_4$: Compressive strengths of mortar specimens.....	21
5.	Distribution of alite, belite and matrix in sample B-18	22
6.	Homogeneous distribution of belite and matrix in sample B-16	22
7.	Belite clinkers (calcareous marl and clayey marl) doped with $BaSO_4$: Compressive strengths of mortar specimens.....	25
8.	Belite clinker (marlaceous limestone and marl) doped with $CaSO_4$: Compressive strengths of mortar specimens.....	28
9.	C_2S stabilized by $Ca_5(PO_4)_3(OH)$: Compressive strengths of paste specimens.....	31
10.	Belites (high grade limestone and quartz) stabilized by $Ca_5(PO_4)_3(OH)$: Compressive strengths of mortar specimens.....	34

LIST OF ILLUSTRATIONS (cont'd)

<u>Figure</u>	<u>Caption</u>	<u>Page</u>
11.	C ₂ S stabilized by V ₂ O ₅ : Compressive strengths of paste specimens.....	36
12.	The effect of BaSO ₄ concentrations on the $\alpha' \xrightarrow{H} \alpha$ -C ₂ S transition temperature	41
13.	DT heating curves of C ₂ S solid solutions with BaSO ₄	43
14.	Effect of Ca ₅ (PO ₄) ₃ (OH) concentrations on the $\alpha' \xrightarrow{H} \alpha$ -C ₂ S transition temperature.....	45
15.	DT heating curves of C ₂ S solid solutions with Ca ₅ (PO ₄) ₃ (OH)	47
16.	Polysynthetic lamellae in β -C ₂ S (sample P-0.5)	50
17.	Detail from Fig. 16, highly enlarged	50
18.	Cross lamellae in sample B-37	51
19.	Detail from Fig. 18, highly enlarged	51
20.	Cross lamellae of the $\alpha \rightarrow \alpha'$ -C ₂ S inversion (sample B-38)	53
21.	Cross lamellae of the $\alpha \rightarrow \alpha'$ -C ₂ S inversion (sample P-5.0 P)	53
22.	Crystals of α -C ₂ S (sample P-5.0 P)	54
23.	Temperature dependent changes in light transmissiveness of C ₂ S thin sections.....	55

LIST OF ILLUSTRATIONS (cont'd)

<u>Figure</u>	<u>Caption</u>	<u>Page</u>
24.	C ₂ S grain: Center of β -polymorph surrounded by α -polymorph (sample P-2.5)	57
25.	Microstructure of V ₂ O ₅ -stabilized C ₂ S (sample V-4)	59
26.	Microstructure of BaSO ₄ -stabilized C ₂ S (sample B-6)	60
27.	Microstructure of Ca ₅ (PO ₄) ₃ (OH)-stabilized C ₂ S (sample P-1.5)	61
28.	Microstructure of BaSO ₄ doped C ₂ S (sample NA-1)...	62
29.	Microstructure of BaSO ₄ doped C ₂ S (sample B-16)...	63
30.	Fracture surface of BaSO ₄ doped belite clinker (sample B-16)	64
31.	Ba distribution in BaSO ₄ doped belite clinker (area as in Fig. 30)	65
32.	Portland cement with C ₆ H ₁₀ O ₅ admixtures: Compressive strengths of mortar specimens.....	71
33.	Particle size distribution of cements (control samples C-1 and D-1)	74
34.	Particle size distribution of cement (control sample P-1)	75
35.	Particle size distribution of limestone	76
36.	Cement with limestone addition: Particle size distribution in sample P-2	78

LIST OF ILLUSTRATIONS (cont'd)

<u>Figure</u>	<u>Caption</u>	<u>Page</u>
37.	Cement with limestone addition: Particle size distribution in sample P-3	79
38.	Cement with limestone addition: Shrinkage of mortar specimens (sample C-1 to C-5)	83
39.	Cement with limestone addition: Shrinkage of mortar specimens (samples D-1 to D-5)	84
40.	Cement with limestone addition: Shrinkage of mortar specimens (samples P-1, P-2 and P-3)	85
41.	Cement with limestone addition: Shrinkage of concrete specimens (samples C-1 to C-5)	90
42.	Cement with limestone addition: Shrinkage of concrete specimens (samples D-1 to D-5)	91
43.	Cement with limestone addition: Shrinkage of concrete specimens (samples P-1, P-2 and P-3)	92
44.	Reaction products in Sorel cement pastes from mixes expected to give phase 5	104
45.	Reaction products in Sorel cement pastes from mixes expected to give phase 3	105
46.	Compressive strengths in Sorel cement mortars from 5:1:13 (sample D-5) and 3:1:11 (sample D-3) mixes	110
47.	Sorel cement with $\text{Ca}_5(\text{PO}_4)_3(\text{OH})$ addition: Reaction products in pastes from mixes expected to give phase 5	112

LIST OF ILLUSTRATIONS (cont'd)

<u>Figure</u>	<u>Caption</u>	<u>Page</u>
48.	Sorel cement with $\text{Ca}(\text{H}_2\text{PO}_4)_2 \cdot \text{H}_2\text{O}$ addition: Reaction products in pastes from mixes expected to give phase 5	113
49.	Sorel cement with $\text{Ca}_5(\text{PO}_4)_3(\text{OH})$ addition: Reaction products in pastes from mixes expected to give phase 3	114
50.	Sorel cement with $\text{Ca}(\text{H}_2\text{PO}_4)_2 \cdot \text{H}_2\text{O}$ addition: Reaction products in pastes from mixes expected to give phase 3	115
51.	Sorel cement with phosphate addition (5:1:13 mix with MgO_{800}) Phases in hardened pastes stored in water	116
52.	Sorel cement with phosphate addition (3:1:11 mix with MgO_{800}): Phases in hardened pastes stored in water	117
53.	Compressive strengths in Sorel cement mortars with $\text{Ca}(\text{H}_2\text{PO}_4)_2 \cdot \text{H}_2\text{O}$ addition. Samples D-T5 and DV-T5 prepared from 5:1:13 mix and samples D-T3 and DV-T3 from 3:1:11 mix	120

LIST OF TABLES

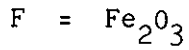
<u>Table</u>	<u>Title</u>	<u>Page</u>
1.	Clinker raw materials	7
2.	C ₂ S stabilized by BaSO ₄ : Initial mix composition and analyses of products	14
3.	Chemical and phase analyses of BaSO ₄ -stabilized belites (high grade limestone and quartz)	17
4.	Chemical and phase analyses of BaSO ₄ doped belite clinkers (marlaceous limestone and marl).....	20
5.	Chemical and phase analyses of BaSO ₄ doped belite clinkers (calcareous marl and clayey marl) ...	24
6.	Chemical and phase analyses of CaSO ₄ doped belite clinkers (marlaceous limestone and marl).....	27
7.	Initial mix compositions and phase analyses of BaCO ₃ CaSO ₄ , CaO and MnO ₂ doped C ₂ S	29
8.	C ₂ S stabilized by Ca ₅ (PO ₄) ₃ (OH): Initial mix composition and analyses of products	30
9.	Chemical and phase analyses of Ca ₅ (PO ₄) ₃ (OH) doped belites (high grade limestone and quartz)	33
10.	β-C ₂ S stabilized by V ₂ O ₅ : Lattice constants and powder data	37
11.	α _L ' -C ₂ S stabilized by V ₂ O ₅ : Lattice constants and powder data	38
12.	Reflection splittings in V ₂ O ₅ stabilized α _L ' - and β-C ₂ S.....	39
13.	C ₂ S doped with BaSO ₄ : Initial mixes and peak temperatures of α _H ' → α-C ₂ S phase transformation.....	40
14.	C ₂ S stabilized by Ca ₅ (PO ₄) ₃ (OH): Initial mixes and peak temperatures of α _H ' → α-C ₂ S phase transformation	44
15.	Element distribution in clinker phases (sample B-16)	48

LIST OF TABLES

<u>Table</u>	<u>Title</u>	<u>Page</u>
16.	Chemical and phase analyses of cements with limestone addition (control samples)	68
17.	Cements with limestone addition: Physical and chemical properties	69
18.	Cements with limestone addition: Mechanical properties (mortar test)	82
19.	Mix proportion and properties of concretes from cements with limestone addition (samples C-1 to C-5)	86
20.	Mix proportion and properties of concretes from cements with limestone addition (samples D-1 to D-5)	87
21.	Mix proportion and properties of concretes from cements with limestone addition (samples P-1, P-2 and P-3)	88
22.	Crystalline reaction products in magnesium oxychloride pastes	100
23.	Crystalline reaction products in air-cured Sorel cement pastes from 5:1:23 mix	107
24.	Initial mix and phase composition in Sorel cement mortars with MgO ₈₀₀	109

LIST OF ABBREVIATIONS AND SYMBOLS

Standard cement nomenclature used:



Other abbreviations used:

w/c = water-cement ratio

C/S = CaO:SiO₂ ratio

XD = X-ray diffraction

Phase 5 = Mg₃(OH)₅ Cl 4H₂O

Phase 3 = Mg₂(OH)₃ Cl 4H₂O

1. INTRODUCTION

The project on strength development in cements concerns the improvement of strength in Portland cement and ameliorated water resistance of hardened Sorel (magnesium oxychloride) cement. Therefore this report deals with two main topics: Portland cement and Sorel cement.

PORTLAND CEMENT

Strength development in Portland cement can be accelerated by:

- increased activity of a particular clinker phase through the influence of minor components;
- modified hydration process through carbonation;
- admixtures either interground with cement clinker or blended with cement.

Stabilizers and clinker reactivity

The characteristics of Portland cement clinkers depend on the composition and fineness of raw mix, on thermal threatment (burning and cooling) and on the reaction and diffusion processes in solid and liquid states. The two principal constituents of Portland cement, alite and belite, are solid solutions of Ca_3SiO_5 and Ca_2SiO_4 incorporating various minor amounts of elements, such as: Al, Fe, Mg, alkalies etc. Calcium aluminates and calcium aluminoferrites as other major constituents are also solid solutions and they too incorporate impurities coming from the raw mix.

The incorporation of foreign atoms into the crystal lattice of pure calcium silicates will either stabilize a metastable phase or promote the formation of a new modification.

When calcium silicate modifications exist as pure phases in the chemical sense, i.e. without impurity atoms incorporated in their crystal lattice, the phases that are stable at higher temperatures can be stabilized by foreign atoms at room temperature. Solid solutions containing foreign atoms can have a higher or lower reactivity than those of pure phases. There is also a relationship between the kind and quantity of foreign atoms incorporated into C_3S and C_2S crystal structures and the hydraulic reactivity of the respective phase.

The investigation of pure phases and their solid solutions with regard to sintering temperatures and the effect of various levels and kinds of foreign atoms is the only possible way to study and define the nature and state of stability as well as the reactivity of various phases in commercial Portland cement clinkers.

Since there are numerous and manifold data in literature on the subject, e.g., those in the survey by Regourd and Guinier (1), the research program demanded a critical re-examination of the effects that various levels and kinds of impurities can have on the stability and reactivity of calcium silicate phases.

The influence of impurities was first tested on the reactivity of C_3S . Stabilizers (TiO and $BaSO_4$) incorporated in the crystal lattice of C_3S did not improve the strength development as expected. Since alites are very reactive they do not possess such a high potential for increase in reactivity as belites which hydrate more slowly. The work was therefore centered primarily on C_2S .

The effectiveness of impurities was tested on both pure dicalcium silicates obtained from reagent grade chemicals and on clinkers prepared from indigenous raw materials. The study included the formation, polymorphic stabilization and hydraulic reactivity of C_2S with particular emphasis upon the strength

development in cement pastes and mortars. After a preliminary testing of various impurities (BaCO_3 , BaSO_4 , CaSO_4 , $\text{Ca}_5(\text{PO}_4)_3(\text{OH})$, V_2O_5 , MnO_2 and CaO above stoichiometric ratio in C_2S), three compounds (impurities) were selected for further consideration: BaSO_4 , $\text{Ca}_5(\text{PO}_4)_3(\text{OH})$ and V_2O_5 . The efficacy of the compounds and economic reasons decided the choice of BaSO_4 and $\text{Ca}_5(\text{PO}_4)_3(\text{OH})$, the first occurring in waste materials of commercially exploited rocks, while V_2O_5 was taken because of Pritts and Daugherty's statement (2) that it is more effective in stabilizing $\beta\text{-C}_2\text{S}$ than Cr^{6+} , B^{3+} or S^{6+} .

Hydration process accelerated by carbonation

Much more has already been done in investigating accelerated strength development caused by CO_2 treatment during cement hydration (Klem and Berger (3), Young, Berger and Breese (4)). The present approach was different, i.e., a compound was tested that decomposes at room temperature releasing CO_2 in contact with water. The compound, diethyl pyrocarbonate is a liquid which can be added easily to mortar or concrete mixes and thus applicable not only in the manufacture of prefabricates, like the CO_2 gas, but also at construction sites.

Cement with limestone addition

For economical reasons additions of 10 to 35% finely ground limestone, dolomite or sand are made in the manufacture of Portland cement in some countries.

The possibility of adding cheap limestone to Portland cement would also interest the Yugoslav cement producers, especially if there was evidence that limestone positively affects the process of cement hydration. To ascertain the actual effect of limestone on strength development it was decided to investigate mortars and concretes prepared from blended cements.

Since limestone is usually added to cement clinker during grinding, specimens were made from such interground cements and also from cements blended with limestone ground separately to different finenesses for the purpose of testing the effect of limestone fineness on the development of strengths in cements.

SOREL CEMENT

Magnesium oxychloride cement is not resistant to water attacks and can therefore be used as a binder only for non-structural interior works, mostly floorings. Some properties of Sorel cement, however, are superior to those of Portland cement, in particular the rapid setting and hardening and the capacity to take large quantities of fillers for heat and sound insulation. Therefore, efforts to enhance the use of this binder have included its use for prefabricated partition walls and other non-structural elements. Thus additional data are required on the reaction products and strength development in magnesium oxychloride pastes and mortars and on the efficacy of some additives to improve water stability of hardened Sorel cements.

For that purpose the investigations included:

the influence of MgO activity on magnesium oxychloride paste composition to explain the reaction mechanism in the $\text{MgO-MgCl}_2\text{-H}_2\text{O}$ system;

the development of strength in $\text{Mg}_3(\text{OH})_5\text{Cl}\cdot 4\text{H}_2\text{O}$ (phase 5) and in $\text{Mg}_2(\text{OH})_3\text{Cl}\cdot 4\text{H}_2\text{O}$ (phase 3) since both phases have cementitious properties but lack strength;

the effectiveness of phosphates, both the soluble $\text{Ca}(\text{H}_2\text{PO}_4)_2 \cdot \text{H}_2\text{O}$ and the insoluble $\text{Ca}_5(\text{PO}_4)_3(\text{OH})$ in ameliorating the water resistance of hardened Sorel cement.

II. PORTLAND CEMENT

1. STABILIZERS AND CLINKER ACTIVITY

A. LITERATURE SURVEY

The aim of the investigation was to ascertain which compounds can stabilize calcium silicates under conditions applicable to the process of manufacture (one sintering operation at $1,450^\circ\text{C}$) and to examine the hydraulic reactivity of solid solutions that had thus been formed. Literature data helped to select the stabilizers for the present work.

Thus, Welch and Gutt (5) emphasize the importance of impurities in the conversion of major clinker phases. They report that the C_2S phase can be stabilized into β -, α' or α -modification by increasing the quantity of phosphates. When stabilized in this manner the β -form has good hydraulic properties, α' -modification has some, while α -polymorph has none.

Suzuki and Yamaguchi (6) have synthesized α' - C_2S by substituting Ba or Sr for Ca and B for Si atoms. The α' -polymorph appeared when C_2S raw mixes with their respective CaO substituted by 0.15-0.30 mol BaO were sintered at 1500°C for approximately 20 minutes and then quenched. The C_2S consisted of 56.12% CaO, 11.21% BaO and 32.67% SiO_2 . With a higher substitution by BaO (approximately 0.7 mol) the quenching gave the α -form. The crystal data for Ba-stabilized α' - C_2S are: $a = 11.07$, $b = 18.80$, $c = 6.85 \text{ \AA}$; space group $C_{mc}2_1$:

Kurdowski (7) has described the distribution of barium, titanium, vanadium and chromium oxides in clinker phases and their effects on cement mortar strengths. According to him the solubility limits of barium oxide in solid solutions are as follows: 1.5 mol % in alite, approximately 5.0 mol % in belite (both at 1600°C) and approximately 1.5 mol % in C_3A (at 1300°C). C_4AF does not form a solid solution with barium. Barium oxide exerts the strongest influence on mortar strengths, with chromium oxide coming next, while titanium and vanadium have practically no influence on the hydraulic activity of clinkers.

Pritts and Daugherty (2) report that stabilized β - C_2S hydrates more slowly than pure and that samples stabilized with V^{6+} are more active than those with Cr^{6+} , B^{3+} and S^{6+} , whereas Ba^{2+} has no stabilizing effects on β - C_2S .

B. EXPERIMENTAL DATA

The first task of the experimental work was to prepare mixes from pure chemicals with varying amounts of stabilizers, to synthesize calcium silicates and to determine their hydraulic activity by simple strength tests on cement pastes. When satisfactory results were obtained, selected samples were subsequently

prepared from industrial minerals (Table 1) with varying amounts of stabilizers and the hydraulic activity of the resulting clinkers was measured with strength tests on cement mortars.

Materials

Reagent grade chemicals were used for the preparation of doped calcium silicates:

CaCO_3 , Alkaloid, Skopje, Yugoslavia
 SiO_2 , Kemika, Zagreb, Yugoslavia
 $\text{Ca}_5(\text{PO}_4)_3(\text{OH})$, Kemika, Zagreb, Yugoslavia
 V_2O_5 , Koch-Light Labor.LTD. Colubrook, Buchs, England
 $\text{CaSO}_4 \cdot 2\text{H}_2\text{O}$, Kemika, Zagreb, Yugoslavia
 $\text{BaCl}_2 \cdot 2\text{H}_2\text{O}$, Kemika, Zagreb, Yugoslavia
 H_2SO_4 (96%), Kemika, Zagreb, Yugoslavia
 BaSO_4 precipitated from $\text{BaCl}_2 \cdot 2\text{H}_2\text{O}$ with sulphuric acid, washed in distilled water, dried, heated at 900°C and ground into powder.

Preparation of specimens

Calcium silicates were synthesized from pure chemicals by high temperature CaO-SiO_2 reaction. The initial mix (160g batches of finely powdered CaCO_3 , SiO_2 and a stabilizer) was mixed well by hand, placed in a rotating homogenizer for three hours, calcined at 1000°C , pressed into pellets and sintered in platinum crucibles in an electric furnace at 1450°C for 90 minutes in the majority of cases. The product was quickly cooled (air quenched) and then ground to the appropriate specific surface (approx. $3600 \text{ cm}^2/\text{g}$ determined by the Blaine permeability method). When necessary the samples were resintered. The sintering temperature and period varied depending on the kind of the stabilizing agent utilized. Practically all the syntheses of pure chemicals were repeated to check the reproducibility of the reaction products.

Table 1. Clinker raw materials

Component (wt. %)	Limestone		Marl			Sand	Gypsum	Pyrite cinder
	1	2	3	4	5	6	7	8
SiO ₂	(n.d.)	4.10	5.35	22.66	38.16	97.20	2.80	10.00
Al ₂ O ₃	(n.d.)	1.45	1.74	6.28	9.86	0.97	0.20	3.35
Fe ₂ O ₃	(n.d.)	0.85	0.81	3.75	8.17	0.30	0.10	79.41
CaO	55.96	51.31	50.08	32.75	20.08	0.63	31.50	0.52
MgO	(n.d.)	0.64	(n.d.)	2.11	(n.d.)	(-)	0.20	(-)
SO ₃	(n.d.)	0.25	(n.d.)	1.10	(n.d.)	(-)	44.00	2.40
Na ₂ O	(n.d.)	0.12	(n.d.)	0.56	(n.d.)	(-)	(n.d.)	(n.d.)
K ₂ O	(n.d.)	0.14	(n.d.)	0.67	(n.d.)	(-)	(n.d.)	(n.d.)
Loss on ignition	43.93	41.14	41.04	29.76	19.78	0.43	20.85	4.32
Balance	0.11	(-)	0.98	0.36	3.95	0.47	0.35	(-)

1 - Calspar or high grade limestone; 2 - marlaceous limestone;
 3 - marlstone or calcareous marl; 4 - marl; 5 - clayey marl; 7 - gypsum
 was a mixture of 86.08% CaSO₄ · 2H₂O and 6.67% CaSO₄; (n.d.) - not
 determined; (-) - not detected

Clinkers were prepared from indigenous raw materials in batches of 1600 g and treated in the same way as the doped calcium silicates. The raw mix components (table 1) were ground to the appropriate fineness determined by the sieve test (no residue on 200 μ m mesh sieve and less than 10% on 90 μ m mesh sieve).

Clinkers containing calcium aluminates and aluminoferrites were interground with gypsum to the specific surface of approximately 3600 cm²/g.

The water: cement ratio for cement pastes was determined by the normal consistency test, as described in Section 3 (Cement with limestone addition).

Paste ingredients were mixed by hand in a bowl, cast into prismatic molds (1x1x4 cm) and after 24 hours removed from the forms and stored in water at 20 \pm 2^oC.

Mortar specimens were prepared from a mixture of cement and graded sand in a ratio of 1:3 at a constant water cement ratio of 0.5, then cast into 4x4x16 cm molds and stored as described in Section 3. The compressive strength was determined on paste and mortar samples cured in water; with the tests being repeated three times to obtain mean values.

Since strength tests on neat cement pastes are not reliable enough, conclusions on strength development were inferred from tests on cement-sand mortar specimens.

Investigative methods

The prepared samples were examined by X-ray diffraction*, analytical chemistry methods, optical** and scanning electron microscopy***, X-ray microanalysis⁺ and by thermal analyses⁺⁺.

*X-ray diffractometer, Philips Gloeilampenfabrieken N.V., Eindhoven, The Netherlands

**Optical microscope, Leitz, Wetzlar, W. Germany

***Scanning electron microscope, Jeolco JSM-U3, Japan Electron Optics Lab. Co., Tokyo

+X-ray analyzer, EDAX International Inc., Prarie, Illinois, USA

++Thermal analyzer, Thermoanalyzer TA-1, Mettler, Greifensee, Switzerland

Raw material, clinker and cement compositions were determined by wet analytical methods (gravimetry for SiO_2 , SO_3 , BaO , P_2O_5 ; complexometry for CaO , MgO , Al_2O_3 and Fe_2O_3 ; flame photometry⁺⁺⁺ for Na_2O and K_2O determination). Free CaO was analyzed by the glycerol (1,2,3-propanetriol)-ethanol method (Lerch and Bogue (8)). The distribution of elements in clinker phases was determined by selective extraction (9-12) by dissolving the silicate phases with salicylic acid (2-hydroxybenzoid acid)-methanol solvent and the aluminate phase with sucrose-water solution as solvent. According to Takashima and Higaki (13) glass does not dissolve when salicylic acid - methanol solution is used.

Samples were tested for compressive strength at the end of the respective hydration period, then ground and washed in acetone to block further hydration. Acetone was removed by filtration and evaporation in vacuum and samples were then kept in vacuum or in a desiccator above KOH . The hydration process was studied by X-ray diffraction examination and differential thermal analyses. Thermal analyses was also used to identify the hydration products (hydrates and hydroxides), determine the temperature of ~~α~~ α - C_2S conversion in doped samples and detect unreacted BaSO_4 in clinker.

The peak temperature for phase transformation of particular C_2S polymorphs served to find whether the added stabilizer had completely or partially passed into solid solution with dicalcium silicate. The method is based on acknowledging that the decrease in the phase conversion temperature depends on the quantity of stabilizer dissolved in C_2S solid solution. It is not often used, yet Pritts and Daugherty (2) applied it to determine the solubility of Cr_2O_3 in β - C_2S .

It has been established (1) that γ - C_2S transforms on heating into α'_L - C_2S in the temperature range of 700-900°C, the conversion enthalpy varying from 10878 to 14393 J mol^{-1} (2600 to 3440 cal/mol). When β - C_2S is the initial

⁺⁺⁺Flame photometer, Lange M6a, Berlin, W. Germany

material it transforms into α'_L -polymorph at the temperature between 600 and 700°C and the conversion enthalpy varies from 1423 to 2720 J mol⁻¹ (340 to 650 cal/mol). The conversion of α'_L -C₂S into α'_H -modification occurs between 1150 and 1190°C, the enthalpy being 720 J mol⁻¹ (172 cal/mol). At 1420-1440°C α'_H -C₂S will convert into α -polymorph, the enthalpy lying between 13389 and 1410 J mol⁻¹ (3200 to 3370 cal/mol).

On cooling, α -C₂S first transforms into α'_H -polymorph, then into α'_L and finally converts into β -form, the conversion temperatures being similar to those in the process of heating. Between 500 and 600°C β -C₂S can transform into γ -modification.

When samples are heated from room temperature upward, all the reaction in phase transformations are endothermal so their differential thermal effects are endothermal too. The situation is diametrically different on cooling when all the reactions are exothermal, which implies that the differential thermal effects will be exothermal as well.

The most impressive peak on the differential thermal curve is brought about by the transformation of $\alpha'_H \rightarrow \alpha$ -C₂S because the conversion enthalpy is high and the temperature range narrow. This fact was applied in the present work to find whether the added stabilizer had passed completely or only partly into C₂S solid solution. The principle cannot be used, however, when calcium aluminates and aluminoferrites are present in the system because the peak of phase transformation will coincide with the peak of melt formation. Both effects are endothermal on heating and exothermal in the process of cooling.

The morphology and elementary analysis of specimens as well as the detection and distribution of impurities were studied by scanning electron microscopy and electron probe X-ray microanalysis.

No attempts were made to draw quantitative conclusions on elementary analysis from the X-ray microanalysis or on polymorph analyses from X-ray diffraction data. However, the experimental conditions were kept constant during the entire work, so the results could be used for comparative analysis.

Quantitative phase analyses of clinker consisted of microscopic detection of belite, alite, free lime, periclase and matrix. The polymorphic modifications of dicalcium silicate were examined with an optical microscope in reflected light, using a method based on literature data (14-18) and developed further in the course of this work. Therefore, it is described in detail in the following paragraphs.

At the sintering temperature dicalcium silicate has the α -form. Successive polymorphous transformations into low-temperature α' , β - and γ -modifications occur in the process of cooling. Each of the polymorphs leaves characteristic traces in the C_2S crystal and they can be made visible in the reflected light of the optical microscope where every modification is recognizable in the belite grain structure. Clinker specimens were treated in the usual manner, viz. ground, polished and etched by 1% HNO_3 in alcohol solution and then making the microstructure visible by removing the film of the reaction products of HNO_3 and clinker sample. Stabilized α -modification keeps its original form of round grains with a smooth surface (Fig. 1a). At a lower temperature the unstable grains of α -polymorph transform into a α' -modification which is characterized by cross striation (intersected lamellae) formed within the original α -modification grain (skeleton structure, Fig. 1b). The conversion of α' - into β -modification manifests itself by very fine transversal and polysynthetic lamellae formed within those of the α' -modification. The skeleton structure of the α' -modification mostly remains unchanged (Fig. 1c). If enlarged 800 times or more the fine lamellae of the β -polymorph are visible within those of the α' -modification. During recrystallization the skeleton structure of the α' -modification can disappear completely or partly so the grain shows a very fine polysynthetic lamellar system typical for the β -modification (Fig. 1d). A volume increase of the unit cell (12%) accompanies the transformation of β into γ -polymorph making the compact belite grain disintegrate into extremely fine crystallites of the γ -modification. Macroscopically the phenomenon causes the entire specimen to turn into a fine powder.

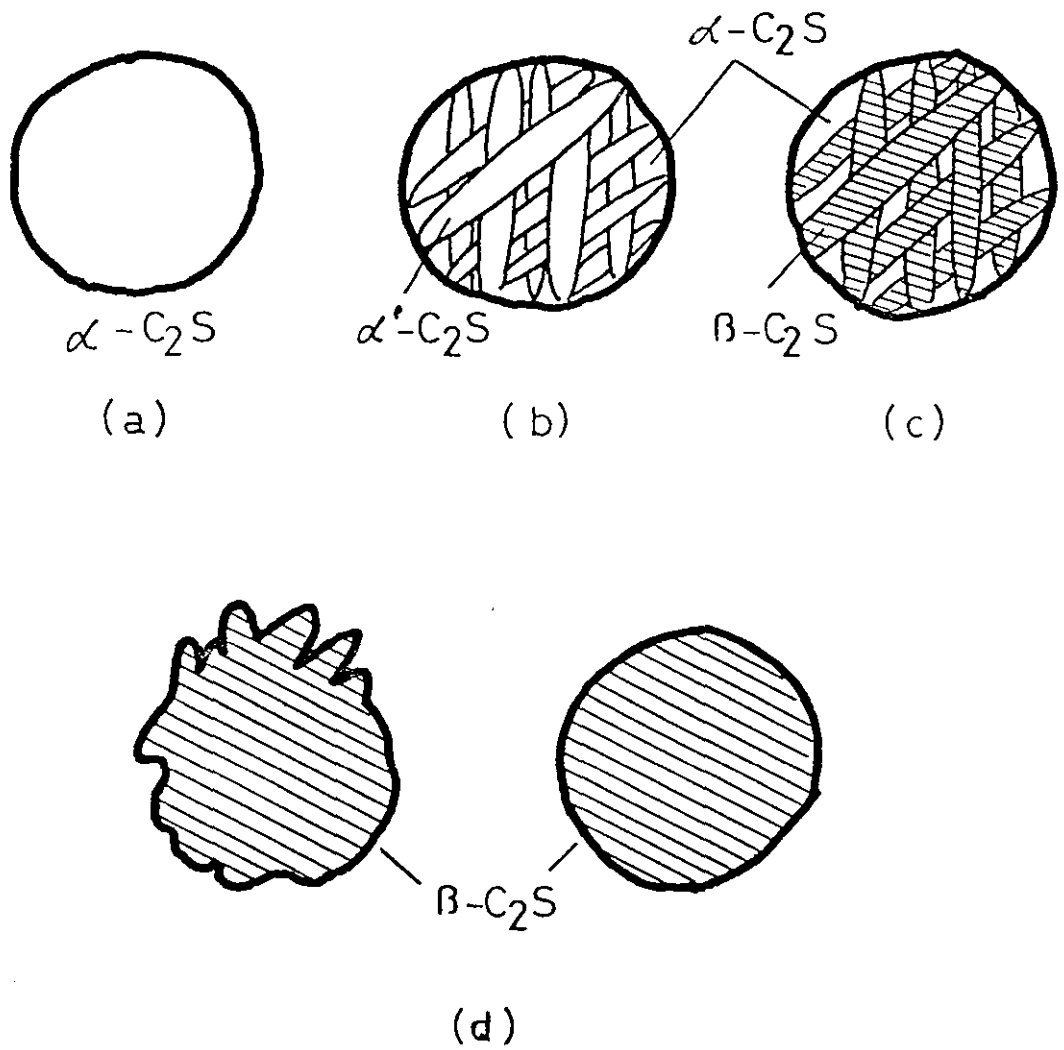


Figure 1. Microstructure of C_2S forms

C. RESULTS AND DISCUSSION

Effects of BaSO_4 on C_2S activity

Raw mix composition, phase composition, the content of SO_3 and free CaO in dicalcium silicate samples are presented in Table 2. The samples were synthesized at 1450°C for 90 minutes. Tabulated data show that the γ - C_2S content in synthesized samples decreases proportionally to the increase of the BaSO_4 content in the initial mix. Thus, for example, the content of γ - C_2S is less than 2% in sample B-1 containing 6.7% of BaSO_4 . With 12.7% or more BaSO_4 in the initial mix, there will be no γ -polymorph but α' and β -modifications combined. Since the synthesized samples contain less SO_3 than originally added, it seems that Ba atoms participate more than SO_4 groups in the stabilization process of α' and β -polymorphs.

Figure 2 shows the development of strengths in pastes with C_2S stabilized by different amounts of BaSO_4 . Four representative samples have been selected: B-1 as β - C_2S (with γ - $\text{C}_2\text{S} < 2\%$) and B-6, B-14 and B-15 which contained coexisting α' and β -modifications due to different BaSO_4 levels in the initial mix.

No clear-cut conclusions can be drawn from strengths obtained on pastes, but some inferences can be made. Thus, for instance, it was observed that 7-day strengths are higher when both α' - and β - C_2S are present (B-6, B-14 and B-15) than when only β - C_2S occurred (B-1). On Ba_2SiO_4 -stabilized samples Bikbau (19) found that the α' -modification had a quicker strength development than the β -form. Samples containing α' and β -modifications (B-14 and B-15) illustrate that at times higher levels of stabilizer cause a decrease in strength. Pritts and Daugherty (2) and also Copeland and Kantro (20) report that the hydration rate decreases with increased concentrations of the stabilizers.

Table 2. C_2S stabilized by $BaSO_4$: Initial mix composition and analyses of products

Sample	Initial mix composition (wt. %)			Analyses							
	CaO	SiO_2	$BaSO_4$	Free CaO (wt. %)	SO_3 (wt. %)	XD			Microscopy		
						$\alpha-C_2S$	$\beta-C_2S$	$\gamma-C_2S$	$\alpha-C_2S$	$\alpha-C_2S$	$\beta-C_2S$
B-22	62.93	33.74	3.33	0.23	0.34	-	+++	+			+++
B-1	60.76	32.58	6.66			-	+++	+	(+)	+	++
	60.76	32.58	6.66	0.85		-	+++	+			
	60.76	32.58	6.66	0.85	0.40	-	+++	-			
B-5	57.49	30.71	11.80	0.64	0.64						
B-6	56.82	30.47	12.71			++	++	-			
	56.82	30.47	12.71	0.26	(n.d.)	+++	+	-			
	56.82	30.47	12.71		0.78	++	++	-			
	56.82	30.47	12.71	0.41	1.20	+++	+	-	(+)	++	(+)
B-14	55.50	30.02	14.48	0.06		+++	+	-			
	55.50	30.02	14.48			+++	+	-			
	55.50	30.02	14.48	1.42	1.45	++	++	-	(+)	++	+
B-15	54.54	29.68	15.78			++	++	-			
	54.54	29.68	15.78	0.06	1.08	+++	+	-	+	+++	+

(+) small quantity

(n.d.) not determined

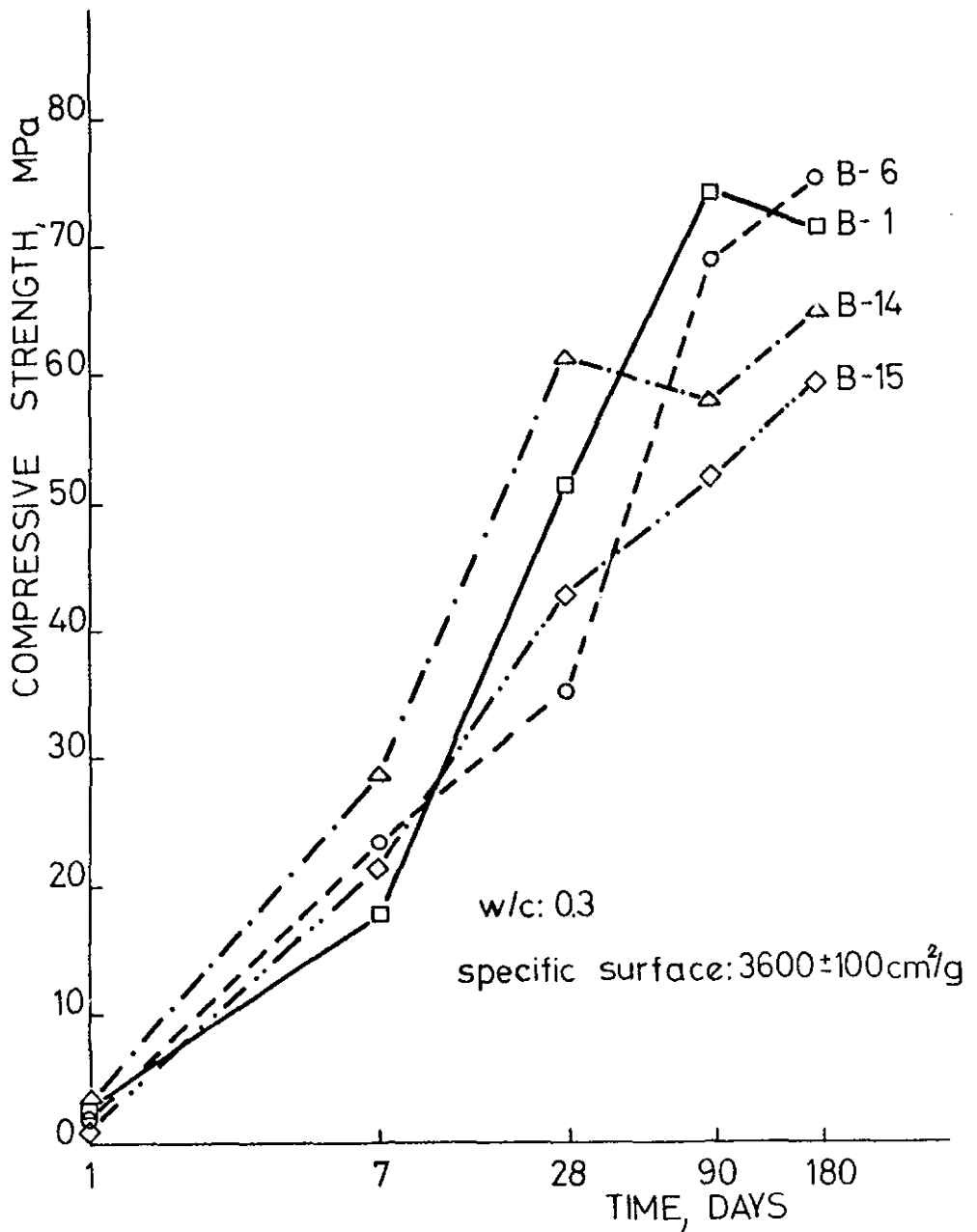


Figure 2. C₂S stabilized by BaSO₄: compressive strength of paste specimens. B-1: 6.66% BaSO₄, B-6: 12.71% BaSO₄, B-14: 14.48% BaSO₄, B-15: 15.78% BaSO₄.

The hydraulic activity of samples was examined by X-ray diffraction analysis and the characteristic diffraction maxima for samples hydrated 1 day and 28 days were compared with the intensity of the internal standard (CaF_2). It was found that the degree of hydration did not considerably differ in coexisting α' - and β -modifications after 28-day hydration.

Reactivity of BaSO_4 -stabilized belites

The results presented in Table 2 indicate that BaSO_4 stabilizes both β - and α' -polymorphs of C_2S in one thermal treatment (1450°C for 90 minutes). To gain more reliable and applicable data on the strength development in dicalcium silicates, BaSO_4 served as stabilizer for belites prepared from indigenous raw materials, i.e. high-grade limestone and quartz sand (Table 1, columns 1 and 6). The synthesis was completed in 90 minutes at 1450°C . Sintered specimens had either β -modification alone (sample B-37) or coexisting β and α' -polymorphs (B-36 and B-38) (Table 3). Since synthesized belites were almost pure C_2S , they were ground to $3600 \pm 100 \text{ cm}^2/\text{g}$ without gypsum addition. Strengths were examined on mortars and the results of mechanical testings are presented in Figure 3. Samples B-36 and B-38 containing both α' - and β - C_2S had better strength development than B-37 with the β -polymorph as the only C_2S form.

Effects of BaSO_4 on the reactivity of belite cements

Since commercial cements are complex systems containing not only alite and belite but also calcium aluminates, aluminoferrites and some other phases, any impurity selected for the incorporation into the crystal lattice of alite and belite can also enter into the crystal lattice of any other clinker phase. Indigenous raw materials usually include some minor elements, such as magnesium, sodium, potassium, titanium, sulphur etc. These elements or their mixes can likewise incorporate into the crystal lattice of the four major clinker constituents and consequently modify their hydraulic activity. When a selected stabilizer (for instance BaSO_4 affirmed to influence the C_2S reactivity) is added to the industrial raw mix, the reactivity of belite will not be affected

Table 3. Chemical and phase analyses of BaSO₄-stabilized belites (high grade limestone and quartz)

Component (wt.%)	Samples		
	B - 36	B - 37	B - 38
SiO ₂	30.87	32.68	28.24
Al ₂ O ₃	0.31	0.32	0.27
Fe ₂ O ₃	0.09	0.10	0.09
CaO	57.62	61.04	55.58
MgO	-	-	-
BaO	8.47	4.39	12.02
SO ₃	2.35	1.21	3.44
Balance	0.29	0.26	0.36
Free CaO	-	0.20	1.34

	XD		Optical microscopy		
	β -C ₂ S	α' -C ₂ S	β -C ₂ S	α' -C ₂ S	α -C ₂ S
B - 36	++	++	+++	+	
B - 37	++++		++++		
B - 38	++	++	++	+	+

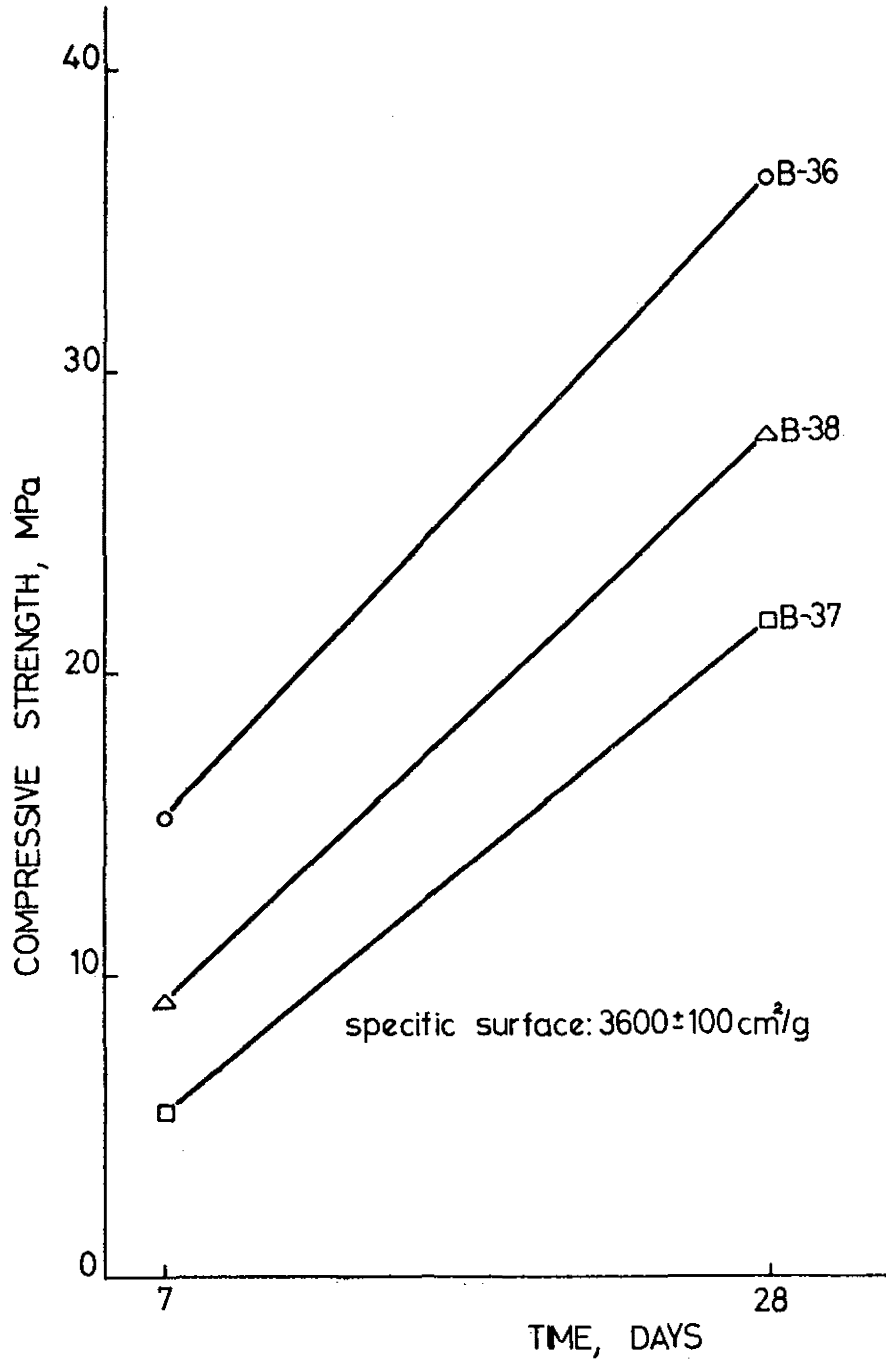


Figure 3. Belites (from high grade limestone and quartz) stabilized by BaSO_4 . Compressive strengths of mortar specimens. B-36: 10.8% BaSO_4 , B-37: 5.6% BaSO_4 , B-38: 15.46% BaSO_4 .

in the same way as when BaSO_4 is the only impurity in dicalcium silicate. Consequently the optional BaSO_4 level for C_2S need not be the optimum for the initial raw mix of belite cements. The level must be explicitly determined for every raw mix and therefore the effectiveness of BaSO_4 was tested also on belite cements.

Two clinkers with high belite content were prepared from marlaceous limestone and marl (Table 1, columns 2 and 4) with BaSO_4 added as stabilizer. Samples were synthesized at 1350°C for 90 minutes, earlier experiments having shown that the reaction was completed at such a temperature.

Chemical and clinker phase analyses are presented in Table 4. Synthesized clinkers were interground with 6.2% gypsum in a ball mill to a specific surface area of $3600 \pm 100 \text{ cm}^2/\text{g}$ and the compressive strengths of mortar specimens are graphically presented in Figure 4. The influence of BaSO_4 on the development of strengths in belite cement is easily discernible by comparison with the strength in a belite cement of similar composition but without BaSO_4 addition (Fig. 7). Higher strengths were observed on sample B-18 with a lower BaSO_4 content (1.64 wt.%) in the raw mix and a phase composition of 18.5% alite and 56.5% belite as determined by optical microscopy. The microstructure of clinker B-18 is presented in Figure 5 where alite crystals with straight lateral edges and round belite grains are clearly visible in the light matrix. Sample B-16, with more BaSO_4 added to the raw mix (8.0 wt.%), had only traces of alite and a very high belite content (75.9%). The content of alite calculated from the four principle oxides (CaO , SiO_2 , Al_2O_3 and Fe_2O_3) should have been 10%. The microstructure of clinker B-16 can be seen in Figure 6 (round dark grey belite grains in light matrix). Since there was no free CaO in either clinker the formation of C_3S must have been prevented by BaSO_4 which favored the formation of C_2S solid solution with BaO , CaO and the sulphate groups.

According to Massazza and Pezzuoli (21), tricalcium silicate tends to transform into CaO and $(\text{Ca},\text{Sr})_2$ mixed crystals in the presence of SrO and SrSO_4 . Jawed and Skalny (22) report that by increasing the SO_3 content of the clinker from 3.97 to 4.24%, the content of belite will be higher and that of alite lower than calculated.

Table 4. Chemical and phase analyses of BaSO₄ doped belite clinkers (marlaceous limestone and marl)

Component (wt. %)	B-16	B-18
SiO ₂	21.46	22.95
Al ₂ O ₃	6.33	5.92
Fe ₂ O ₃	2.83	3.15
CaO	53.97	60.32
MgO	1.93	2.42
BaO	7.34	2.08
SO ₃	4.41	0.86
K ₂ O	0.72	0.42
Na ₂ O	0.45	0.65
Balance	0.56	1.16
Free CaO	-	(n.d.)

	Calculated (Bogue)					Optical microscopy				X D		
	C ₃ S	C ₂ S	C ₃ A	C ₄ AF	Balance*	C ₃ S	C ₂ S	Matrix	Free CaO	C ₂ S	Free CaO	
B-16	10.0	53.9	12.0	8.6	15.5	0.2	75.9	α'(α)	23.9	-	α'(α)	-
B-18	26.9	45.5	10.4	9.6	7.6	18.5	56.5	β(α')	24.8	0.2	β + α'	-

(n.d.) not determined; () small quantity; * MgO, BaO, SO₃, alkalis

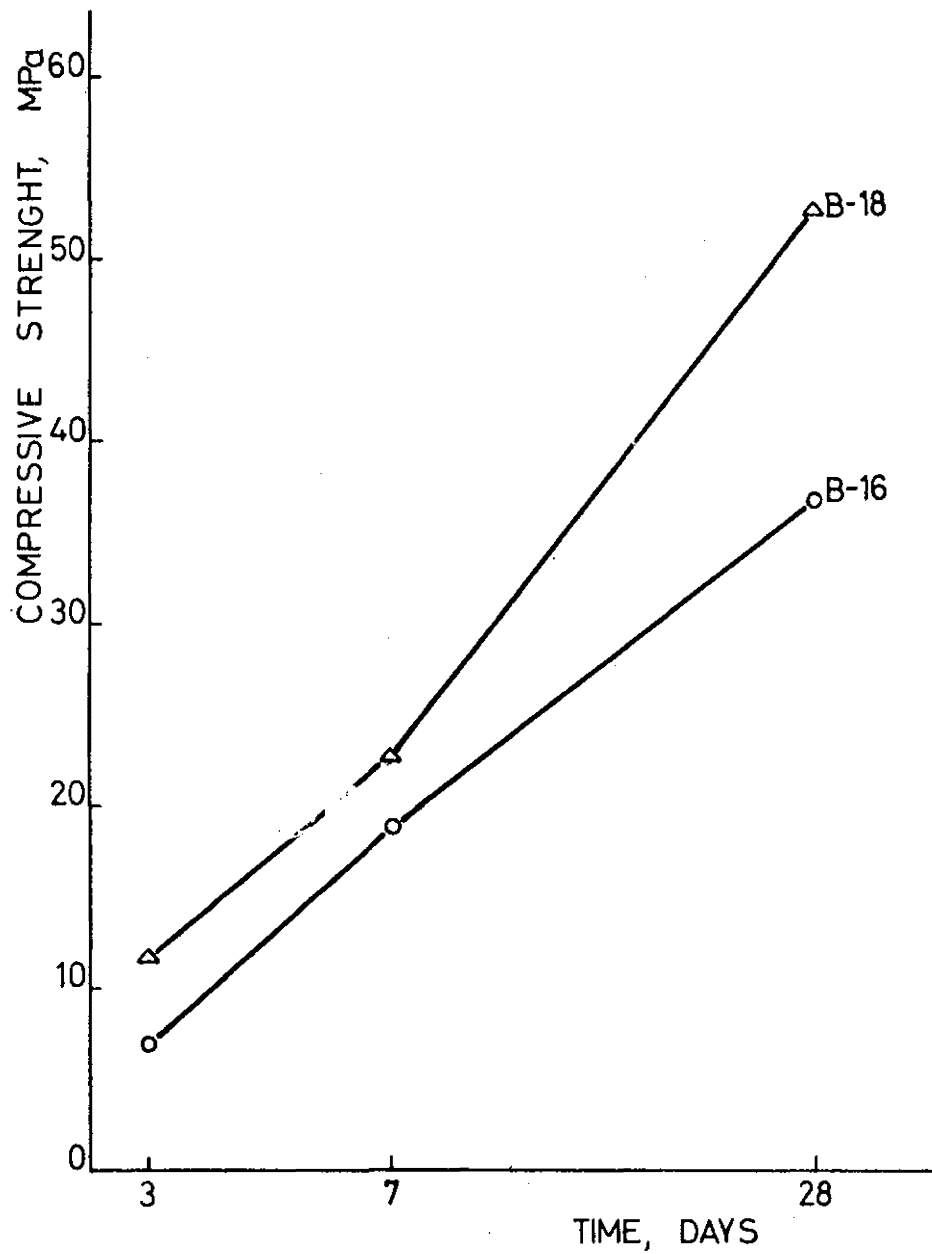


Figure 4. Clinkers (from marlaceous limestone and marl) stabilized by BaSO₄. Compressive strengths of mortar specimens. B-18: 1.64% BaSO₄, B-16: 8% BaSO₄.

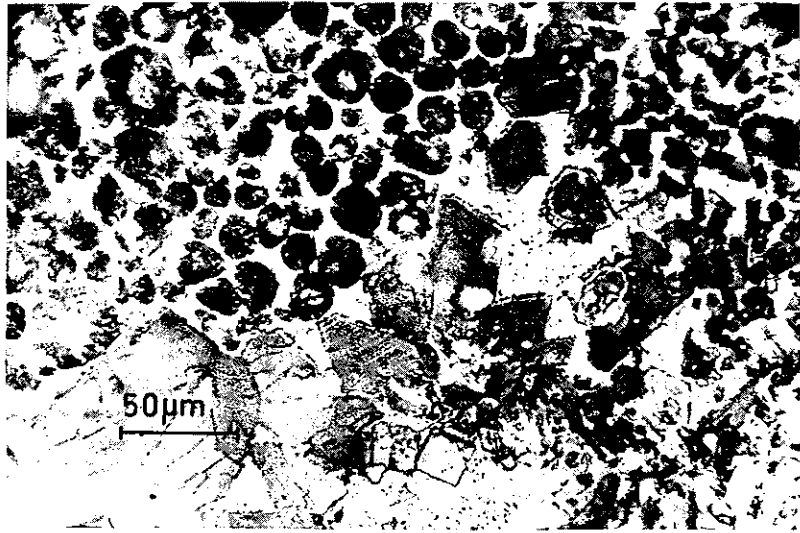


Fig. 5 Distribution of alite, belite and matrix in sample B-18.

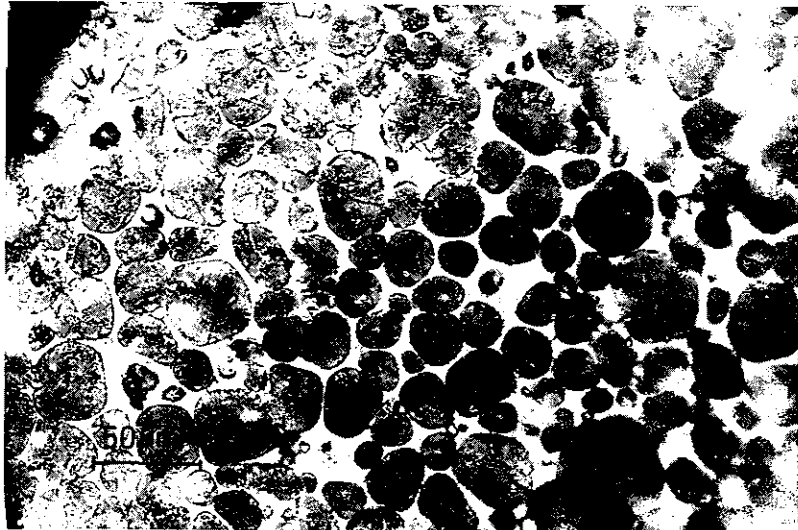


Fig. 6 Homogeneous distribution of belite and matrix in sample B-16.

To verify whether BaSO_4 added to the raw mix improved the hydraulic reactivity of belite and diminished the formation of alite in the clinker, a new series of clinkers with higher alite content was prepared for phase analysis and mechanical testing. The raw mix consisted of calcareous marl, clayey marl (Table 1, columns 3 and 5) with SiO_2 (reagent grade) added to correct the silica ratio and BaSO_4 as stabilizer. The control sample had no BaSO_4 addition. Samples were synthesized at 1350°C for 90 minutes. Chemical and clinker phase analysis are presented in Table 5. Gypsum (7.3%) was interground with the clinker to a specific surface of $3600 \pm \text{cm}^2/\text{g}$. The compressive strengths tested on mortar specimens are graphically presented in Figure 7. All samples with BaSO_4 had strengths superior to that of the control sample which contained only $\beta\text{-C}_2\text{S}$ while samples doped with BaSO_4 had coexisting β - and α' -polymorphs. The effectiveness of BaSO_4 to improve the strength development has thus been definitely confirmed. The phase analyses of belite clinkers stabilized by BaSO_4 corroborate the mentioned finding that barium sulphate also affects the lowering of alite content in clinker. With the increase of BaSO_4 (from 1.5 to 3.8%) in the initial mix, the content of alite in clinker decreased from 35.5% (without stabilizer) to 24.4% (with maximum addition of BaSO_4), while the belite content increased from 43.5 to 54.0%.

Effects of CaSO_4 on the reactivity of belite clinker

As already mentioned sulphate ions can substitute silicate groups in C_2S solid solution with BaSO_4 . It would therefore be interesting to study how sulphate groups without barium ions influence the reactivity of belite clinker. Mehta and Brady (23) report that CaSO_4 added to the raw mix to give 2% SO_3 in the clinker favorably influences the development of 1- and 3-day strengths of clinkers with a calculated composition of 52% C_3S and 22% C_2S .

To compare the effectiveness of CaSO_4 on strength development in belite cements to that of BaSO_4 , two clinkers were prepared: one as a control sample, the other with 2% $\text{CaSO}_4 \cdot 2\text{H}_2\text{O}$ added to the raw mix of a composition similar to that for the clinker with BaSO_4 (sample B-18). The synthesis was

Table 5. Chemical and phase analyses of BaSO₄ doped belite clinkers (calcareous marl and clayey marl)

Component (wt. %)	NA (control sample)	NA - 1	NA - 2	NA - 3
SiO ₂	24.18	23.27	23.88	23.82
Al ₂ O ₃	5.60	5.39	5.56	5.52
Fe ₂ O ₃	3.93	3.76	3.90	3.88
CaO	63.69	61.27	62.21	62.70
MgO	0.68	0.67	0.69	0.67
BaO	-	2.51	1.25	1.04
SO ₃	0.20	1.30	0.67	0.53
Na ₂ O	0.24	0.23	0.24	0.24
K ₂ O	0.66	0.63	0.65	0.66
Balance	0.82	0.97	0.95	0.94

	Calculated (Bogue)					Optical microscopy				XD
	C ₃ S	C ₂ S	C ₃ A	C ₄ AF	Balance*	C ₃ S	C ₂ S	Matrix	Free CaO	C ₂ S
NA	32.3	45.0	8.2	12.0	2.5	35.5	43.5	31.0	-	β
NA - 1	31.0	43.3	7.9	11.4	6.4	24.4	54.0	21.4	0.2	β, α'
NA - 2	28.8	46.7	8.1	11.8	4.6	27.3	46.9	23.6	2.2	β, α'
NA - 3	31.6	44.5	8.1	11.8	4.0	34.0	44.0	21.5	0.5	β, α'

* MgO, BaO, SO₃, alkalies

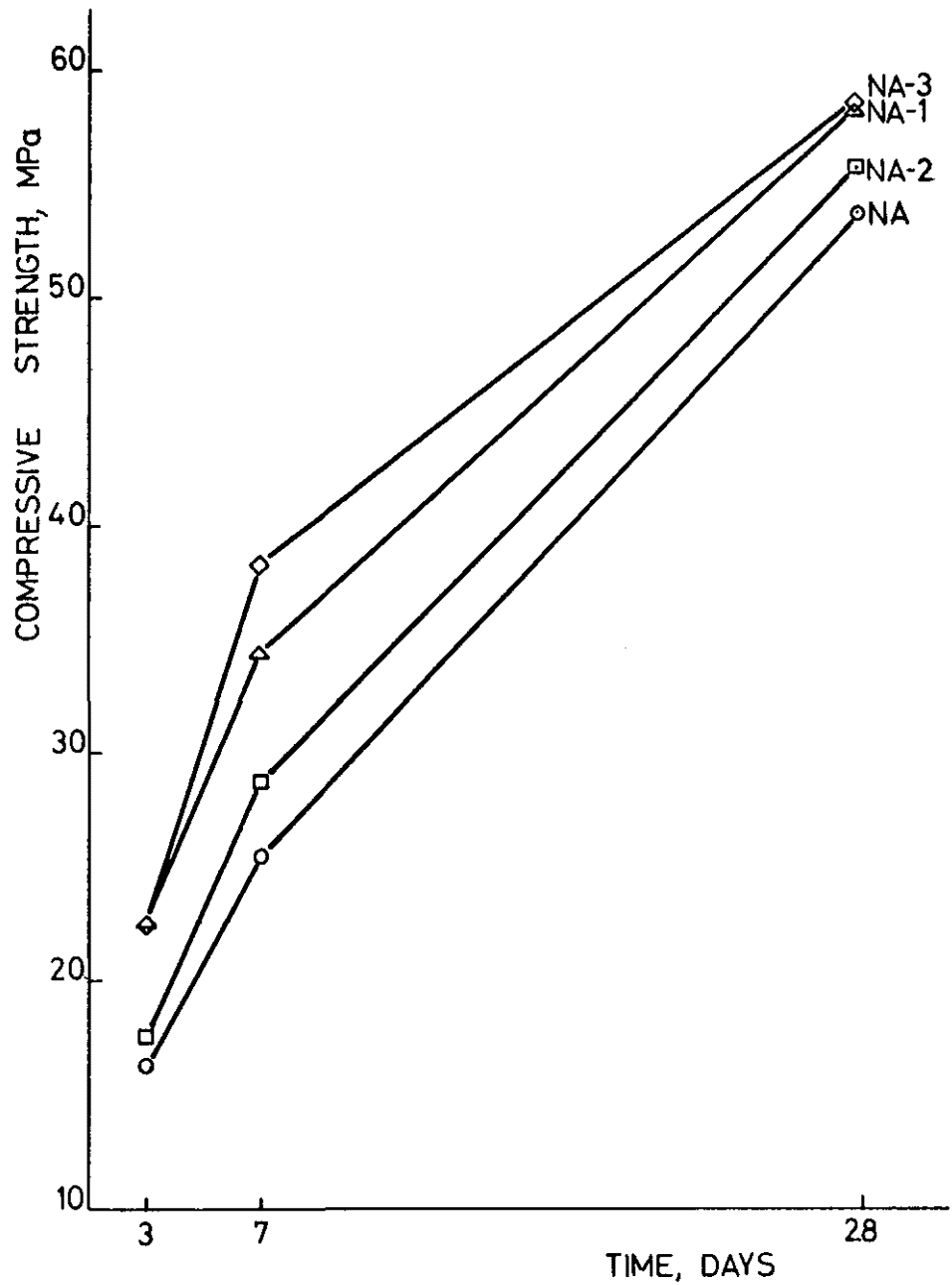


Figure 7. Belite clinkers (from calcareous marl and clayey marl) doped with BaSO_4 ; NA-1: 3.81% BaSO_4 ; NA-2: 1.92% BaSO_4 ; NA-3: 1.57% BaSO_4 .

accomplished at 1300°C for 90 minutes. Chemical and phase analyses are presented in Table 6. The clinkers were ground to a specific surface of $3500 \pm 100 \text{ cm}^2/\text{g}$ and gypsum added to give 3.5% SO_3 in the cements. Strength development in the CaSO_4 doped clinker is illustrated in Figure 8, which shows that the strength is higher than in the control sample, but lower than in the BaSO_4 -stabilized clinker (Fig. 4).

C_2S doped with BaCO_3 , MnO_2 , CaSO_4 and CaO

Dicalcium silicates were prepared from pure chemicals with the addition of BaCO_3 , MnO_2 , CaSO_4 and CaO in excess of the theoretically required value for C_2S , the synthesis being identical to that of the BaSO_4 doped C_2S . The tested compounds did not stabilize α' and β -modifications of C_2S (Table 7) under conditions analogous to those for the stabilization with BaSO_4 .

Reactivity of C_2S and belite stabilized by $\text{Ca}_5(\text{PO}_4)_3(\text{OH})$

The raw mix composition and phase analyses of the prepared C_2S are presented in Table 8. Samples were synthesized at 1450°C for 90 minutes, ground, compacted and repeatedly treated thermally under identical conditions because the free CaO content exceeded 1.5% after the first sintering. Samples bear the mark P (abbreviation for P_2O_5) with the number showing the percentage by weight of P_2O_5 in a particular sample. The reaction product in sample P-0.5 was β - C_2S , whereas samples with 1.5% P_2O_5 had β - and α' -modifications coexisting, the content of the α' -polymorph increasing proportionally with the increase of the P_2O_5 level and attaining the maximum at 5% P_2O_5 when the α -modification started to form as well.

The strength development in C_2S pastes stabilized by $\text{Ca}_5(\text{PO}_4)_3(\text{OH})$ is illustrated in Figure 9, showing that samples with the α' -form as the main reaction product (sample P-5.0) have better strengths than those with β - C_2S

Table 6. Chemical and phase analyses of CaSO_4 doped belite clinkers (marlaceous limestone and marl)

Component (wt. %)	BK - 3 (control sample)	BK - 2 (CaSO_4 doped clinker)
SiO_2	23.83	23.45
Al_2O_3	7.29	6.85
Fe_2O_3	3.36	3.31
CaO	61.40	60.93
MgO	1.96	1.85
SO_3	0.65	1.71
Balance	1.15	1.88
Free CaO	0.67	0.38

	Calculated (Boque)					Optical microscopy				XD			
	C_3S	C_2S	C_3A	C_4AF	Balance [*]	C_3S	C_2S	Matrix	Free CaO	C_3S	C_2S	C_3A	C_4AF
BK - 3	15.3	56.8	13.6	10.2	4.4	Sample too purous				10	47(β)	6	9
BK - 2	19.1	52.8	12.6	10.1	5.4	10.5	62.0	27.0	0.5	5	55(β)	4	9

* MgO, SO_3 , alkalis; () small quantity

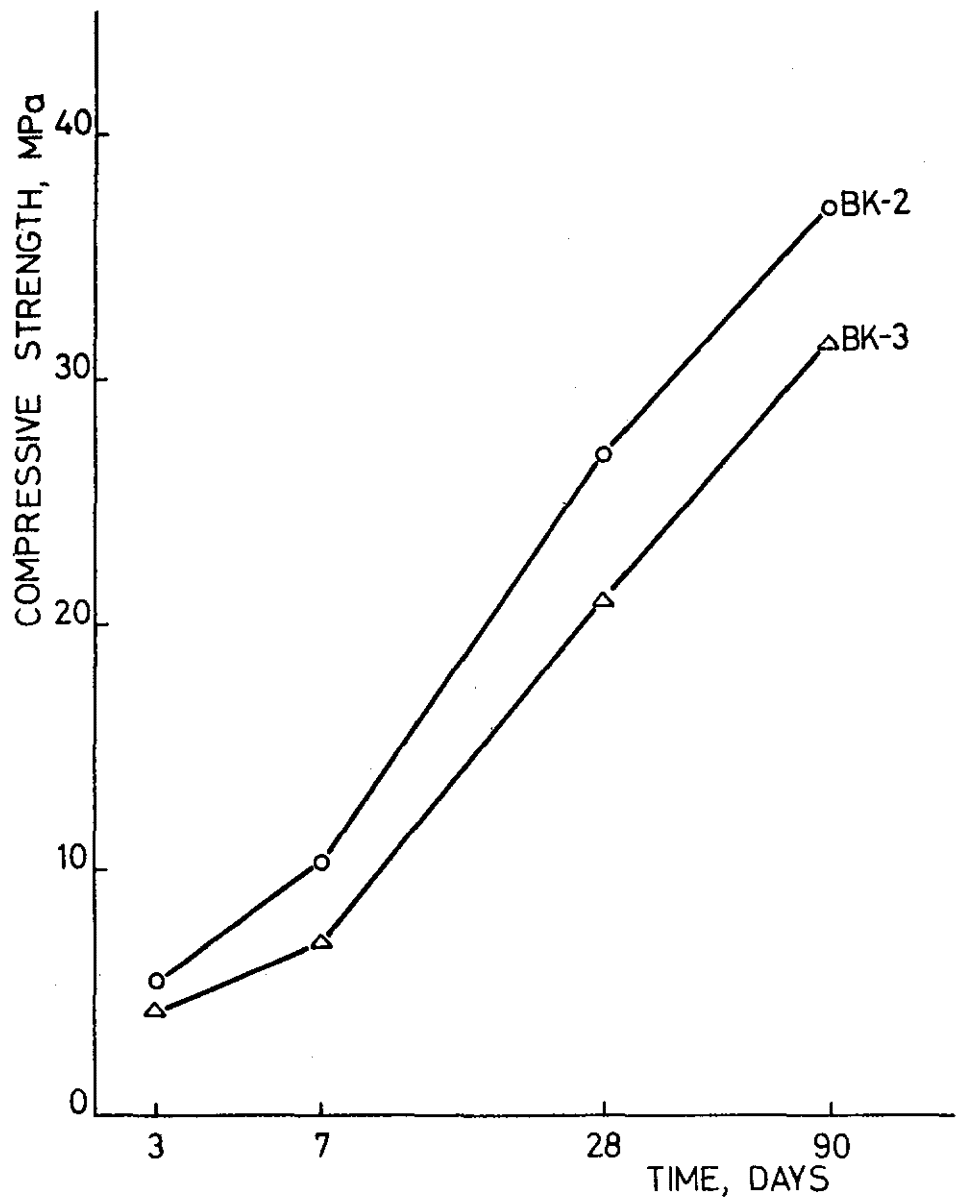


Figure 8. Belite clinker (from marlaceous limestone and Marl) doped with CaSO_4 : Compressive strengths of mortar specimens. BK-2: 2% $\text{CaSO}_4 \cdot 2\text{H}_2\text{O}$; BK-3: control

Table 7. Initial mix compositions and phase analyses of BaCO_3 , CaSO_4 , CaO and MnO_2 doped C_2S

Initial mix composition (wt. %)			XD			Sintering	
CaO	SiO_2	BaO (a)	CaO	$\gamma\text{-C}_2\text{S}$	$\beta\text{-C}_2\text{S}$	Temp. ($^\circ\text{C}$)	Time (min.)
58.55	33.02	8.43		*		1450	90
58.67	33.06	8.27		*		1450	90
58.93	33.14	7.93		*		1450	90
58.42	32.99	8.59		*		1450	90
58.18	32.91	8.91		*		1450	90
CaO	SiO_2	MnO_2					
64.22	34.40	1.38		+++		1450	90
63.16	33.84	3.00		+++		1450	90
CaO	SiO_2	CaSO_4					
64.43	34.70	0.87	(+)	++	++	1270	90
						1400	90
64.05	34.60	1.35	(+)	++	++	1270	90
						1400	90
63.52	34.48	2.00	(+)	++	++	1290	90
						1400	90
63.27	33.89	2.84	(+)	++	++	1400	3x- 120
CaO	SiO_2	C : S (c)					
66.22	33.78	2.1		*		1450	90
67.25	32.75	2.2		*		1450	2x 90
65.00	35.00	2.0	++	(+)	+	(b) 1100	105+90+ +1800+ +120
67.25	32.75	2.2	+	(+)	+++	1100	90+1800+ +120

* dusting at cooling, phases not determined

(+) small quantity

(b) prepared according to (2)

(a) BaO in BaCO_3

(c) molar ratio

Table 8. C_2S stabilized by $Ca_5(PO_4)_3(OH)$: Initial mix composition and analyses of products

Sample	Raw mix composition (wt. %)			Analyses						
	CaO	SiO_2	$Ca_5(PO_4)_3(OH)$	Free CaO (wt. %)	XD			Microscopy		
					$\alpha' (\alpha)$	β	γ	α	α'	β
P-0.5	64.35	34.46	1.18		(+)	+++	-	-	-	++++
P-1.5	62.86	33.68	3.46	0.96	(+)	+++	-			
	62.86	33.68	3.46		+	++	-		+	++
	62.86	33.68	3.46		+	++	-		+	++
P-2.0	62.12	33.28	4.60	0.90					+	++
	62.12	33.28	4.60		++	++	-		+	++
P-2.5	61.40	32.90	5.70	1.15	(+)	++	-			
	61.40	32.90	5.70						+	++
	61.40	32.90	5.70		++	+	-		+	++
P-5.0	57.92	31.03	11.05	0.32	+++	-	-	(+)	+++	(+)
	57.92	31.03	11.05		+++	(+)	-	(+)	+++	(+)
	57.92	31.03	11.05		+++	(+)	-			
P-7.5	54.66	29.28	16.06	0.32				+	+++	-
	54.66	29.28	16.06		+++	-	-	+	+++	-

(+) small quantity

- not detected

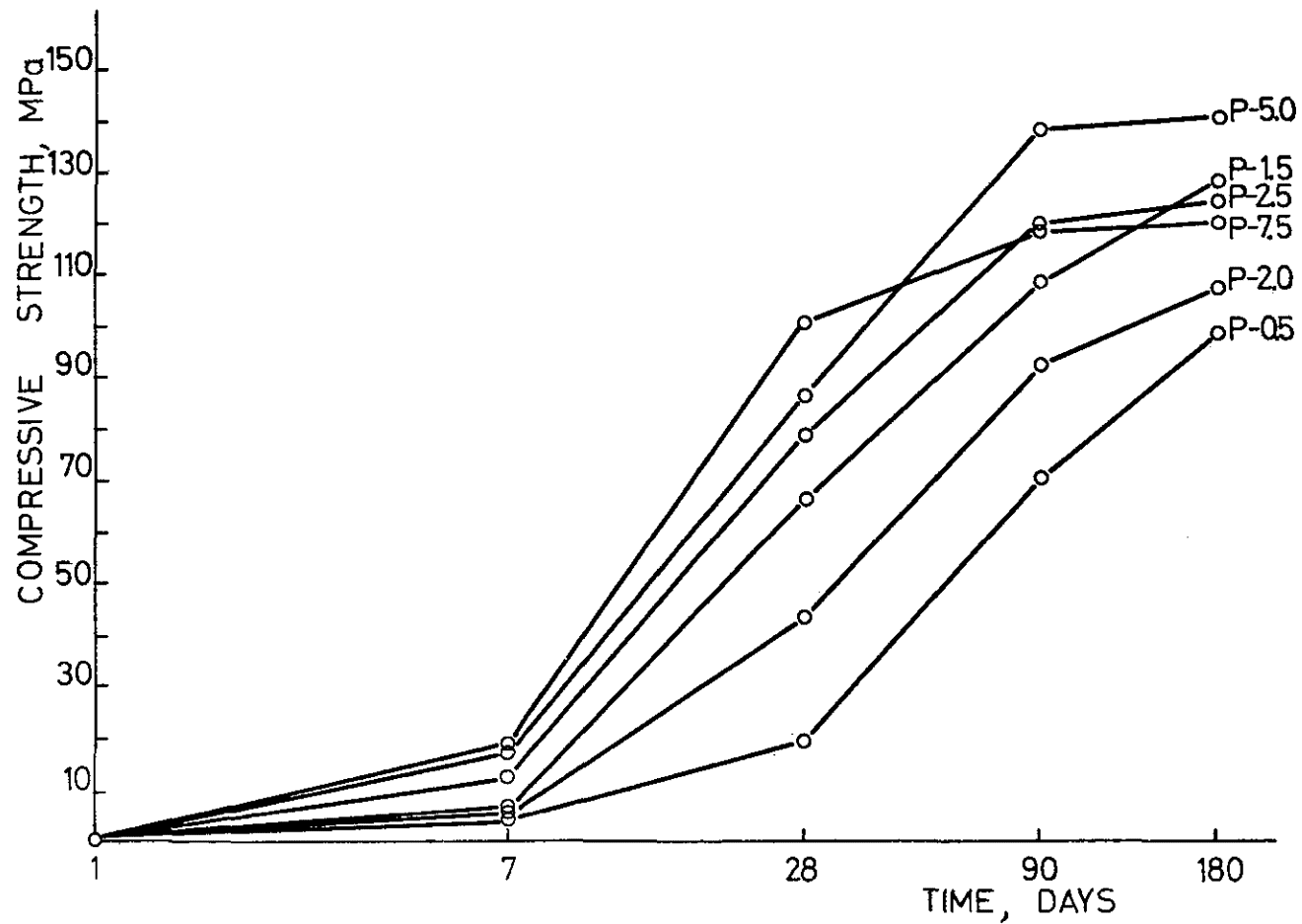


Figure 9. C₂S stabilized by Ca₅(PO₄)₃(OH). Compressive strengths of paste specimens. Amount of additive: P-0.5: 1.18%; P-1.5: 3.46%; P-2.0: 4.60%; P-2.5: 5.70%; P-5.0: 11.05%; P-7.5: 16.06%.

in prevalence. The presence of the α -polymorph (sample P-7.5) probably lowers the strength at later ages (90 and 180 days). X-ray diffraction examinations of the hydraulic activity of the α' and the β -modifications in $\text{Ca}_5(\text{PO}_4)_3(\text{OH})$ -stabilized C_2S demonstrated that at the age of 28 days the activity of α' -polymorph was slightly better than that of β -modification.

To secure results more reliable than those obtained on pastes, strengths were determined on mortars prepared with belites from limestone, quartz sand (Table 1, columns 1 and 6) with $\text{Ca}_5(\text{PO}_4)_3(\text{OH})$ added to give either 2.5% (sample P-2.5P) or 5.0% (sample P-5P) of P_2O_5 in the clinkers. The samples were synthesized at 1450°C for 90 minutes and since there were no crystallized aluminates and aluminoferrites in the interstitial phase (approx. 2%), the clinkers were ground without gypsum to a specific surface of $3600 \pm 100 \text{ cm}^2/\text{g}$. Table 9 shows the chemical composition and phase analysis of the prepared belites and Figure 10 their compressive strengths. Sample P-5P with the α' -polymorph predominating obviously has somewhat higher strength than sample P-2.5P where β - C_2S is the main reaction product. In belites stabilized by phosphate, strengths develop very slowly during the first month and are remarkably lower than BaSO_4 doped belites (Fig. 3).

Effects of V_2O_5 on C_2S activity

Experiments were made using the initial mix prepared from pure chemicals (reagent grade) with an addition of V_2O_5 in varying percentages (from 0.38 to 11 wt.%). The doped mixes were synthesized at 1400°C for 90 minutes and the thermal treatment repeated whenever the reaction was not completed on first sintering. Samples with 0.38 to 4.0% V_2O_5 had either β - C_2S alone or coexistent β - and γ -modifications. With V_2O_5 content over 4%, β - and α' -polymorphs appeared together. By further increasing the level of V_2O_5 the β -polymorph content decreased and the α'_L -modification formed when V_2O_5 content was 7%.

Table 9. Chemical and phase analyses of $\text{Ca}_5(\text{PO}_4)_3(\text{OH})$ doped belites (high grade limestone and quartz)

Component (wt. %)	Samples	
	P - 2.5 P	P - 5.0 P
SiO_2	32.88	31.24
Al_2O_3	0.27	0.46
Fe_2O_3	0.31	-
CaO	63.80	64.05
MgO	-	-
SO_3	-	-
P_2O_5	2.27	4.02
Balance	0.47	0.23

	Optical microscopy				XD		
	C_3S	$\beta\text{-C}_2\text{S}$	$\alpha'\text{-C}_2\text{S}$	Free CaO	C_3S	$\beta\text{-C}_2\text{S}$	$\alpha'\text{-C}_2\text{S}$
P - 2.5 P	(+)	+++	(+)	-	<5%	+++	(+)
P - 5.0 P	(+)	+	+++	-	<5%	+	+++

(+) small quantity

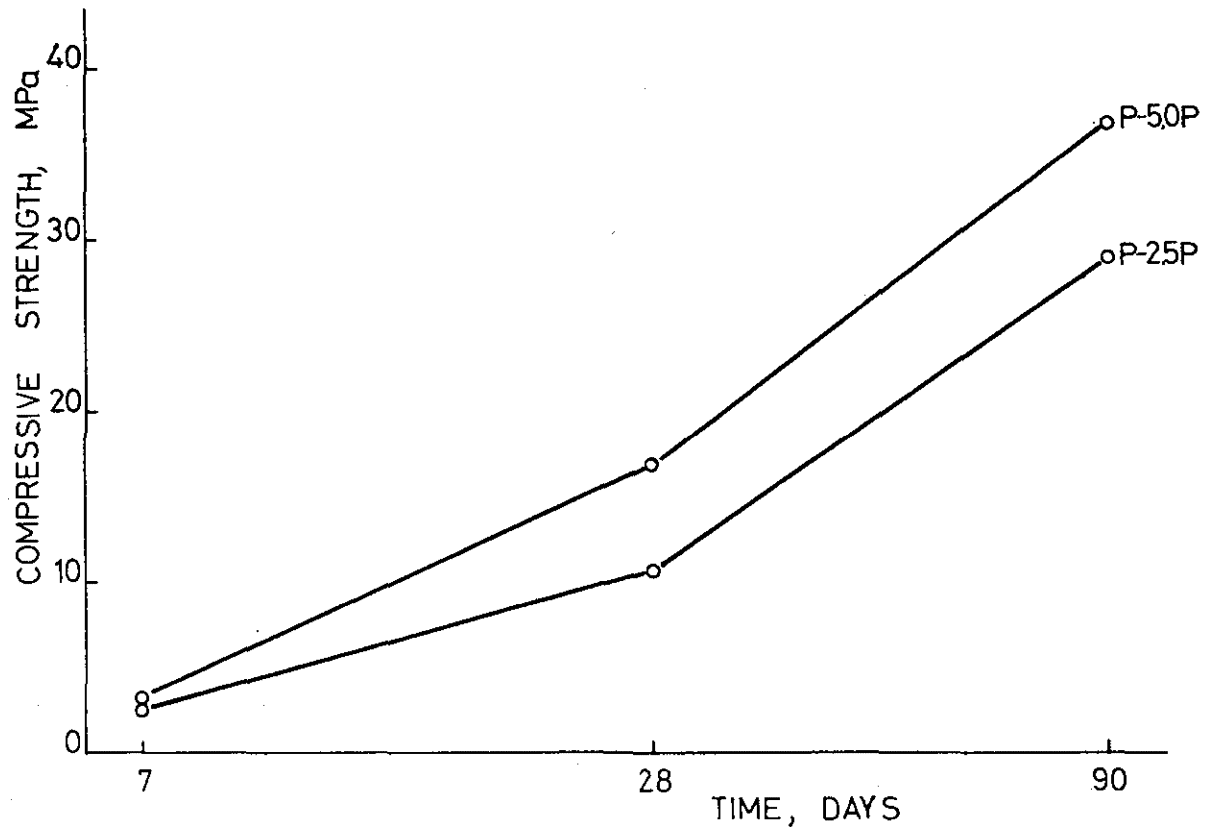


Figure 10. Belites (from high grade limestone and quartz) stabilized by $\text{Ca}_5(\text{PO}_4)_3(\text{OH})$. Amount of stabilizer: P-2.5:5.70%; P-5.0:11.05%.

Strength data for cement pastes are presented in Figure 11. Samples are marked V to denote V_2O_5 with the number indicating the percentage of the stabilizer. For the first 90 days, α' - C_2S had similar or slightly higher strengths than β - C_2S , but at later ages β - C_2S attains better strengths.

Strengths were not tested on mortars because no V_2O_5 belite clinkers were prepared due to the toxicity of vanadium compounds (recommended limit in air 0.5 mg/m^3 particulates and 0.005 mg/m^3 vapor, ref. 25).

Saalfeld (26) obtained β -polymorph with 1-2% V_2O_5 and α -modification with 5% V_2O_5 (at 1500°C). According to his later finding (27) V_2O_5 cannot stabilize the α' -form. This work, however, shows otherwise and Tables 10 and 11 give the lattice constants and powder data determined for V_2O_5 -stabilized β - and α'_L - C_2S doped with V_2O_5 . During the $\alpha'_L \rightarrow \beta$ transition some orthorombic reflections split and new lines appear (Table 12).

Additional data on polymorphs and stabilizer distribution

Differential thermal analyses:

Peak temperatures of the endothermal $\alpha'_H \rightarrow \alpha$ - C_2S phase transformation were measured on C_2S samples doped with various $BaSO_4$ levels (Table 13) to determine whether the stabilizer added to the raw mix had completely passed into solid solution with C_2S during synthesis or remained in part as a separate phase. This was decided by recourse to the relationship of the temperature of $\alpha'_H \rightarrow \alpha$ - C_2S phase transformation to the stabilizer level in the raw mix shown by 0 entries on Figure 12. The Δ points denote the temperatures of phase transformations in certain samples (B-1, B-6, B-14, B-15, and B-38). Compared to the phase transformation curve these temperatures were higher than expected for samples with a defined percentage of stabilizer in the raw mix, indicating that the samples contained unreacted $BaSO_4$ which had not entered into solid solution with C_2S . This was confirmed by differential thermal analyses, because there was an endotherm at 1170°C for the $BaSO_4$ phase transformation. Free $BaSO_4$ in these samples was detected by X-ray diffraction method, both on samples and on residues after the selective separation of the silicate phase.

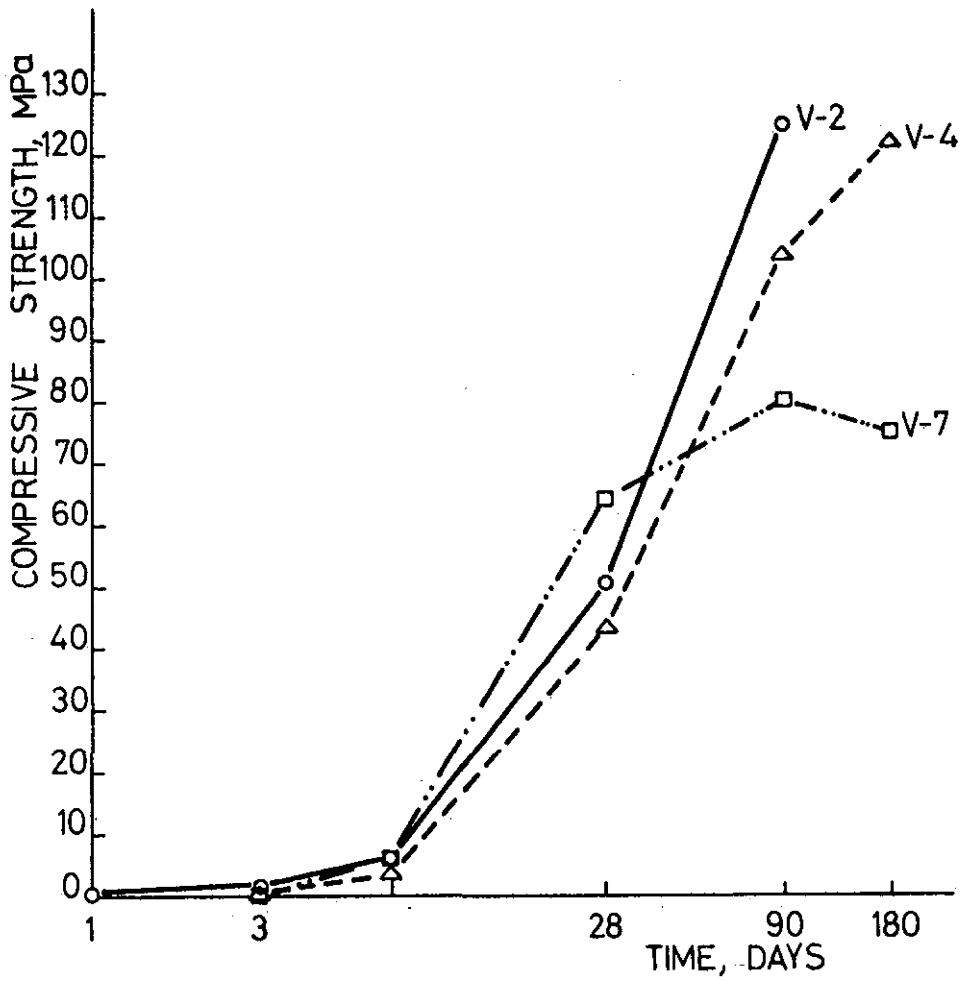


Figure 11. C₂S stabilized by V₂O₅. Compressive strengths of paste specimens. V-2: 2% V₂O₅; V-4: 4% V₂O₅; V-7: 7% V₂O₅.

Table 10. β -C₂S stabilized by V₂O₅: Lattice constants and powder data

β -C ₂ S; monoclinic with $a = 5.51(2)$, $b = 6.75(2)$, $c = 9.32(3)$ Å = 94.6(1) ^o ; the space group P2 ₁ /n							
d _{obs.} (Å)	d _{calc.} (Å)	hkl	I	d _{obs.} (Å)	d _{calc.} (Å)	hkl	I
4.90	4.90	$\bar{1}01$	6	2.281	2.282	023	19
4.646	4.645	002	8	2.200	2.196	014	17
3.948	3.970	$\bar{1}11$	1	2.189	2.188	031	45
3.824	3.827	012	6	2.165	2.163 2.157	$\bar{2}12$ 123	12
3.780	3.783	111	1	2.132	2.130	220	7
3.376	3.377	020	7	2.100	2.105	$\bar{2}21$	2
3.236	3.241	$\bar{1}12$	8	2.091	2.094	$\bar{1}14$	6
3.173	3.175	021	6	2.085	2.083	130	5
3.042	3.046	112	8	2.050	2.048	221	12
2.876	2.876	120	24	2.042	2.041	$\bar{2}13$	10
2.810	2.814	013	15	2.026	2.026	032	13
2.785	2.795 2.780	$\bar{1}03$ 121	99	2.020	2.019	131	16
2.738	2.744 2.731	200 022	100	1.984	1.983	$\bar{2}22$	19
2.720	2.716	121	36	1.910	1.913	024	6
2.607	2.608	103	45	1.897	1.897 1.892	213 222	12
2.538	2.543	210	10	1.847	1.845	$\bar{1}24$	3
2.440	2.451 2.433	$\bar{2}02$ 113	15	1.820	1.821	033	3
2.405	2.407 2.400	211 122	17	1.806	1.808 1.804	$\bar{2}23$ 105	12
2.323	2.322	004	2	1.791	1.791	015	8
2.304	2.304	$\bar{2}12$	6	1.766	1.768	301	2

Table 11. α'_L -C₂S stabilized by V₂O₅: Lattice constants and powder data

α'_L -C ₂ S; orthorhombic with a = 11.08(5), b = 18.80(10), c = 6.82(3)Å; the space group P _{mcn}							
d _{obs.} (Å)	d _{calc.} (Å)	hkl	I	d _{obs.} (Å)	d _{calc.} (Å)	hkl	I
3.93	3.910	221	5	2.360	2.350	080	5
3.87	3.870	041	11	2.308	2.307	062	7
3.412	3.410	002	10	2.225	2.222	081	19
3.209	3.211	112	7	2.212	2.215	113	23
	3.206	022			2.210	023	
	3.200	311					
3.164	3.173	241	12	2.180	2.167	123	12
2.900	2.904	202	16	2.164	2.150	402	6
2.881	2.891	132	25	2.085	2.069	422	8
	2.883	331			2.089	530	
2.840	2.847	061	9	2.059	2.062	281	12
					2.052	223	
2.772	2.774	222	73	2.040	2.046	043	7
2.760	2.770	400	71	1.981	1.985	461	11
					1.994	233	
2.750	2.760	042	55	1.948	1.955	442	15
2.722	2.727	260	100	1.938	1.935	082	18
2.650	2.635	350	5	1.846	1.840	063	3
2.550	2.532	261	14	1.811	1.812	0.10.1	6
2.470	2.476	421	5	1.768	1.773	462	5
2.455	2.470	242	7	1.725	1.727	423	3
2.404	2.386	440	12	1.707	1.705	004	6

Table 12. Reflection splittings in V_2O_5 stabilized
 α'_L - and β - C_2S

α'_L - C_2S (orthorhombic, Table 11)	β - C_2S (monoclinic, Table 10)	α'_L - C_2S (cont.)	β - C_2S (cont.)
—————	$\bar{1}01$	062 —————	023
—————	002	081 —————	014
221 ————	$\bar{1}11$	023 —————	031
—————	111	—————	$\bar{1}23$
041 —————	012	123 —————	
002 —————	020	402 —————	220
241 ————	$\bar{1}12$	422 ————	$\bar{2}21$
—————	112	—————	221
022 —————	021	281 —————	$\bar{1}14$
202 —————	120	—————	130
132, 331 ————		—————	$\bar{2}13$
061 —————	013	461 ————	213
260 ————	$\bar{1}03$	043 —————	032
—————	103	223 —————	131
222 ————	$\bar{1}21$	442 ————	$\bar{2}22$
—————	121	—————	222
400 —————	200	082 —————	024
042 —————	022	—————	$\bar{1}24$
—————	210	063 —————	033
440 —————	$\bar{2}02$	462 ————	$\bar{2}23$
350 —————		—————	223
261 —————	113	—————	$\bar{1}05$
421 —————	211	—————	105
242 —————	122	0.10.1 ————	015
080 —————	004	—————	301
—————	$\bar{2}12$	423 —————	
—————	212	004 —————	040

Table 13. C_2S doped with $BaSO_4$: Initial mixes and peak temperatures of $\alpha'_H \rightarrow \alpha-C_2S$ phase transformation

Sample	Raw mix composition (wt. %)			Peak temperatures ($^{\circ}C$)	$BaSO_4$ detected
	CaO	SiO_2	$BaSO_4$		
Control	65.11	34.89	0	1445	-
B-22	62.93	33.14	3.33	1420	-
B-1	60.76	32.58	6.66	1380	-
	60.76	32.58	6.66	1400	+
B-24	58.66	31.23	10.11	1354	-
B-23	58.04	30.89	11.07	1353	-
B-5	57.49	30.71	11.80	1348	-
B-32	57.28	30.64	12.08	1317	-
	57.28	30.64	12.08	1313	-
B-36*	56.45	30.27	12.63	1324	-
B-6	56.82	30.47	12.71	1360	+
	56.82	30.47	12.71	1370	+
B-33	56.29	30.29	13.42	1300	-
	56.29	30.29	13.42	1319	-
B-34	55.95	30.18	13.87	1298	-
	55.95	30.18	13.87	1309	-
B-14	55.50	30.02	14.48	1351	+
B-35	54.65	29.73	15.62	1289	-
B-15	54.54	29.68	15.78	1345	+
B-38*	54.10	27.52	17.81	1339	+
	54.10	27.52	17.81	1262	-

* B-36 and B-38 from limestone and sand, and the others from chemicals, grade p.a.

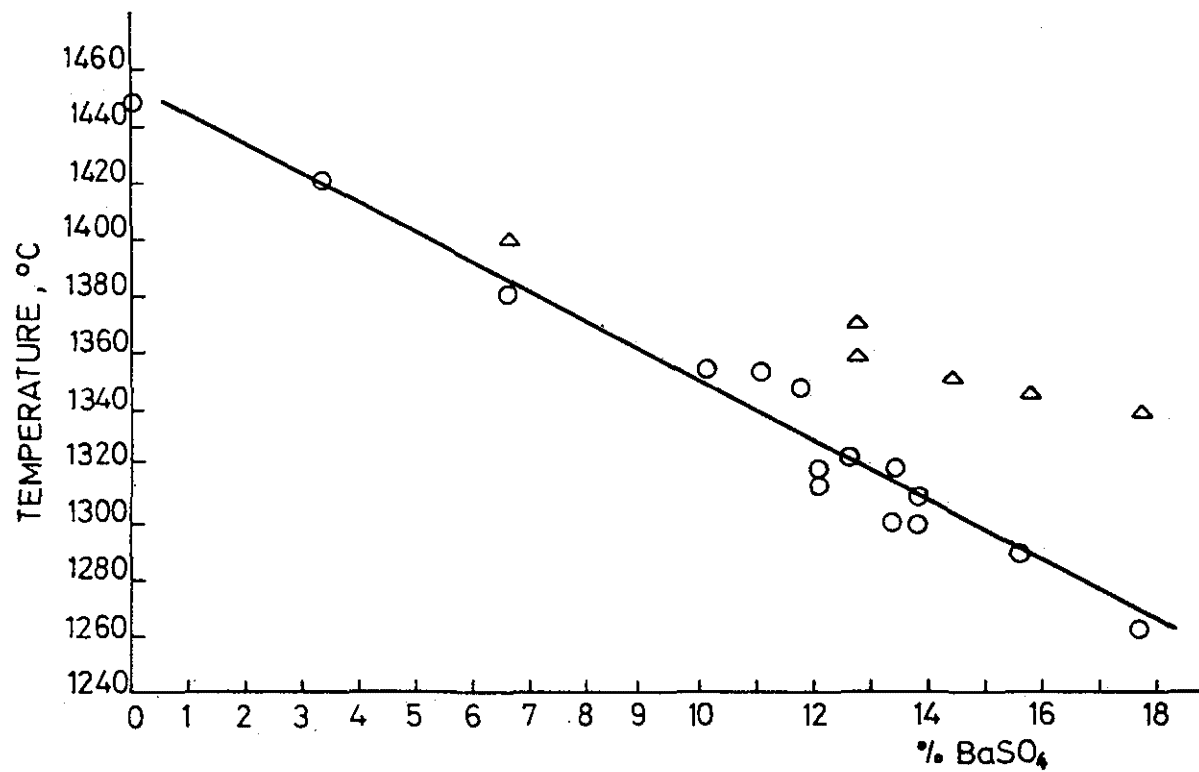


Figure 12. The effect of BaSO₄ concentration on the α -C₂S transition temperature.
 O - completely reacted samples.
 Δ - samples contain some unreacted BaSO₄.

In sample B-38 (Table 13, Fig. 12) the peak temperature of the $\alpha'_H \rightarrow \alpha-C_2S$ phase transition was 1339°C but after four repeated syntheses at 1450°C for 90 minutes it descended to 1262°C, i.e. to the value on the phase transformation curve which corresponds to the temperature of the phase transition in C_2S solid solution with the respective percentage of stabilizer. After such a thermal treatment there was no endotherm for the phase transformation of unreacted $BaSO_4$ on the DTA curve of the sample. The initial SO_3 content in sample B-38 was 3.44%. After repeated synthesis it decreased to 1.34%, indicating that the formed C_2S solid solution had more Ba atoms than SO_4 groups. During the formation of the $BaSO_4-C_2S$ solid solution, $BaSO$ decomposed and a part of the SO_4 evaporated as SO_3 . Unlike barium carbonate, $BaSO_4$ promotes the formation of solid solution with C_2S and acts both as a mineralizer in the sintering process and as a stabilizer for the α' and β -polymorphs. Figure 12 shows that the maximum incorporation level was not attained with 17.8% $BaSO_4$ in the raw mix, because the peak temperature continued to decrease with increased $BaSO_4$ percentage. Once the limit of solubility has been achieved the temperature of the phase transformation will cease to decrease regardless of the quantity of $BaSO_4$ added to the raw mix.

Figure 13 shows the differential thermal curves in the range between 1150 and 1450°C, with endotherms for the $\alpha'_H \rightarrow \alpha-C_2S$ phase transition in samples stabilized by different levels of $BaSO_4$ in the raw mix. The sample without $BaSO_4$ has a sharp peak for the $\alpha'_H \rightarrow \alpha-C_2S$ transition demonstrating that the transformation takes place within a narrow temperature range. In samples prepared from raw mixes with higher $BaSO_4$ percentages, the effects of phase transformation are broader indicating that the stabilizer was not homogeneously distributed in the C_2S solid solution.

Apatite $Ca_5(PO_4)_3(OH)$, doped samples were analyzed in the same manner. The values of peak temperatures for the endothermal $\alpha'_H \rightarrow \alpha-C_2S$ transformation in samples examined in this study are shown in Table 14. The phase transformation curve for $\alpha'_H \rightarrow \alpha-C_2S$ was plotted using experimentally obtained data for the phase transition temperatures as a function of the apatite levels in the raw mix (Fig. 14). The temperatures of the phase transformation did not differ much

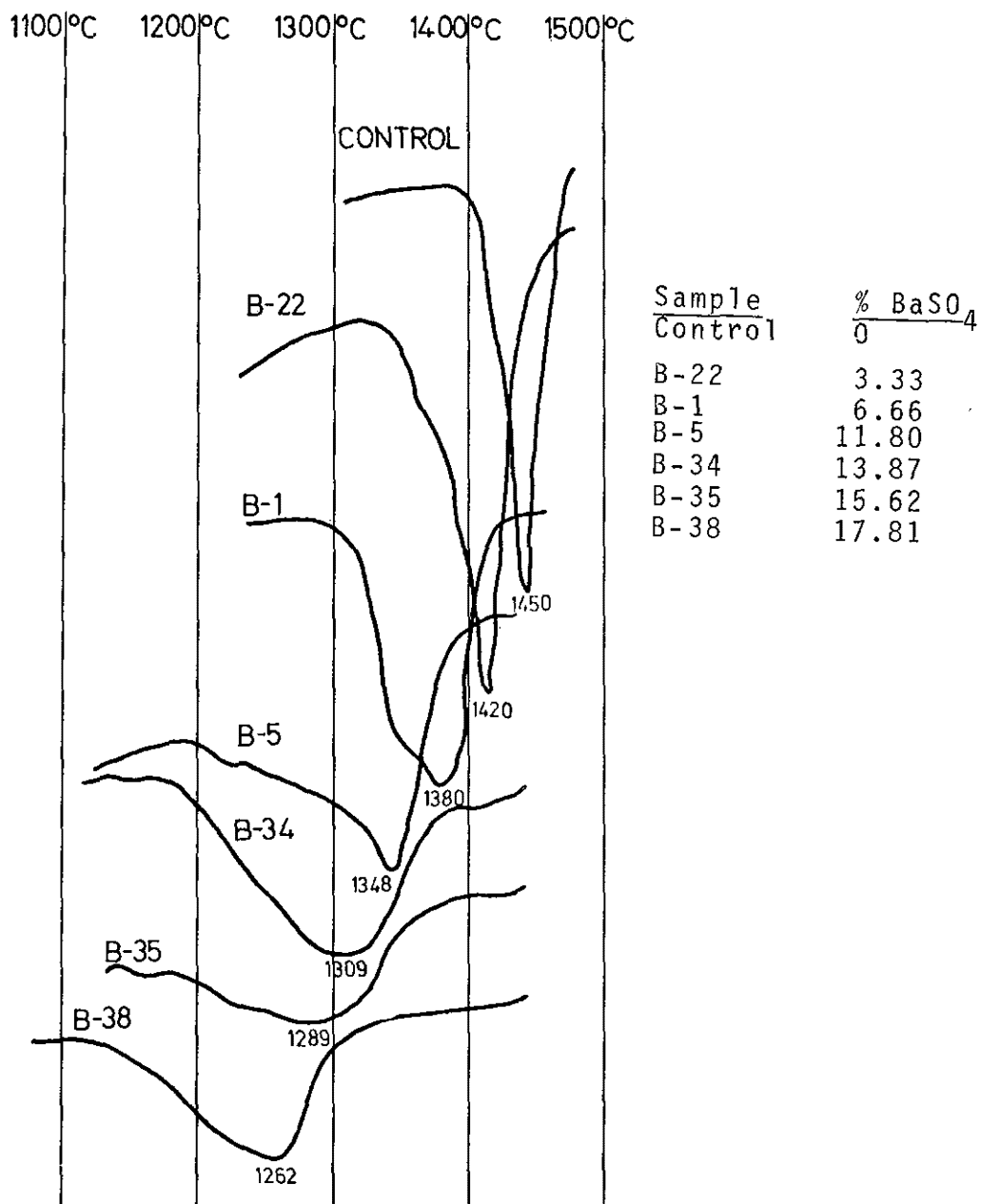


Figure 13. DTA heating curves of C₂S solid solutions with BaSO₄ (10°/min, Pt/P+Rh 10, Pt crucible).

Table 14. C_2S stabilized by $Ca_5(PO_4)_3(OH)$: Initial mixes and peak temperatures of $\alpha'_H \rightarrow \alpha-C_2S$ phase transformation

Sample	Raw mix composition			Peak temperatures ($^{\circ}C$)
	CaO	SiO ₂	$Ca_5(PO_4)_3(OH)$	
Control	65.11	34.89	0	1445
P-0.5	64.35	34.46	1.18	1407
	64.35	34.46	1.18	1406
P-1.5	62.86	33.68	3.46	1371
	62.86	33.68	3.46	1374
	62.86	33.68	3.46	1355
P-2.0	62.12	33.28	4.60	1337
	62.12	33.28	4.60	1335
P-2.5	61.40	32.90	5.70	1303
	61.40	32.90	5.70	1291
	61.40	32.90	5.70	1302
P-5	57.92	31.03	11.05	1106
	57.92	31.03	11.05	1122
P-7.5	54.66	29.28	16.06	1055
	54.66	29.28	16.06	1070

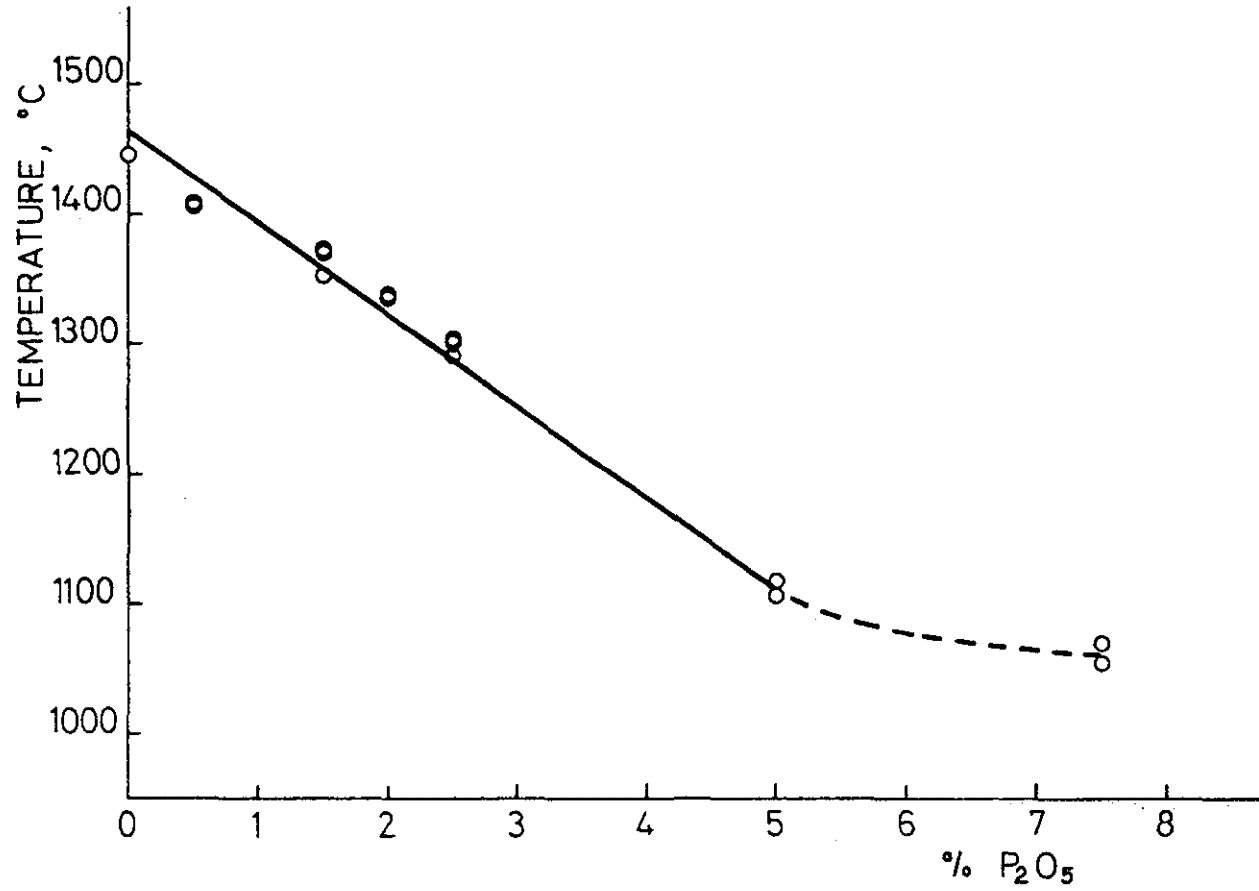


Figure 14. Effect of $\text{Ca}_5(\text{PO}_4)_3(\text{OH})$ concentrations on the $\alpha_H \rightarrow \text{C}_2\text{S}$ transition temperature

from the values of the phase transformation line. Figure 15 shows the DTA curves within the 950-1450°C temperature range for apatite-stabilized specimens. The endotherms for the phase transformation are broader when the samples have a higher percentage of stabilizer, so it can be deduced that the distribution of the stabilizer in the C₂S solid solution was not homogeneous for samples doped with Ca₅(PO₄)₃(OH).

Homogeneous solid solutions can be obtained by repeated syntheses for which the thermally treated samples must again be ground, homogenized and compacted. This, however, was not the intention of the present work which was designed to investigate the influence of stabilizers on strength development under conditions similar to those in the process of manufacture. According to Pritts and Daugherty (2) repeated thermal treatments of samples will decrease the rate of hydration of dicalcium silicate since "it is possible that the large decrease in hydration rate upon refiring arises from the heterogeneous to homogeneous change in stabilizer distribution within the C₂S lattice. Or, an alternative explanation for the rapid hydration of the "heterogeneously" stabilized preparations is concerned with crystallite size. Refiring samples could allow crystals to grow larger. Samples fired only once could contain smaller crystallites which could hydrate faster." It follows that an accurate estimation of the influence of stabilizer levels on the hydration rate of particular C₂S polymorphs requires the examination of both the crystallite size and the homogeneity in solid solutions.

Selective extraction method:

Differential thermal analysis was not appropriate to determine whether the stabilizer had completely passed into solid solution with C₂S in sample B-16 which contained calcium aluminates and aluminoferrites. As belite was the sole calcium silicate in the sample, it was of interest to find the basic: acidic oxide ratio in C₂S. Therefore, the silicate phase was separated by selective extraction and the oxide distribution obtained as presented in Table 15. Sample B-16 contained 71% silicate phase, 9% aluminate phase and 20% of the other phases, including glass. Of the 7.34% BaO, there was 1.89% in the silicate

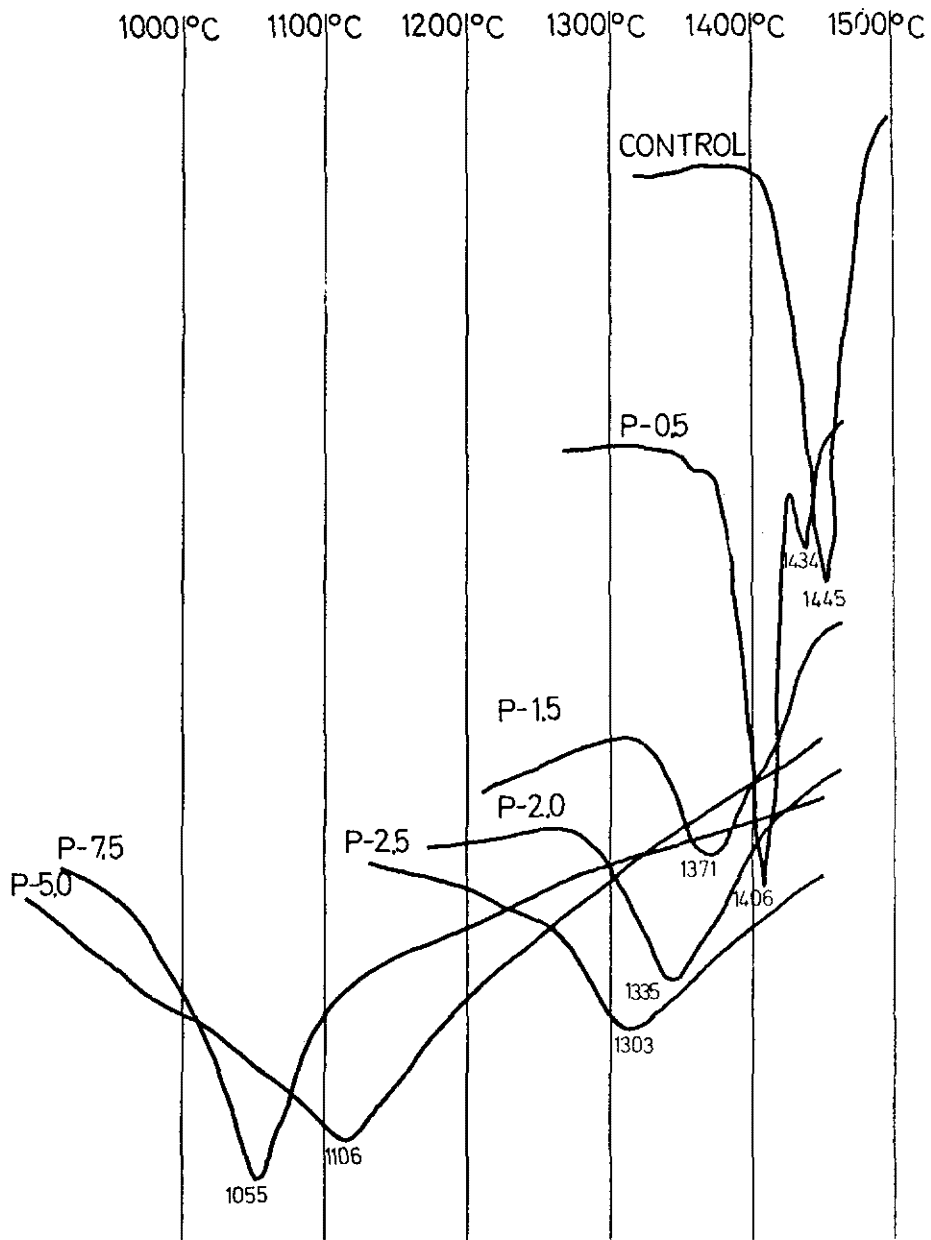


Figure 15. DTA heating curves of C₂S solid solutions with Ca₅(PO₄)₃(OH) (10°/min, Pt/Pt+Rh 10%, Pt crucible). Percent additive: Control: 0; P-0.5:1.18; P-1.5:3.46; P-2.0:4.60; P-2.5: 5.70; P-5.0:11.05; P-7.5:16.06.

Table 15. Element distribution in clinker phases (sample B-16)

Component (wt. %)	Silicate phase (71%) ⁺	Interstitial phase (29%) ⁺	Total (100%)	Original sample analyses	△
SiO ₂	20.24	2.05	22.29	21.46	+0.83
Al ₂ O ₃	1.44	4.50	5.94	6.33	-0.39
Fe ₂ O ₃	0.79	2.04	2.83	2.83	-
CaO	45.22	9.23	54.45	53.81	+0.64
MgO	0.43	1.32	1.75	1.93	-0.18
BaO	1.89	4.67	6.56	7.34	-0.78
SO ₃	0.57	3.31	3.88	4.41	-0.53
Balance	0.30	2.00	2.30	1.89	+0.41

$$c/S^* \quad 2.39$$

$$\frac{C+B+M}{S+\bar{S}+A+F}^* \quad 2.28$$

+ determined by selective solution method

* molar ratios (B = BaO)

phase and the balance in the interstitial phase. It should be noted that no barium oxide was identified in the aluminate phase separated by selective extraction. The silicate phase had only 0.57% SO_3 out of the total 4.41%. Since the silicate phase included 1% (mol) BaO and 0.6% (mol) SO_3 , it is obvious that from the BaSO_4 added to the raw mix more Ba ions than SO_4 groups were incorporated within the C_2S lattice. Barium ions and sulphate groups were mostly found in the interstitial phase. The presence of BaSO_4 was identified by X-ray diffraction both in the original sample and in the residue after extraction of the silicate phase. X-ray microanalysis detected barium and sulphur in the interstitial phase in addition to calcium, aluminum, silicon and iron. Thus, we can conclude that both the silicate and the interstitial phase contained some BaSO_4 , a part of which remained unreacted, while in the aluminate phase there were no stabilizing atoms.

Sample B-16 had no free CaO , the silicate phase was C_2S and the basic:acidic oxide ratio was 2.28 (Table 15). However, should BaSO_4 precipitate during extraction of the silicate phase, the quantity of Ba atoms and SO_4 groups incorporated in the silicate phase would be higher than that shown in Table 15.

Korneyev (28) reports that γ - and β - forms of dicalcium silicate have been found at molar ratios of $\text{CaO}:\text{SiO}_2 = 2.0 - 2.2$. Further investigations are needed to establish whether the CaO enrichment of dicalcium silicate is brought about by C_2S solid solution with BaSO_4 only, or by the presence of other atoms (Fe and Al) as well.

Optical microscopy:

The identification of polymorphous modifications of C_2S by optical microscopy in reflected light is described in a foregoing chapter B (Experimental data: Investigation methods) and patterns typical for particular C_2S polymorphs are illustrated there by some examples.

Figures 16 to 19 refer to samples P-0.5 and B-37, illustrating the manner of β - C_2S identification. Figure 16 shows the β -polymorph in sample P-0.5 which has no striation (intersected lamellae), characteristic of the α - $\text{C}_2\text{S} \rightarrow \alpha'$ -transformation (as in sample B-37, Fig. 18); complete grains exhibit only the

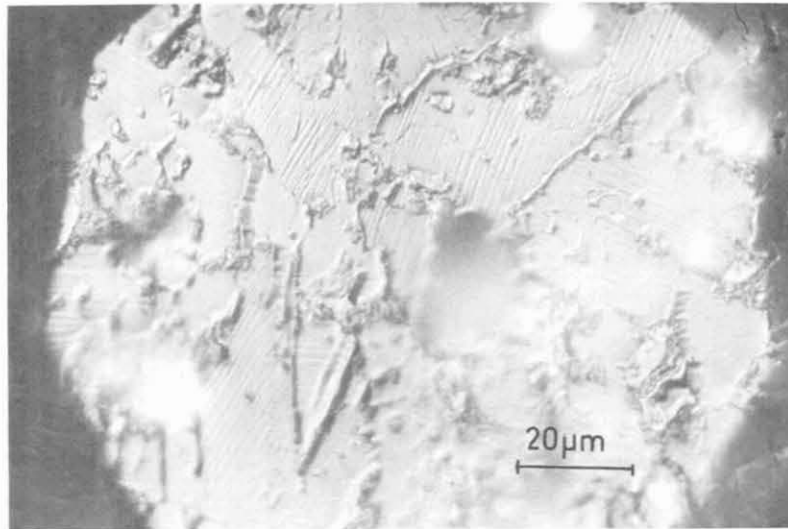


Fig. 16 Polysynthetic lamellae in $\beta\text{-C}_2\text{S}$, sample P-0.5

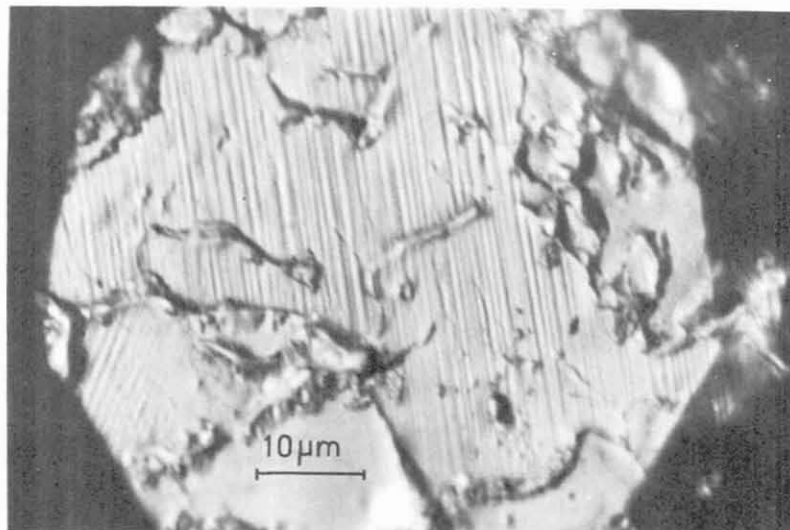


Fig. 17 Detail from Fig. 16, grossly enlarged.

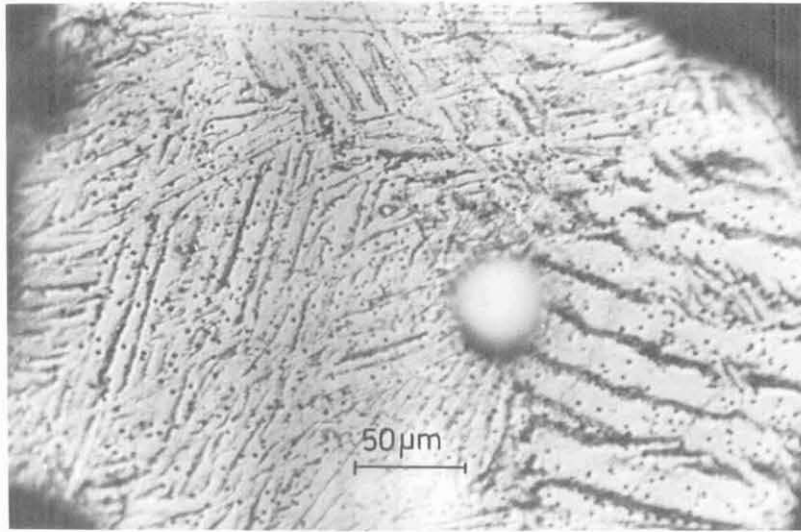


Fig. 18 Cross lamellae in sample B-37.

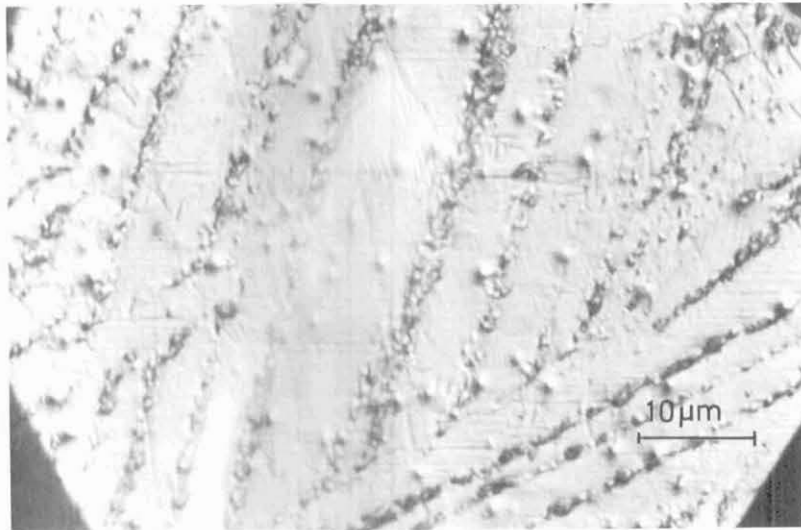


Fig. 19 Detail from Fig. 18, grossly enlarged.

polysynthetic lamellae formed by the phase transition of α' -C₂S into β -polymorph (cf. Fig. 1d). Figure 17 is more indicative because sample P-0.5 is grossly enlarged. Sample B-37 (Fig. 18, enlarged x 320) has only the cross striation typical for $\alpha \rightarrow \alpha'$ -transition. The transformation of α' -C₂S into the β -polymorph is evident in Figure 19 (sample B-37 enlarged x 1600), where the α' -form striae are transversally laminated by polysynthetic lamellae characteristic of the β -form (cf. Fig. 1c).

Figure 20 (sample B-38) and 21 (sample P-5.0P) show the respective α' -grains under maximal enlargement (1600 x). The characteristic striation of the α' -polymorph remained smooth, keeping its original form (cf. Fig. 1b) and thus confirming that the grains, (Figures 20 and 21) belong to the α' -modification. Sample P-5.0P also has α -C₂S crystals recognizable by allotriomorphic grains (Figure 22). Since all the specimens were subjected to identical etching treatment, the C₂S crystal grains with no marks (Figure 22) must evidently be those of the α -C₂S (cf. Fig. 1a).

The DTA method has shown that the temperatures of $\alpha'_H \rightarrow \alpha$ -C₂S phase transition can be lowered by as much as 200°C depending on the percentage of the stabilizer added (Figures 12 and 14). Samples with higher percentages have broader endotherms for the $\alpha'_H \rightarrow \alpha$ -C₂S transformation (Figures 13 and 15) because the stabilizer was not homogeneously distributed in the C₂S solid solution.

Inferences derived from thermal analyses were confirmed by crystallo-optical characteristics of different dicalcium silicate polymorphs studied by the method developed by S. Chromy (24). It allows the identification of particular C₂S modifications, the assessment of temperatures for phase transitions and visual observation of the effect brought about by $\alpha' \rightarrow \alpha$ -C₂S phase transition. The procedure is based on the following principle: when C₂S specimens are heated to 1500°C on the heating stage of the optical microscope continuous changes in the birefringence are noticeable, with marked fluctuations for phase transitions affecting the intensity of the light transmitted through the crystal section. Changes in light intensity are registered by a photometer with an X-Y recorder and a curve can be plotted showing the light intensity (photometric values) as a function of the sample temperature (Fig. 23). It is

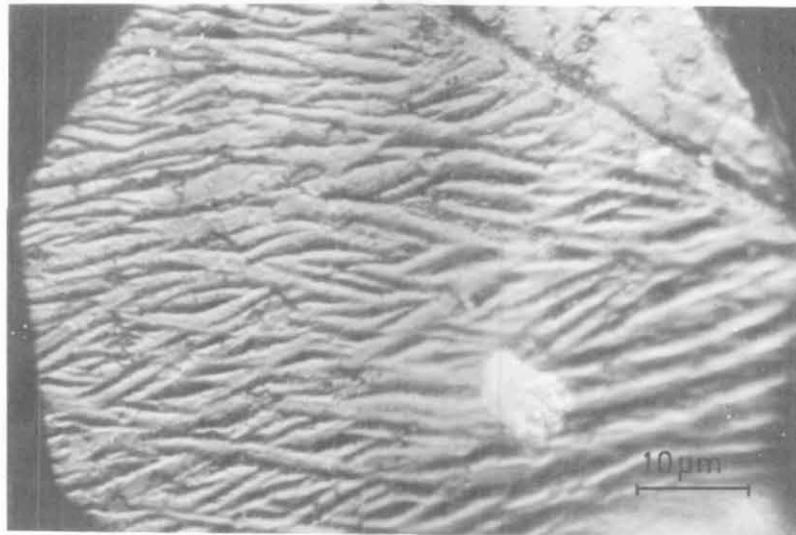


Fig. 20 Cross lamellae of the $\alpha \rightarrow \alpha' - C_2S$ inversion, sample B-38.

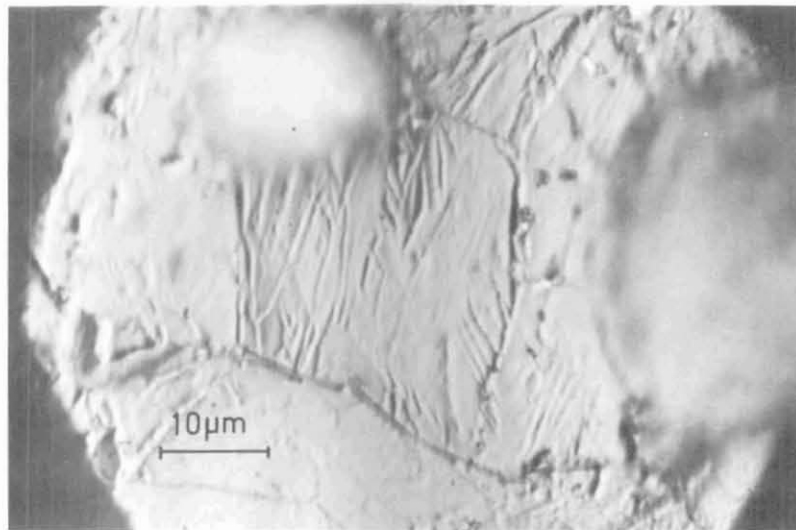


Fig. 21 Cross lamellae of the $\alpha \rightarrow \alpha' - C_2S$ inversion, sample P-0.5 P.

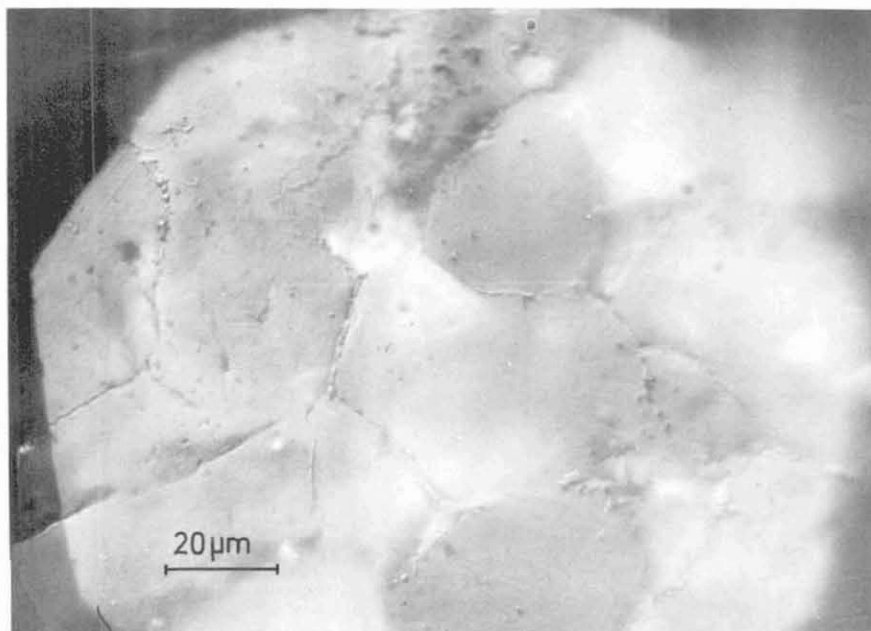


Fig. 22 Crystals of the α -C₂S, sample P-5.0 P

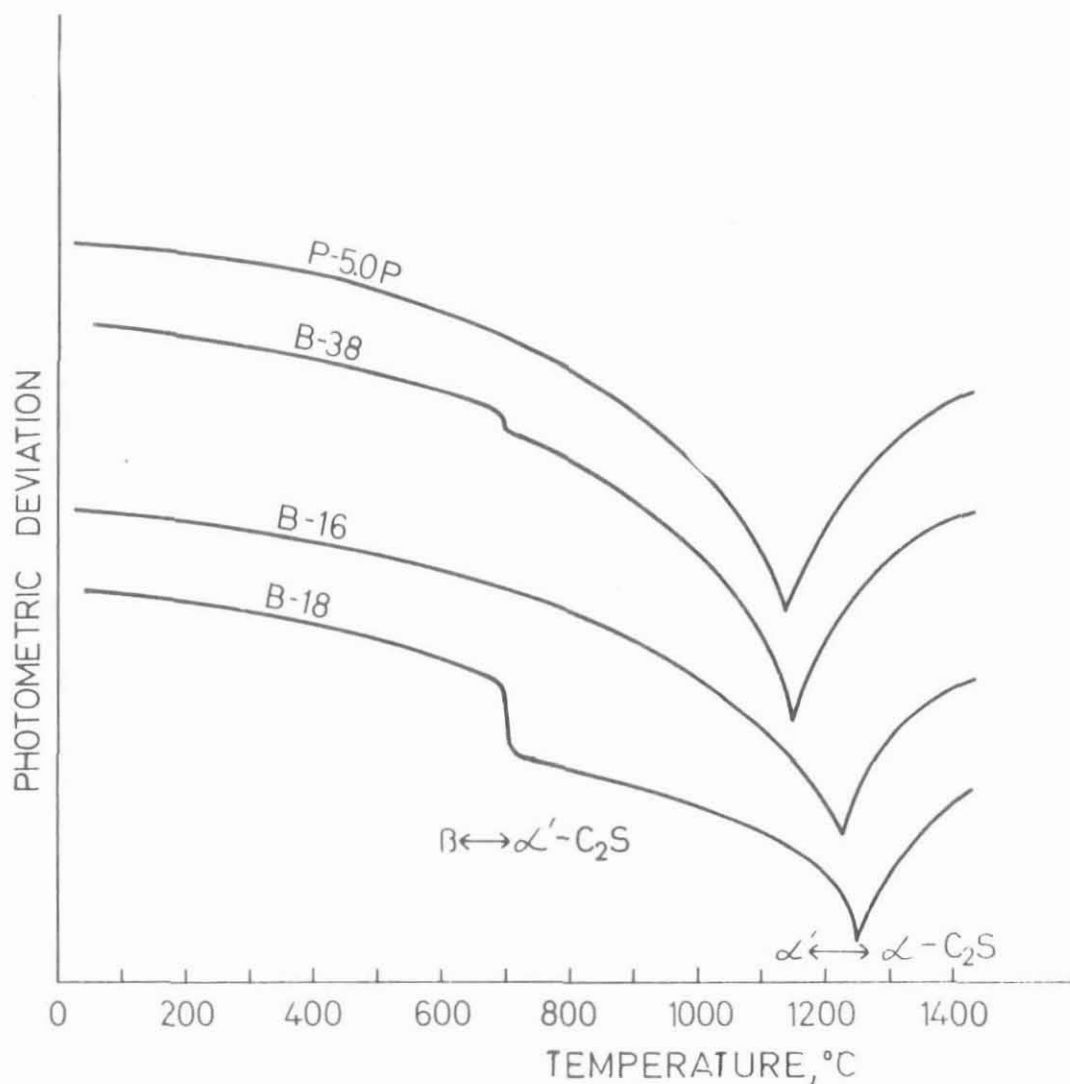


Figure 23. Temperature dependent changes in light-transmissiveness of C_2S thin sections. Curves B-18 and B-38 show inflection at $700^\circ C$ indicating $\beta \rightarrow \alpha'-C_2S$ inversion. Curves B-18, B-16, B-38 and P-5.0P minima between 1100 and $1250^\circ C$ indicates $\alpha' \rightarrow \alpha-C_2S$ phase transformation. Additives: P-5.0P: 11.05% $Ca_5(PO_4)_3OH$; B-16: 8.0% $BaSO_4$; B-18: 1.64% $BaSO_4$; B-38: 17.81% $BaSO_4$.

possible in this way to determine the temperatures for $\beta \rightarrow \alpha' - C_2S$ and $\alpha' \rightarrow \alpha - C_2S$ conversions in a sample with the β polymorph and also the temperature of the $\alpha' \rightarrow \alpha - C_2S$ phase transition in an $\alpha' - C_2S$ specimen. The data obtained confirm that samples P-5.0P and B-16 had $\alpha' - C_2S$, whereas α' and $\beta - C_2S$ were coexistent in samples B-38 and B-18. The inflection intensity demonstrated that the content of the β -modification was higher in sample B-18 than in B-38. Those samples were analyzed by S. Chromy at the Research Institute for Building Materials, Brno, Czechoslovakia.

The effect visually observed in the microscope is also worth mentioning. Since the crystals are isotropic at the moment of $\alpha'_H \rightarrow \alpha - C_2S$ conversion, the grains transmit no light through the crossed nicols of the optical microscope. In our study the transformation did not occur simultaneously either in all the crystal grains or within every grain. When a belite grain was observed during heating, the polymorphous transformation was noticed to begin from the edge towards the center, the direction being reversed during cooling. The temperature of the phase transition was lowered because of higher concentrations of the stabilizer at the periphery of the grains. In other words: grains with lower phase transformation temperatures have a larger concentration of the stabilizing ions than those where the temperatures of the phase conversion are higher. The visual observation can thus lead to the conclusion that there is a different range of concentrations for the stabilizer in single C_2S crystallites and within every grain. This is in conformity with the broadening of the DTA curves for samples with higher levels of stabilizer where the $\alpha'_H \rightarrow \alpha - C_2S$ phase transition effect covers a wider temperature range. The nonhomogeneous distribution of the stabilizer in the C_2S solid solution is also evidenced by the fact that there are often grains with $\beta - C_2S$ in the center and $\alpha' - C_2S$ at the periphery, like in sample P-2.5 (Fig.24).

Scanning electron microscopy:

Investigations of the specimen surface have shown that the shape of the belite grain and the physical bond between the grains are essentially dependent on the type of stabilizer.

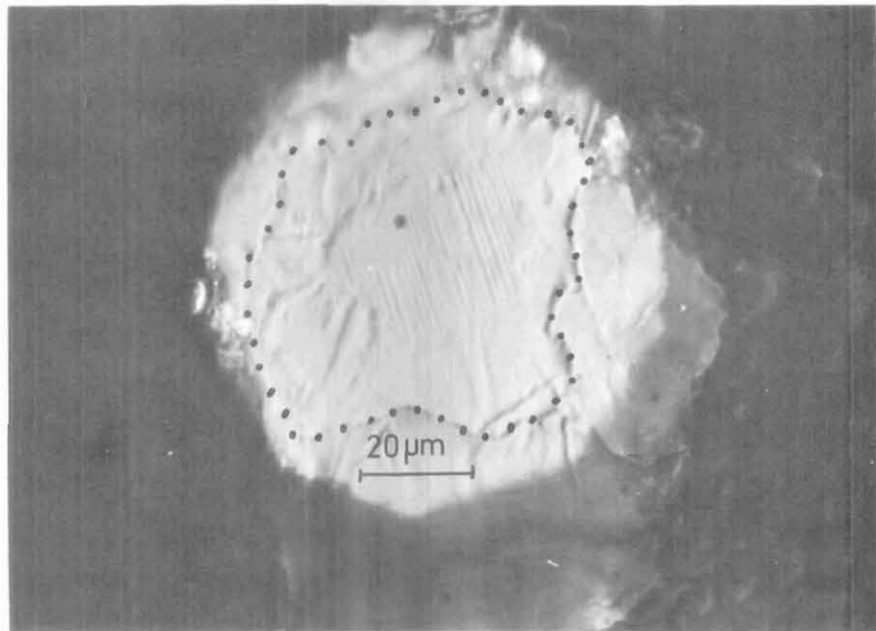


Fig. 24 C₂S grain: Centre of β-polymorph surrounded by α'-polymorph (dashed line denotes the boundary of grain), sample P-2.5)

Belites doped with V_2O_5 have larger, interconnected grains (approx. 50 μ m) and their surface is cross striated due to the $\alpha \rightarrow \alpha'_H - C_2S$ phase conversion (Fig. 25). The $BaSO_4$ stabilized belites present a loosely connected conglomerate with the size of the grains between 20-30 μ m (Fig. 26). Belites doped with apatite have a very porous structure consisting of loosely connected 5-15 μ m grains of dicalcium silicate (Fig. 27).

The belite grains of samples NA-1 and B-16 are equally interesting. The surface of the NA-1 belite grains is widely striated due to the $\alpha \rightarrow \alpha'_H - C_2S$ conversion and then laminated by transversal, very fine polysynthetic lamellae originating from the $\alpha' \rightarrow \beta - C_2S$ phase transformation (Fig. 28). The cross striation of the α' -polymorph is very distinctive in sample B-16, with no sign of further transformations (Fig. 29).

The distribution of the stabilizer was studied using a microanalyzer. All the doped specimens had a stabilizer (Ba and S, and P or V respectively) in the dicalcium silicate grains, with an excess in some samples where the stabilizer had not completely passed into solid solution with C_2S (e.g. sample B-16). By comparing the microstructure of the broken sample B-16 (Fig. 30) and the distribution of Ba atoms (Fig. 31) it is obvious that barium has mostly concentrated in some parts of the interstitial phase (very light in Fig. 30). The microanalysis of these parts of the interstitial phase (marked 0 in Fig. 30) revealed a high concentration of Ba and S atoms with some Al, Ca, Fe and Si in addition. The morphological characteristics of these parts of the interstitial phase lead us to conclude that there is probably a glass phase rich in $BaSO_4$. The analysis of a microsection in the C_2S grain (marked + in Fig. 30) detected some Ba, S and Al atoms in addition to a high concentration of Ca and Si atoms. The SEM and microanalyzer examinations were made at the University of Illinois, Urbana, Ill. in collaboration with professor J. F. Young.

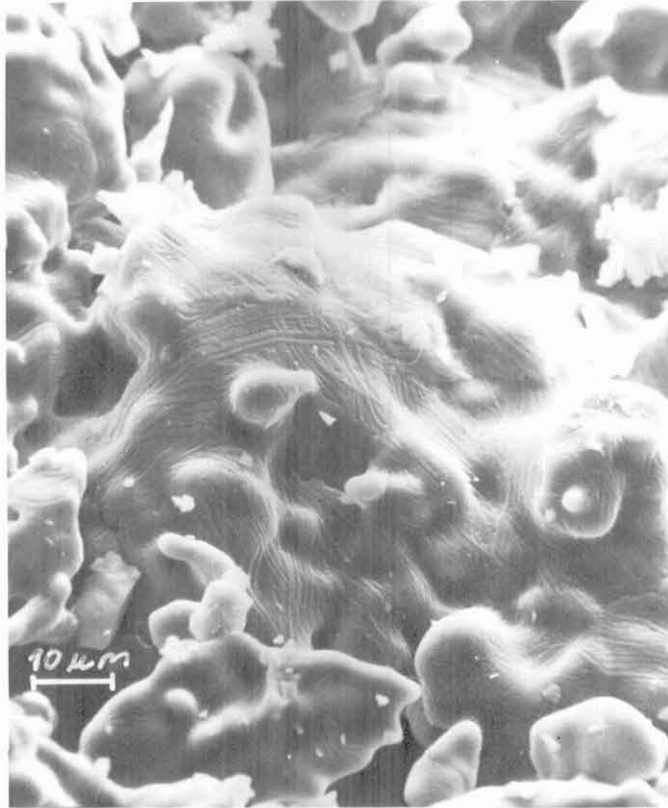


Fig. 25 Microstructure of V₂O₅-stabilized C₂S, sample V-4

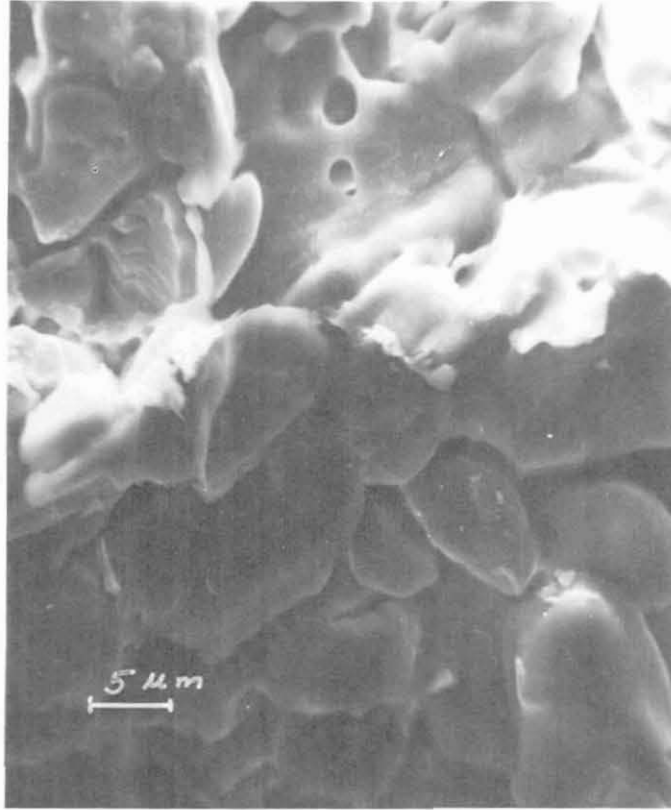


Fig. 26 Microstructure of BaSO₄-stabilized C₂S, sample B-6.

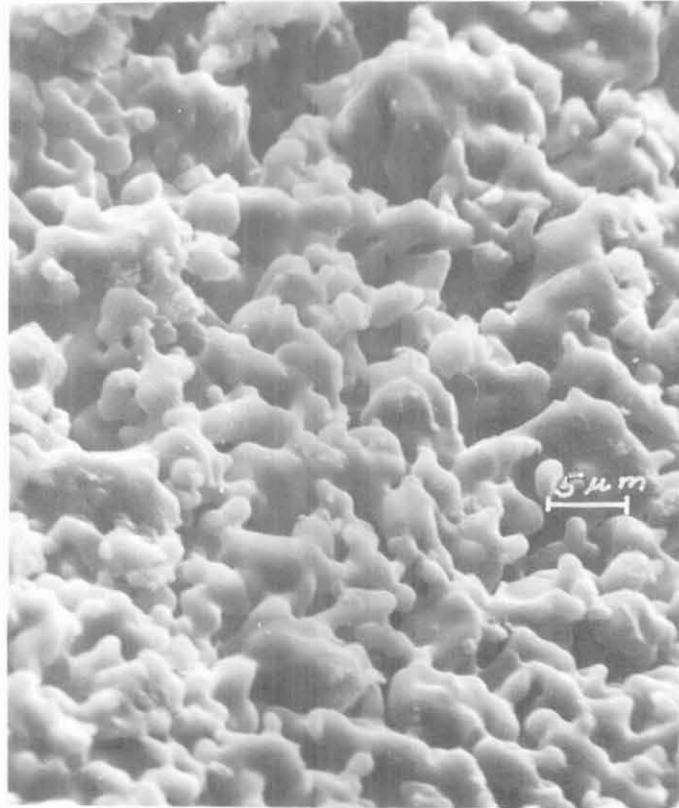


Fig. 27 Microstructure of $\text{Ca}_5(\text{PO}_4)_3(\text{OH})$ -stabilized C_2S , sample P-1.5.

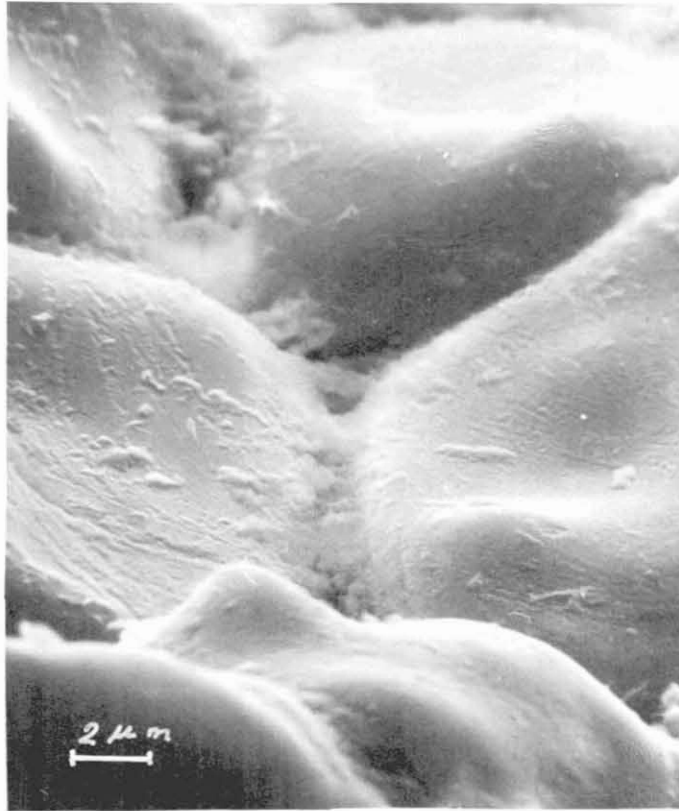


Fig. 28 Microstructure of BaSO₄ doped C₂S, sample NA-1.

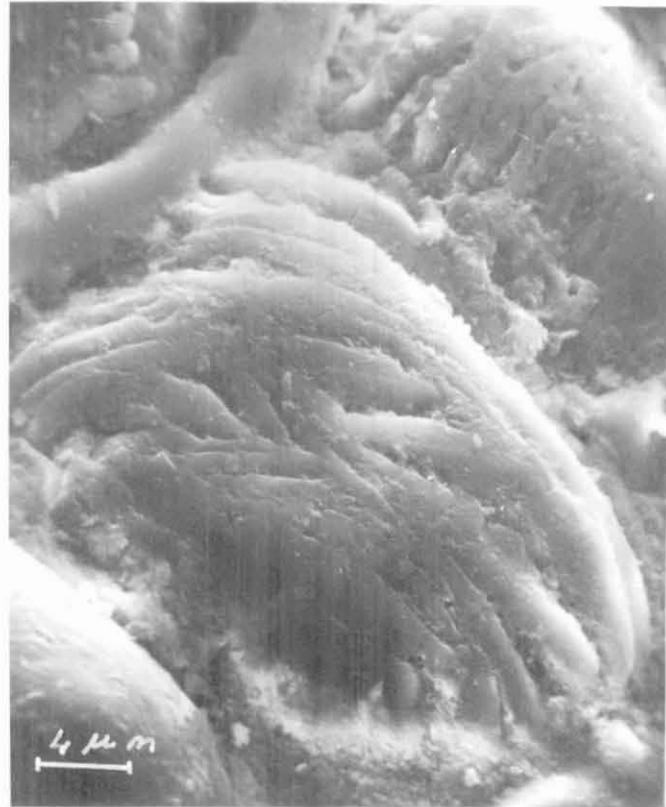


Fig. 29 Microstructure of BaSO₄ doped C₂S, sample B-16.

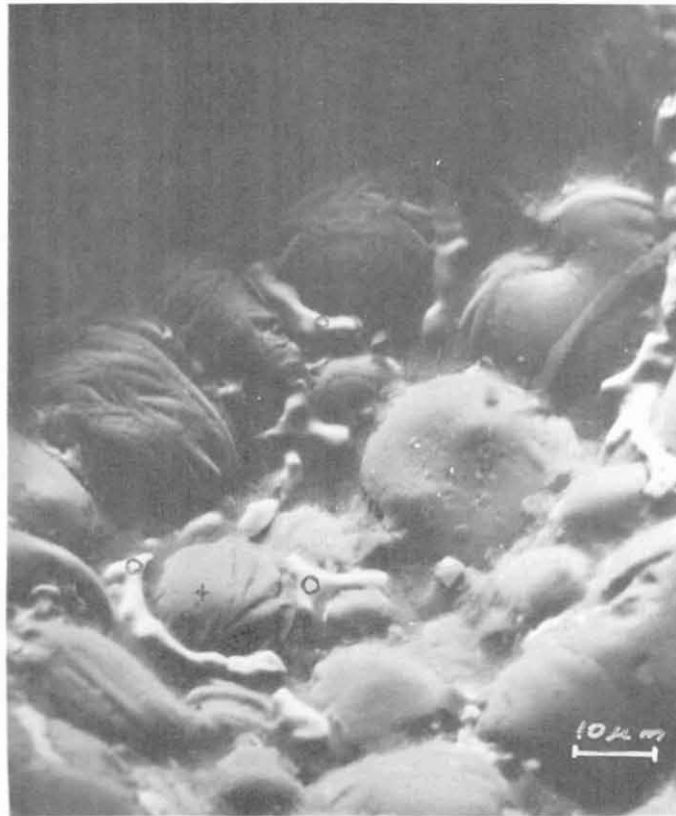


Fig. 30 Fracture surface of BaSO₄ doped belite clinker, sample B-16.

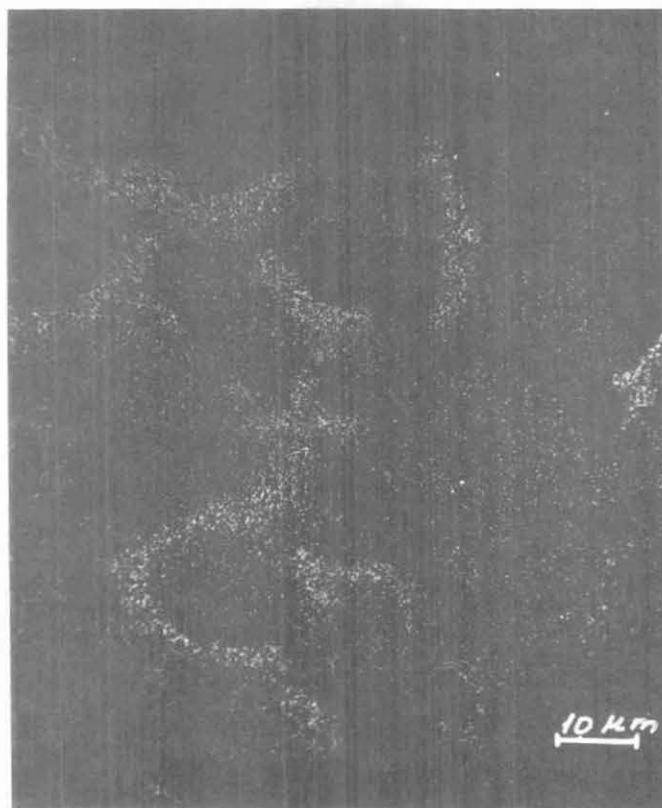


Fig. 31 Ba distribution in BaSO₄ doped belite clinker
(same area as in Fig. 30).

D. CONCLUSIONS

The compounds BaSO_4 , $\text{Ca}_5(\text{PO}_4)_3(\text{OH})$ and V_2O_5 stabilize the β -, α' and/or α -modification of C_2S depending on the quantities added to the raw mix. The stabilization of α -polymorph necessitates the largest addition of the stabilizers and has therefore not been included in the present study.

The crystal growth of C_2S is affected differently by various kinds of stabilizers. While C_2S stabilized by V_2O_5 has larger grains (approx. $50\mu\text{m}$) than BaSO_4 -stabilized C_2S with grain size of $20\text{--}30\mu\text{m}$, the smallest grains ($5\text{--}15\mu\text{m}$) are those of C_2S doped with $\text{Ca}_5(\text{PO}_4)_3(\text{OH})$. During the first month of hydration α' - C_2S demonstrates a more rapid strength development than β - C_2S . Test results obtained on pastes indicate that at later hydration periods β -polymorph attains higher strengths than α' -modification. This has yet to be confirmed on mortars, so relevant investigations are in progress.

The development of strength is influenced differently by various stabilizers. In phosphate-stabilized belites strengths develop very slowly in the first month of hydration and their values are lower than for BaSO_4 doped belites.

If BaSO_4 serves as a stabilizer there will be more Ba atoms than SO_4 groups incorporated in the belite solid solution. During the incorporation BaSO_4 decomposes and some sulphates evaporate from the system as SO_3 . Belite clinkers containing up to 35% alite and BaSO_4 addition attain better strengths than those of a similar composition but without BaSO_4 . With an increased percentage of BaSO_4 in the raw mix the prepared clinker will have a smaller alite content, no free lime and a higher content of belite with CaO in excess of the quantity required for C_2S . This has been determined on a clinker prepared from indigenous raw materials with BaSO_4 added as the stabilizer. When there is BaSO_4 in excess it distributes in the belite clinker as follows: one part into the silicate phase, one part remains unreacted and the balance goes into the interstitial phase, including glass. There was no incorporation of BaSO_4 in the aluminate phase. In addition to being a stabilizer BaSO_4 also acts as a mineralizer, which can be deduced from the fact that BaCO_3 does not stabilize the α' and β -modifications of C_2S under the same conditions as BaSO_4 (1450°C for 90 minutes).

The polymorphous modifications of C_2S were examined by optical microscopy in reflected light, applying a modified method which consists of the observation of characteristic marks visible in the crystal after polymorphous transformations of C_2S . Every polymorph leaves typical marks after being etched with 1% HNO_3 alcohol solution and the layer of reaction products removed.

The DTA method has provided additional data that stabilizers can lower the temperatures of the $\alpha'_H \rightarrow \alpha - C_2S$ phase transition even by $200^\circ C$ depending on the quantity added. The thermal effects of $\alpha'_H \rightarrow \alpha - C_2S$ conversion in samples with higher levels of stabilizer are much broader, indicating that the stabilizer was not homogeneously distributed in the C_2S solid solution.

2. HYDRATION PROCESS ACCELERATED BY CARBONATION

Materials

$C_6H_{10}O_5$ diethyl pyrocarbonate (ethoxyformic anhydride)
density 1.12 g/cm^3 , Bayer A.G., Leverkusen, West
Germany

Cement P-1 (Tables 16 and 17).

Preparation of specimens

Cement pastes (w/c wt. ratio = 0.33 with various quantities of $C_6H_{10}O_5$ admixture) were mixed by hand and compacted for two minutes in $1 \times 1 \times 4 \text{ cm}$ molds on a vibrating table (3000 vibrations per minute, range of vibration $0.75 + 0.1 \text{ mm}$).

The mortar was prepared by mixing cement and graded sand (1:3) with the corresponding amount of water and $C_6H_{10}O_5$ added subsequently. All the components were mixed by hand for three minutes, then cast into molds and vibrated. After 24-hour storage at $20^\circ C \pm 2^\circ C$ at a relative humidity greater than 90%, the forms were removed and the specimens were stored in water at the same temperature until the time of testing. All tests were repeated three times to obtain mean values.

Table 16. Chemical and phase analyses of cements with limestone addition (control samples)

Component (wt.%)	C - 1	D - 1	P - 1
SiO ₂	20.52	21.19	20.94
Al ₂ O ₃	4.92	5.49	5.17
Fe ₂ O ₃	1.84	2.30	2.62
CaO	62.28	61.99	63.25
MgO	2.51	1.81	1.78
SO ₃	3.24	2.54	3.00
Na ₂ O	0.46	0.42	0.33
K ₂ O	0.80	0.75	0.79
Insol.	1.57	0.40	0.25
Loss on ign.	1.04	1.69	1.01
Free CaO	0.28	0.57	0.25
MnO ₂	(n.d.)	0.33	n.d.
Balance	0.54	0.52	0.63

	Calculated (Bogue)				XD			
	C ₃ S	C ₂ S	C ₃ A	C ₄ AF	C ₃ S	C ₂ S	C ₃ A	C ₄ AF
C - 1	53.8	18.2	9.9	5.6	58	18	6	3
P - 1	51.3	21.3	9.3	7.9				

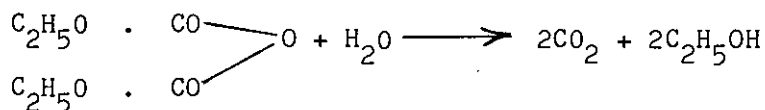
(n.d.) not determined

Table 17. Cements with limestone addition: Physical and chemical properties

SAMPLE	TYPE OF CEMENT	DENSITY (g/cm ³)	SPECIFIC SURFACE (cm ² /g)	CONSIS- TENCY IN (%)	SETTING TIME		LOSS ON IGNITION (%)	SO ₃ (%)
					INITIAL (HRS, MIN)	FINAL (HRS, MIN)		
C-1	CONTROL SAMPLE	3.08	3310	28.4	3.35	4.10	1.04	3.24
C-2	CEMENT + 5% LIMESTONE (5800 cm ² /g)	3.07	3560	27.0	2.40	3.20	3.10	3.14
C-3	CEMENT + 10% LIMESTONE (5800 cm ² /g)	3.04	3870	26.2	2.15	3.00	5.37	3.02
C-4	CEMENT + 5% LIMESTONE (9000 cm ² /g)	3.07	3620	27.0	2.50	3.30	3.06	3.32
C-5	CEMENT + 10% LIMESTONE (9000 cm ² /g)	3.04	3920	25.9	2.25	3.05	5.03	3.12
D-1	CONTROL SAMPLE	3.08	3525	24.3	2.20	3.15	1.69	2.54
D-2	CEMENT + 5% LIMESTONE (5800 cm ² /g)	3.07	3850	24.6	2.40	3.07	3.75	2.41
D-3	CEMENT + 10% LIMESTONE (5800 cm ² /g)	3.02	3810	25.3	2.25	3.53	5.81	2.17
D-4	CEMENT + 5% LIMESTONE (9000 cm ² /g)	3.07	3840	24.8	2.25	3.15	-	-
D-5	CEMENT + 10% LIMESTONE (9000 cm ² /g)	3.02	3960	26.7	2.05	3.20	-	-
P-1	PURE CEMENT (CLINKER + GYPSUM)	3.05	3410	24.6	2.25	3.25	1.01	3.00
P-2	CEMENT + 5% LIMESTONE	3.08	3620	24.2	2.50	3.40	3.12	2.85
P-3	CEMENT + 10% LIMESTONE	3.01	3780	23.8	2.45	3.35	5.13	2.70

Results

Diethyl pyrocarbonate is a stable liquid at low temperatures (4°C) and suitable for storage. When added to a mixture of cement, sand or gravel and water it decomposes, releasing CO₂ as follows:



The CO₂ released in the process of cement hydration was expected to react with Ca(OH)₂ and C-S-H gel thus accelerating the hydration process, whereas ethyl alcohol would evaporate without affecting the process of hydration.

Experiments on cement pastes with different quantities of C₆H₁₀O₅ and water were made to determine the optimal amount of the admixture. Contrary to expectations, the strength was lower in the majority of cases, probably because CO₂ formed too early and there was also an unexpected effect of the ethyl alcohol. The strength increased only in some instances when the water: C₆H₁₀O₅ wt. ratio was approximately 20:1. The results obtained on pastes were checked on three series of mortars prepared with different additions of C₆H₁₀O₅, and on a control sample without admixture.

The mix proportion of the mortars was defined by the water: cement (w/c) and water: C₆H₁₀O₅ (w/a) weight ratios:

<u>Sample</u>	<u>w/c</u>	<u>w/a</u>
control	0.48	-
1	0.49	34.2
2	0.48	16.9
3	0.46	11.3

Compressive strengths are graphically presented in Figure 32.

No further investigations on the carbonation of cement with C₆H₁₀O₅ are envisaged because of the negligible improvement of strengths in all the cases.

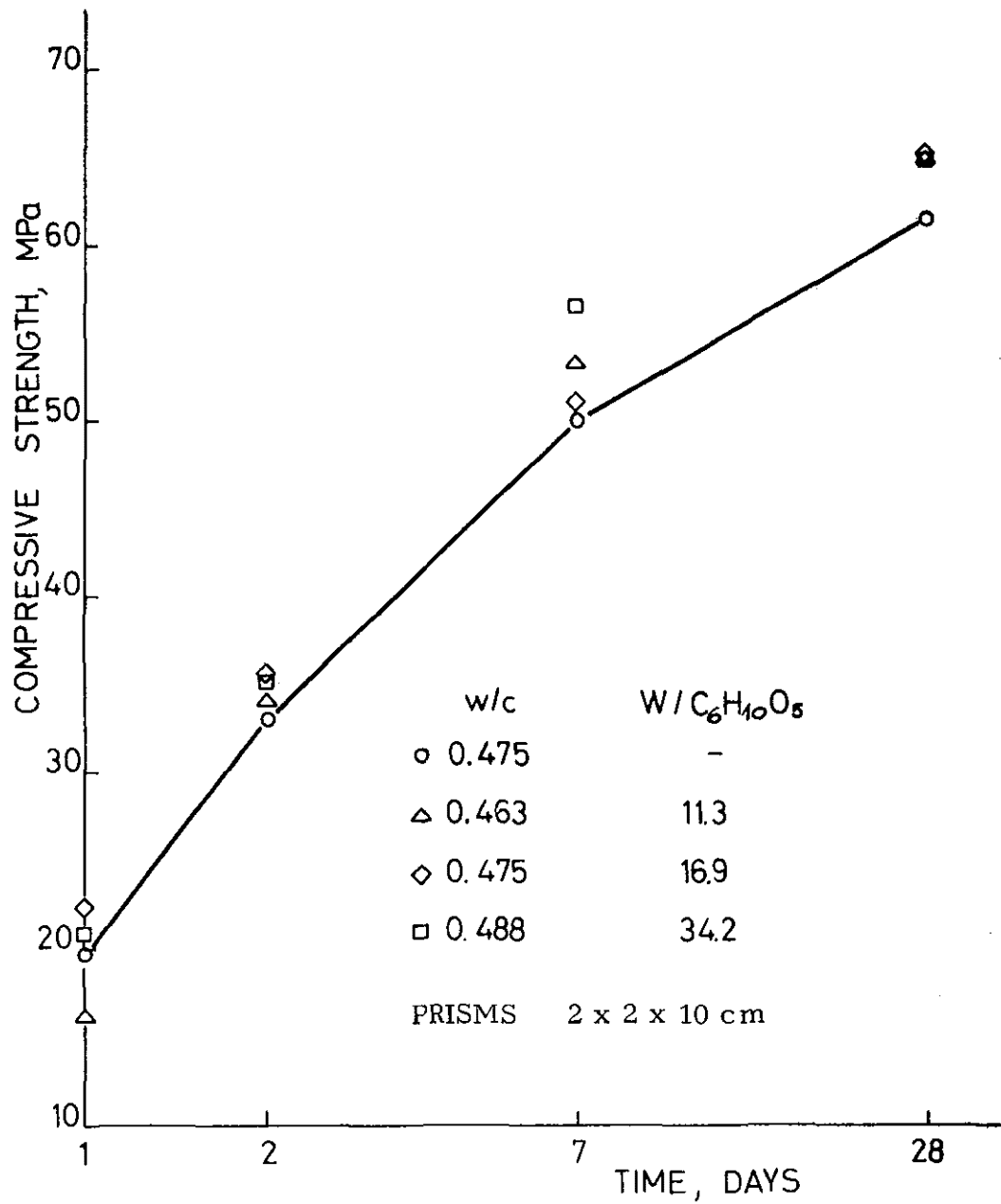


Figure 32. Portland cement with $C_6H_{10}O_5$ admixtures. Compressive strength of mortar specimens.

3. CEMENT WITH LIMESTONE

A. LITERATURE SURVEY

As early as 1938, Bessey (29) suggested that CaCO_3 probably reacts with C_3A to form calcium carboaluminates. Recent investigators, like Seligman and Greening (30), Feldman, Ramachandran and Sereda (31), and Spohn and Lieber (32) support the idea that calcium carbonate added to cement influences the hydration of C_3A and C_4AF leading to the formation of calcium carboaluminates ($\text{C}_3\text{A} \cdot \text{CaCO}_3 \cdot 10-11\text{H}_2\text{O}$). Lea (33) reports that limestone or marl interground with cement clinker can have variable effects. Some hard limestones and marls ground with certain clinkers to substitute 10% of the clinker do not reduce the strength of concrete at a constant slump. In other cases a small substitution of approximately 2% limestone increases the final strength, most likely because limestone acts as a grinding aid.

Soroka and Stern (34) and Soroka and Setter (35) investigated the effects that the content and fineness of fillers can have on the development of strengths in mortars prepared from cement at a constant ratio with the sand reduced for the quantity of added calcium carbonate or other filler. They found that the final strength increased both with the content and fineness of the filler and ascribed this to accelerated cement hydration and higher density of the mix with fillers. According to these authors, the accelerating effects of limestone may partly be attributed to the formation of crystal nuclei, which stimulate the $\text{Ca}(\text{OH})_2$ crystallization. With very finely ground limestone as filler (specific surface of $10,300 \text{ cm}^2/\text{g}$ monocalcium carbonate formed as well but did not effect the strength development.

Bobrowski, Wilson and Daugherty (36) substituted a part of gypsum by limestone and investigated the system consisting of 2% gypsum, 6% limestone and 92% clinker. The hydration reaction began with the formation of $\text{C}_3\text{A} \cdot \text{CaCO}_3 \cdot 12\text{H}_2\text{O}$, but afterwards the product stabilized into $\text{C}_3\text{A} \cdot x\text{CaCO}_3 \cdot 11\text{H}_2\text{O}$ where $x = 0.5 \rightarrow 0.25$. Gypsum disappeared in the course of hydration and calcium sulfoaluminate formed. A partial substitution of limestone for gypsum would reduce the false set of cement and lower the production costs, but also decrease the mortar strengths generally and the early concrete strength in particular.

B. EXPERIMENTAL DATA

Materials

Blended cements were prepared from two Yugoslav commercial Portland cements. Cement C-1 used as a control sample was pure cement clinker ground with approximately 5% gypsum, while cement D-1 was a control sample which contained an additional 13% of blast furnace slag.

The clinker for cements ground with limestone (cements P-1 to P-3) came from the same factory as cement D-1. Chemical and phase analyses of the control samples (C-1, D-1 and P-1) are presented in Table 16 and their particle size distributions in Figures 33 and 34.

Limestone consisting of 97.7% CaCO_3 was ground in a laboratory mill to a specific surface of $5800 \text{ cm}^2/\text{g}$ and $9000 \text{ cm}^2/\text{g}$ respectively and used for the preparation of C- and D-series of blended cements. The particle size distribution for the limestone is presented in Figure 35.

The mortar mix was prepared with graded standard sand (2.00 - 0.09 mm) containing not less than 96% SiO_2 as specified by the Yugoslav standard.

The concrete aggregate was river gravel (approximately 95% limestone) of 32 mm maximum grain size graded down according to Fuller's curve. The bulk density of the aggregate was 2.65 g/cm^3 .

Preparation of specimens

Blended cements were prepared by mixing Portland cement and ground limestone in a rotating homogenizer for five hours. There were two series C- and D- with five combinations each:

C-1 and D-1: pure cement (control samples)

C-2, D-2, C-3 and D-3: cements with additions of 5 and 10% of limestone ground to a specific surface of $5800 \text{ cm}^2/\text{g}$.

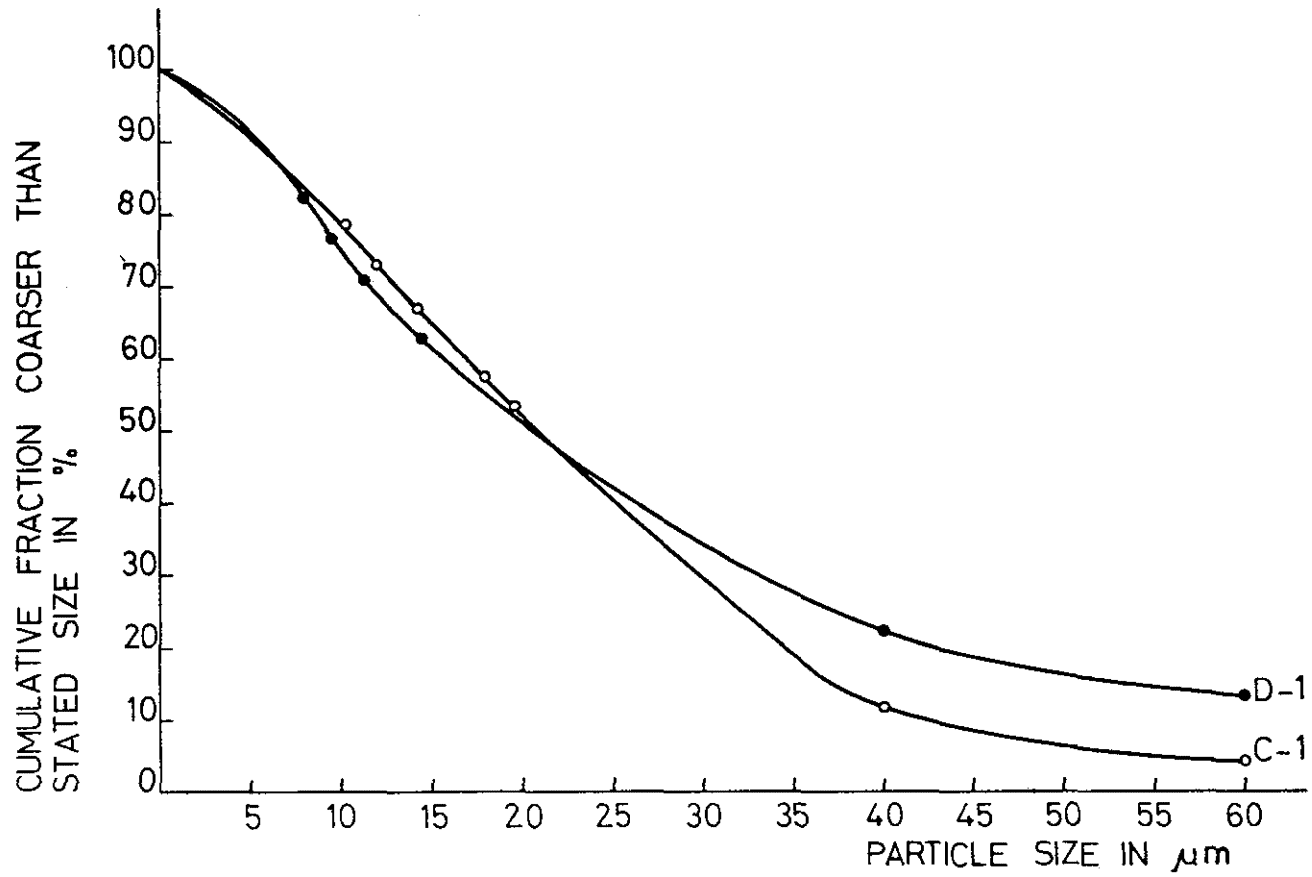


Figure 33. Particle size distribution of cements (control samples C-1 and D-1)

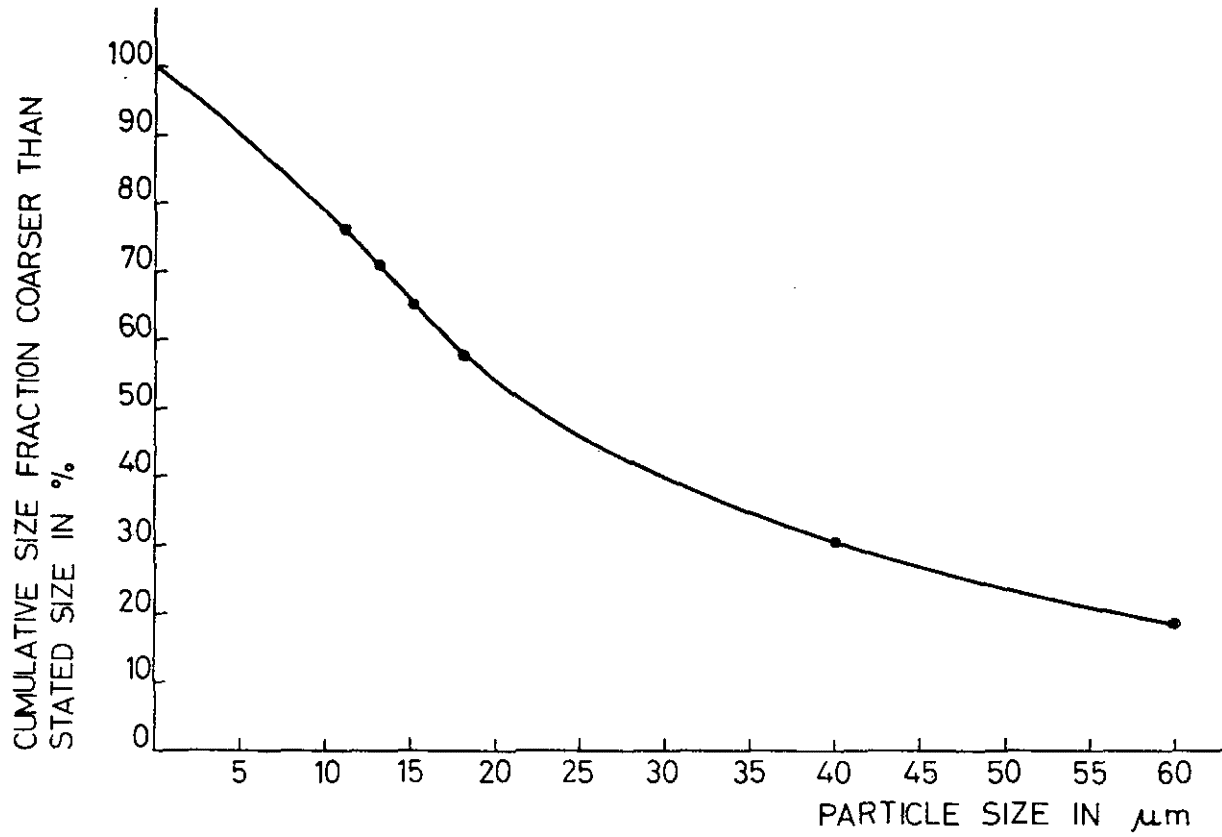


Figure 34. Particle size distribution of cement (control sample P-1)

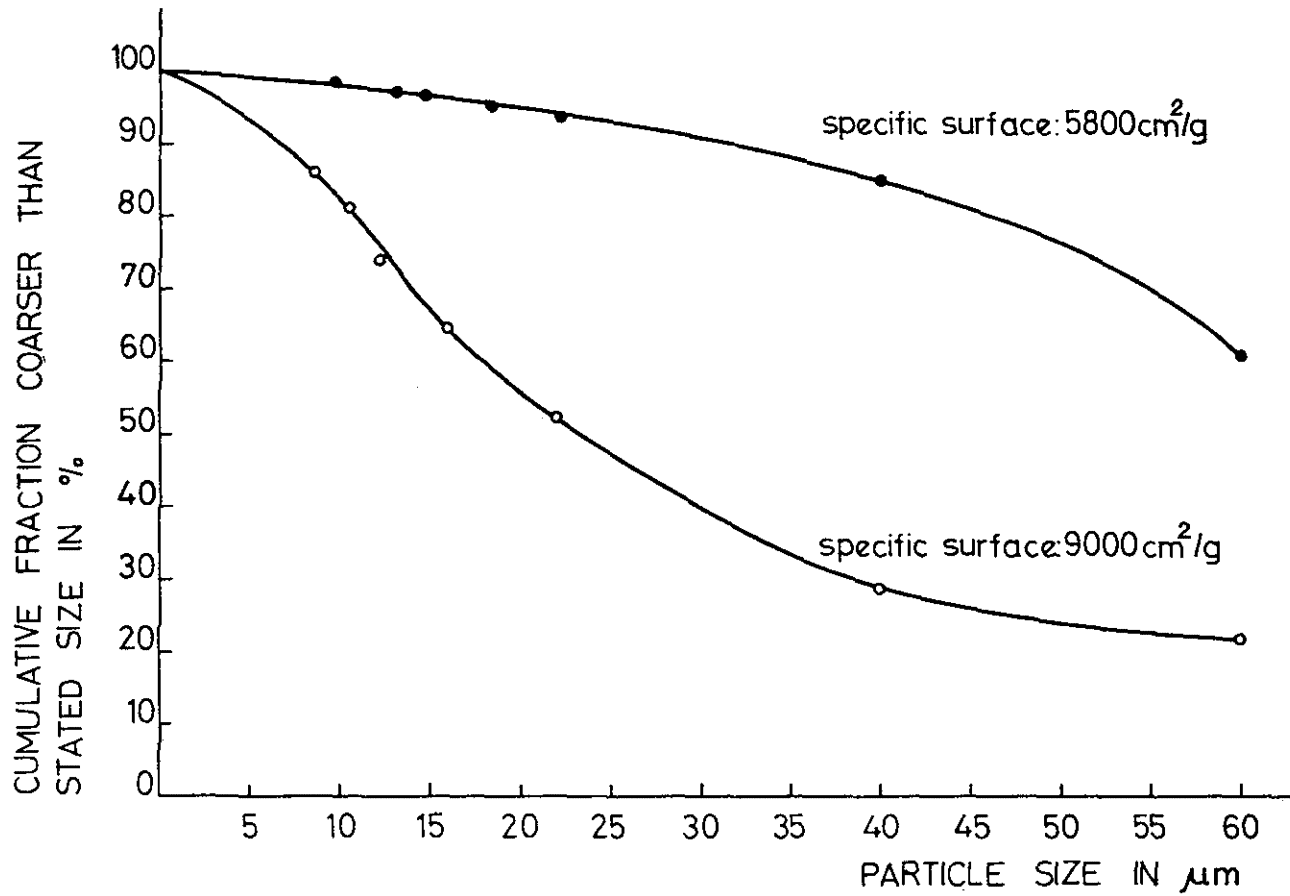


Figure 35. Particle size distribution of limestone

C-4, D-4, C-5 and D-5: cements with additions of 5 and 10% of limestone ground to a specific surface of $9000 \text{ cm}^2/\text{g}$.

The interground cements were mixtures of Portland cement clinker, limestone and gypsum ground in a ball mill for one hour. There were three combinations:

P-1: control sample (95% clinker + 5% gypsum)

P-2: cement with 5% limestone (90% clinker + 5% limestone + 5% gypsum)

P-3: cement with 10% limestone (85% clinker + 10% limestone + 5% gypsum).

Particle size distributions for cement P-2 and P-3 are presented in Figures 36 and 37. Strengths were tested on mortar specimens prepared in compliance with the Yugoslav standard (based on the RILEM-CEMBUREAU method and ISO Recommendation 679). The mix ratio was cement:graded sand 1:3 by weight and the w/c ratio constant at 0.5. The mortar was mixed mechanically and compacted for two minutes in $4 \times 4 \times 16 \text{ cm}$ molds on a vibrating table (3000 vibrations per minute, range of vibration $0.75 \pm 0.1 \text{ mm}$).

Concrete specimens for strength testing contained $300 \text{ kg}/\text{m}^3$ of cement, the workability of the concrete being constant - (constant Abrams slump test). The concrete was mixed in a laboratory mixer (0.1 m^3) and compacted in $12 \times 12 \times 36 \text{ cm}$ molds by a vibrating rod (25 mm diameter with 3000 vibrations per minute).

After conditioning for 24 hours, at $20 \pm 2^\circ\text{C}$ and a minimum relative humidity of 90%, the molds were removed and the mortar specimens stored in water at the same temperature ($20 \pm 2^\circ\text{C}$) for future testing. The concrete prisms were kept in an air conditioned room at $20 \pm 2^\circ\text{C}$ with a relative humidity of 95%.

Specimens for measurement of drying shrinkage were kept in an air-conditioned room at $20 \pm 2^\circ\text{C}$ and 60% relative humidity.

Investigation methods

The specific surface of cements was measured by the air premeability method (Blaine).

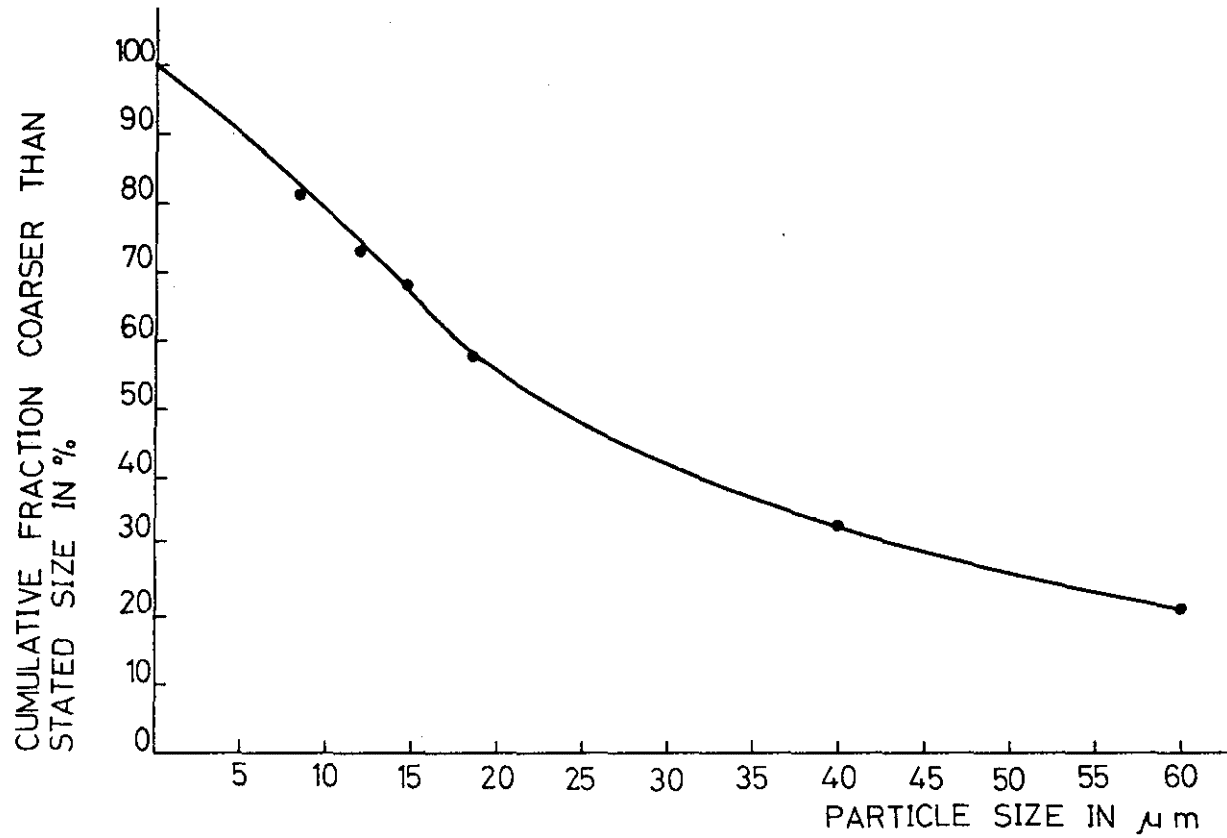


Figure 36. Cement with limestone addition: Particle size distribution in sample P-2

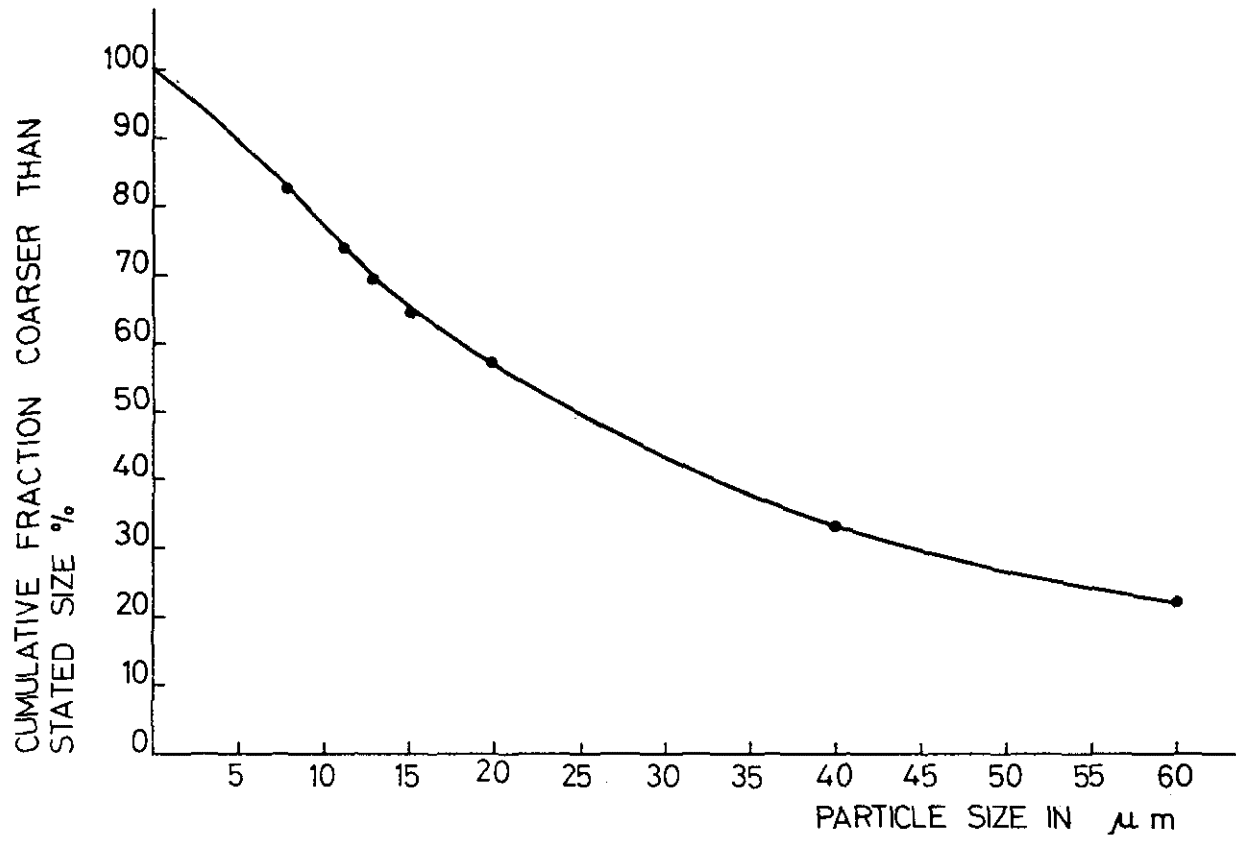


Figure 37. Cement with limestone addition: Particle size distribution in sample P-3

Water required for standard consistency of cement paste was determined by a flat-ended Vicat plunger (penetration to 5-7 mm from the bottom of the Vicat conical ring filled with paste).

The setting time (initial and final) was determined by the Vicat needle on cement paste of standard consistency. Drying shrinkage on mortar specimens was measured after a 24-hour conditioning in molds and two days in water. For additional testing the prisms were kept in an air-conditioned place at $20 \pm 2^{\circ}\text{C}$ with relative humidity of 60%.

The drying shrinkage of concrete was measured one day after the removal from the molds; the specimens then being air-cured under the same conditions as mortar prisms. The change in length was measured at regular intervals, both on mortar and concrete samples, till three months of aging.

The workability of the concrete (consistency) was determined by three various tests: the Abrams slump test, the Swedish Vebe test and the flow test (DIN 1048).

The air content in fresh concrete was determined by the pressure method (ASTM C 231-68).

Compressive strengths of mortars and concretes were obtained on 6 prisms at 1 (in some cases only), 3, 7 and 28 days and the flexural strength on 3 specimens after 3, 7 and 28 days of aging.

C. RESULTS AND DISCUSSION

Physical and chemical properties of tested cements are presented in Table 17. Since the ignition loss is limited to 5% by the Yugoslav standard, cements with 10% limestone can theoretically have a loss on ignition close to this value. However, they will not satisfy this requirement if the cement itself has a slightly higher loss on ignition (e.g., mixed cements C-3, C-5, D-3 and D-5 and interground cement P-3).

Mechanical properties (mortar tests) are presented in Table 18. Compared to the control samples, there are no apparent differences in the compressive strength of cement mortars containing 5% limestone of either fineness. Specimens with 10% limestone display lower compressive strengths in most cases. The flexural strengths follow a similar trend. In comparison to control samples, interground cements have lower strengths (max. 19%) than mixed cements (max. 11%). The decrease is not significant and the tested samples actually satisfy the strength requirements of the Yugoslav standard for Portland cement class PC 450 (compressive strength 18.0 MPa after 3 days and 40.5 MPa after 28 days of aging).

The drying shrinkage of mortars is shown in Figure 38 to 40. Shrinkage started immediately upon drying and increased faster in samples containing limestone, but at the age of three months the relative difference between the shrinkage of cement mortars with limestone and that of the control samples was smaller than at earlier ages. The shrinkage values for cements with limestone are not substantially different from those obtained on other Yugoslav cement mortars.

The mix proportion and properties of concretes are presented in Tables 19 to 21. No regularity was observed either in the increase or the decrease of strengths in concrete specimens containing cements with limestone when compared with control samples (cements without limestone).

Table 18. Cements with limestone addition: Mechanical properties (mortar test)

SAMPLE	TYPE OF CEMENT	FLEXURAL STRENGTH (MPa)				COMPRESSIVE STRENGTH (MPa)			
		1 DAY	3 DAYS	7 DAYS	28 DAYS	1 DAY	3 DAYS	7 DAYS	28 DAYS
C-1	CEMENT	-	6.3	7.3	8.9	-	35.9	41.4	51.2
C-2	CEMENT+5% LIMESTONE (5800 cm ² /g)	-	6.4	7.2	8.7	-	33.4	42.6	48.6
C-3	CEMENT+10% LIMESTONE (5800 cm ² /g)	-	5.8	7.2	8.3	-	32.8	39.0	46.8
C-4	CEMENT+5% LIMESTONE (9000 cm ² /g)	-	6.2	7.3	8.8	-	33.6	40.7	50.8
C-5	CEMENT+10% LIMESTONE (9000 cm ² /g)	-	6.0	7.0	8.4	-	32.0	38.3	48.3
D-1	CEMENT	3.4	5.2	7.0	8.2	13.6	28.8	39.5	47.5
D-2	CEMENT+5% LIMESTONE (5800 cm ² /g)	3.9	5.5	7.0	8.0	14.2	29.8	38.3	48.9
D-3	CEMENT+10% LIMESTONE (5800 cm ² /g)	3.5	5.7	6.7	7.8	12.4	27.8	37.0	46.5
D-4	CEMENT+5% LIMESTONE (9000 cm ² /g)	3.8	5.7	7.2	8.0	13.0	29.0	40.4	49.8
D-5	CEMENT+10% LIMESTONE (9000 cm ² /g)	3.6	5.7	6.5	7.9	13.2	28.0	36.2	45.8
P-1	PURE CEMENT (CLINKER + GYPSUM)	4.6	6.5	7.2	8.6	19.5	34.5	44.1	47.5
P-2	CEMENT+5% LIMESTONE	4.3	6.4	7.1	8.3	18.1	35.3	41.8	49.2
P-3	CEMENT+10% LIMESTONE	3.8	6.0	6.6	8.1	16.0	30.8	38.0	44.8

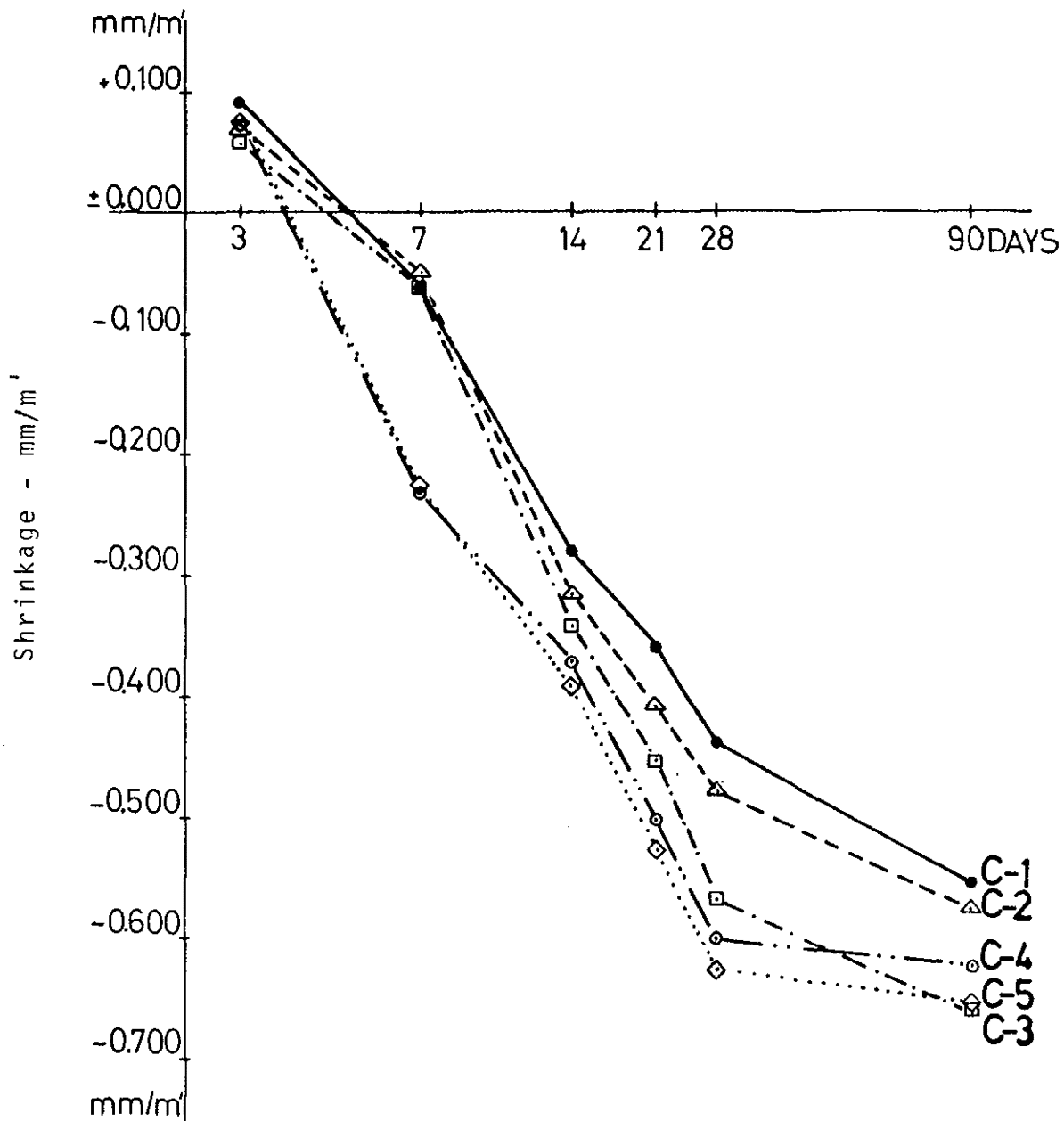


Figure 38. Cement with limestone addition.
 Shrinkage of mortar specimens.
 C-1 : cement
 C-2 : cement +5% limestone, 5800cm²/g
 C-3 : cement +10% limestone, 5800cm²/g
 C-4 : cement +5% limestone, 9000cm²/g
 C-5 : cement +10% limestone, 9000cm²/g

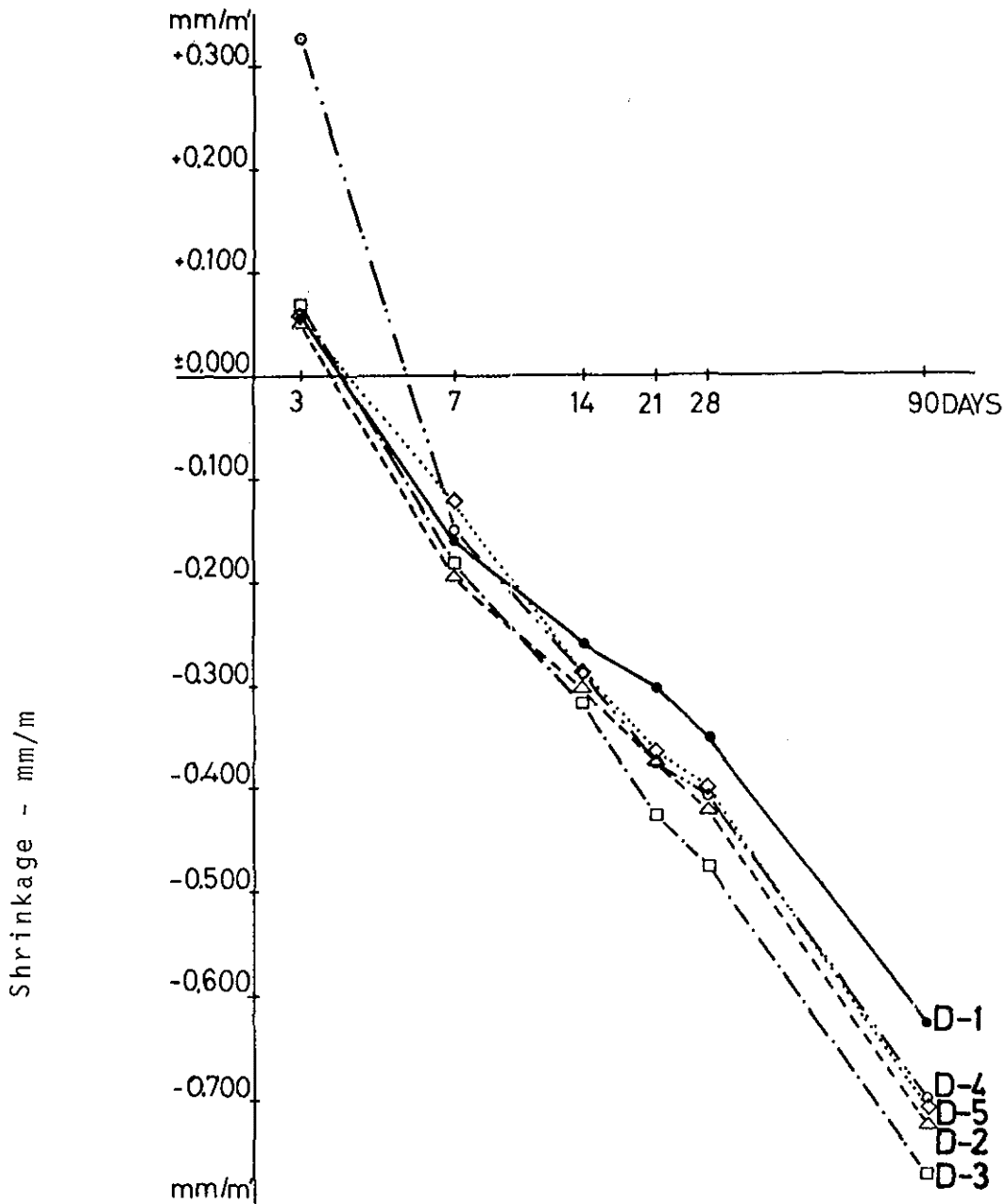


Figure 39. Cement with limestone addition.
 Shrinkage of mortar specimens.
 D1 : cement
 D2 : cement + 5% limestone
 D3 : cement + 10% limestone
 D4 : cement + 5% limestone
 D5 : cement + 10% limestone

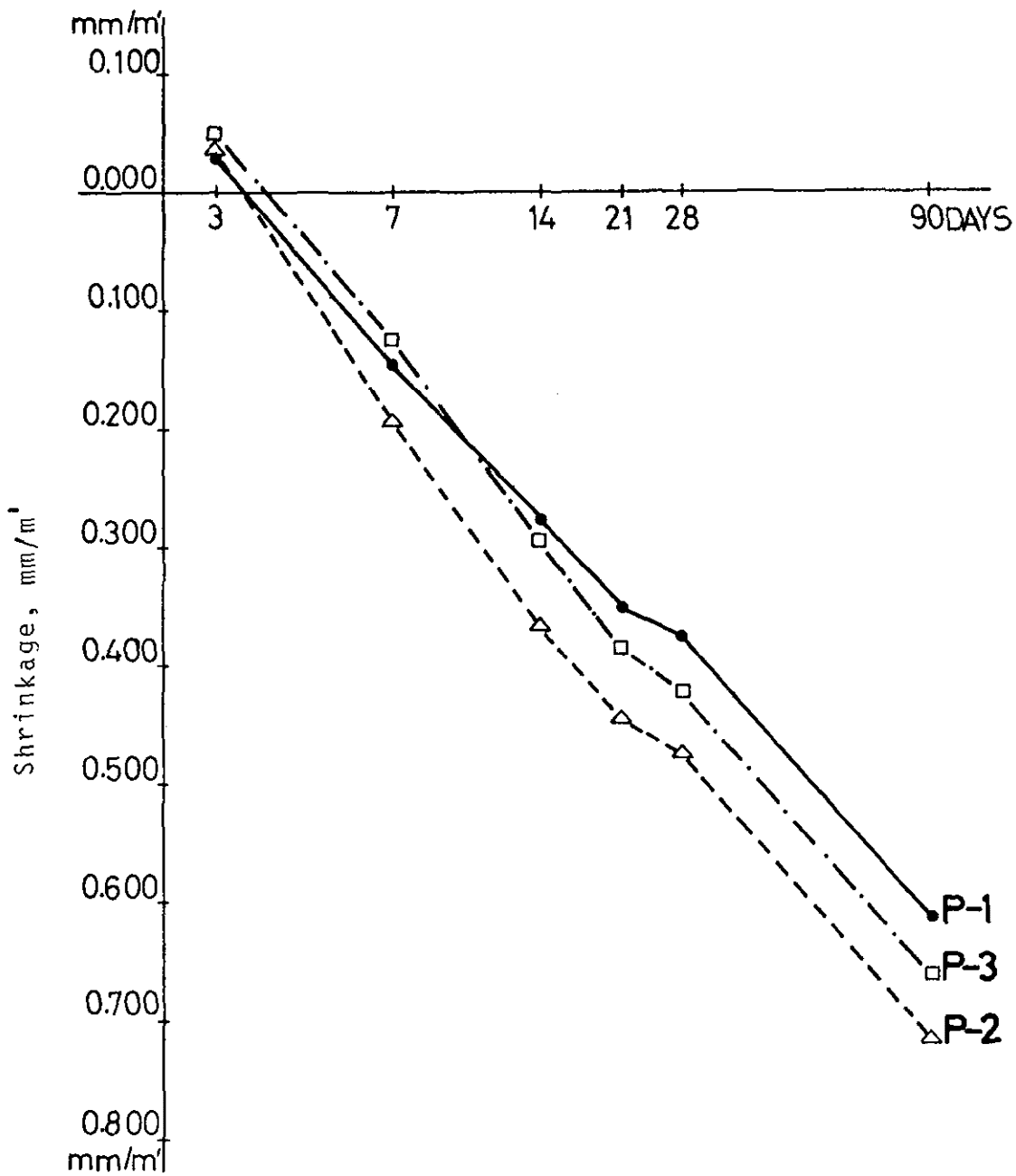


Figure 40. Cement with limestone addition.
 Shrinkage of mortar specimens.
 P-1 : Pure cement (clinker plus gypsum)
 P-2 : Cement + 5% limestone
 P-3 : Cement + 10% limestone

Table 19. Mix proportion and properties of concretes from cements with limestone addition

SAMPLE		C-1	C-2	C-3	C-4	C-5	
MIX PROPORTION	CEMENT (kg/m ³)	300	300	300	300	300	
	LIMESTONE CONTENT (%)		5	10	5	10	
	WATER : CEMENT	0.56	0.56	0.55	0.56	0.49	
	AGGREGATE (kg/m ³)	1939	1939	1931	1939	1978	
FRESH CONCRETE	CONSISTENCY ACCORDING TO	SLUMP (cm)	4	4	4.7	3.7	4.5
		VeBe (VB°)	3.8	3.5	3.0	4.5	3.5
		FLOW TEST (cm)	34	34	36	31	36
	AIR CONTENT (%)	1.9	1.7	1.7	2.6	3.1	
	BULK DENSITY (kg/dm ³)	2.43	2.40	2.36	2.36	2.35	
-HARDENED CONCRETE	COMPRESSIVE STRENGTH (MPa) AFTER DAYS	3	18.9	21.2	17.9	20.5	21.2
		7	23.6	24.7	19.4	22.0	21.7
		28	31.3	32.0	26.5	27.9	26.4
	FLEXURAL STRENGTH (MPa) AFTER DAYS	3	5.5	5.9	5.0	5.5	4.7
		7	6.5	6.4	5.9	5.2	5.1
		28	7.4	7.0	6.1	7.3	6.6

Table 20. Mix proportions and properties of concretes from cements with limestone addition

SAMPLE		D-1	D-2	D-3	D-4	D-5	
MIX PROPORTION	CEMENT (kg/m ³)	300	300	300	300	300	
	LIMESTONE CONTENT (%)	-	5	10	5	10	
	WATER : CEMENT	0.56	0.53	0.55	0.57	0.53	
	AGGREGATE (kg/m ³)	1926	1949	1929	1918	1945	
FRESH CONCRETE	CONSISTENCY ACCORDING TO	SLUMP (cm)	5	5	5	4.5	5
		VeBe (VB ^o)	3.3	2.3	2.4	2.5	2.6
		FLOW TEST (cm)	42	43	40	40	39
	AIR CONTENT (%)	1.8	1.9	1.7	1.9	2.8	
	BULK DENSITY (kg/dm ³)	2.39	2.37	2.35	2.37	2.36	
	HARDENED CONCRETE	COMPRESSIVE STRENGTH (MPa) AFTER DAYS	3	19.6	20.2	20.4	21.8
7			23.9	23.7	25.6	25.9	23.9
28			32.2	28.0	33.1	34.3	31.3
FLEXURAL STRENGTH (MPa) AFTER DAYS		3	4.3	4.8	5.2	5.1	4.3
		7	5.5	6.0	5.8	6.3	5.0
		28	6.7	7.1	7.4	7.0	6.6

Table 21. Mix proportions and properties of concretes from cements with limestone addition

SAMPLE		P - 1	P - 2	P - 3	
MIX PROPORTION	CEMENT (kg/m ³)	300	300	300	
	LIMESTONE CONTENT (%)	-	5	10	
	WATER : CEMENT	0.56	0.53	0.53	
	AGGREGATE (kg/m ³)	1924	1950	1944	
FRESH CONCRETE	CONSISTENCY ACCORDING TO	SLUMP (cm)	5	5	5
		V _e B _e (VB ^o)	3.3	2.3	2.8
		FLOW TEST (cm)	37	38	40
	AIR CONTENT (%)	1.9	2.6	2.5	
	BULK DENSITY (kg/dm ³)	2.41	2.39	2.36	
	HARDENED CONCRETE	COMPRESSIVE STRENGTH (MPa) AFTER DAYS	3	28.2	27.1
7			29.7	31.0	26.7
28			36.8	32.6	29.7
FLEXURAL STRENGTH (MPa) AFTER DAYS		3	5.8	5.0	5.0
		7	6.0	5.6	6.1
		28	6.7	6.8	7.5

The concrete shrinkage in samples with limestone increased proportionally to the content and fineness of the added limestone (Figs. 41 to 43). The relative difference in shrinkage between the control samples and the specimens prepared from cements with limestone additions were most noticeable at the age between one and two months, diminishing later so that the final results did not differ significantly from the values obtained on concretes prepared with other Yugoslav cements.

The results for both concrete and mortar specimens did not indicate that limestone acted as an accelerator of the hydration process.

D. CONCLUSIONS

The results of the investigation show that, as a rule, the addition of 10% limestone brings about lower strengths in cement mortars. A similar trend was not observed on concrete samples, but judging by the strength tests on mortars and concretes, it is obvious that limestone does not promote the development of strength.

Since intergrinding limestone with cement clinker can be advantageous to cement plants and the physical properties (consistency, setting time and shrinkage) of such interground cements are acceptable, there is no special objection to small additions of limestone (max. 5%). In such a case, however, the optimal content of gypsum must also be determined because limestone partially substitutes for gypsum and acts as a set regulator.

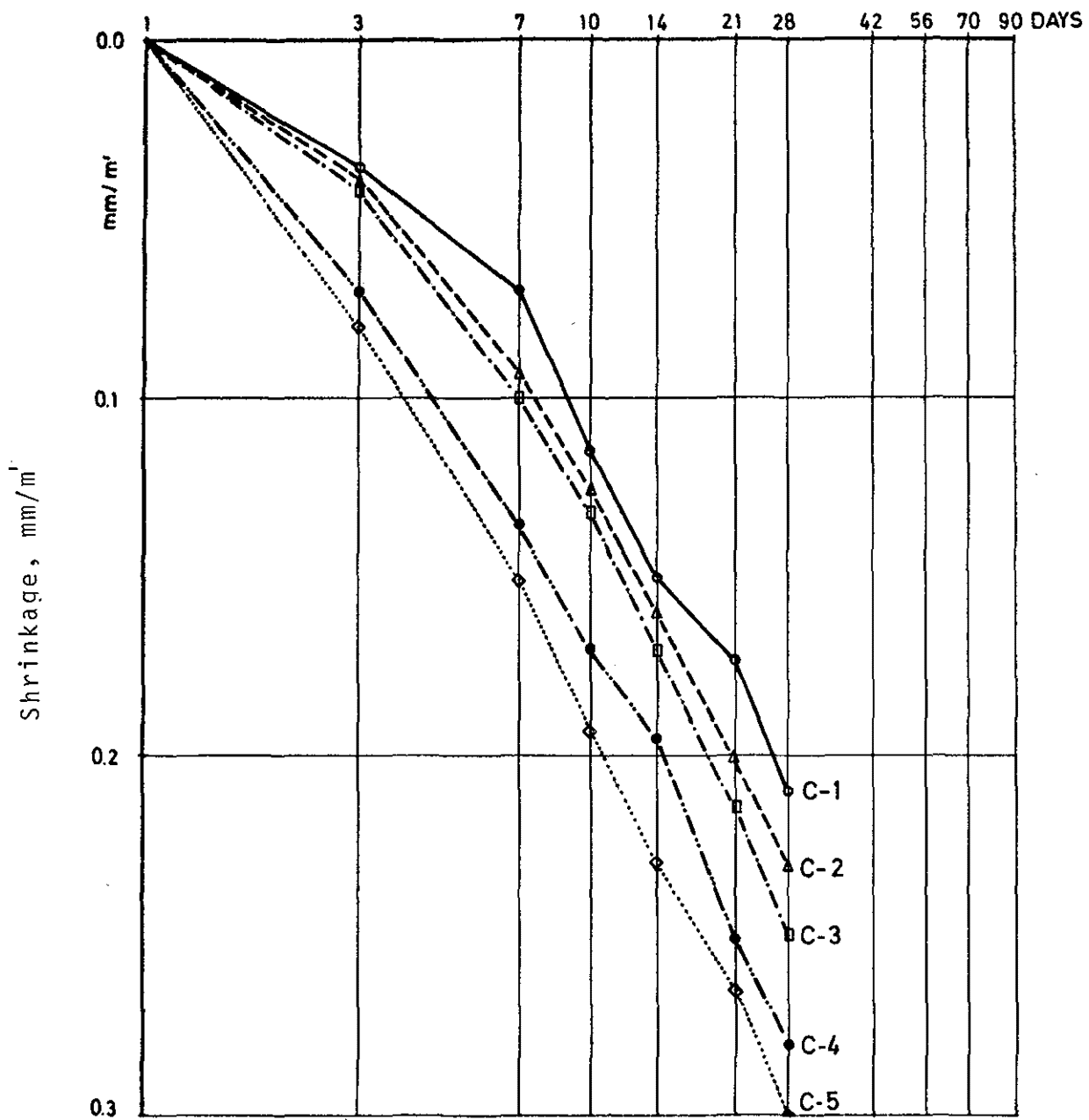


Figure 41. Cement with limestone addition.
 Shrinkage of concrete specimens.
 C-1 : cement
 C-2 : cement + 10% limestone, $5800 \text{ cm}^2/\text{g}$
 C-3 : cement + 5% limestone, $5800 \text{ cm}^2/\text{g}$
 C-4 : cement + 5% limestone, $9000^2/\text{g}$
 C-5 : cement + 10% limestone, $9000^2/\text{g}$

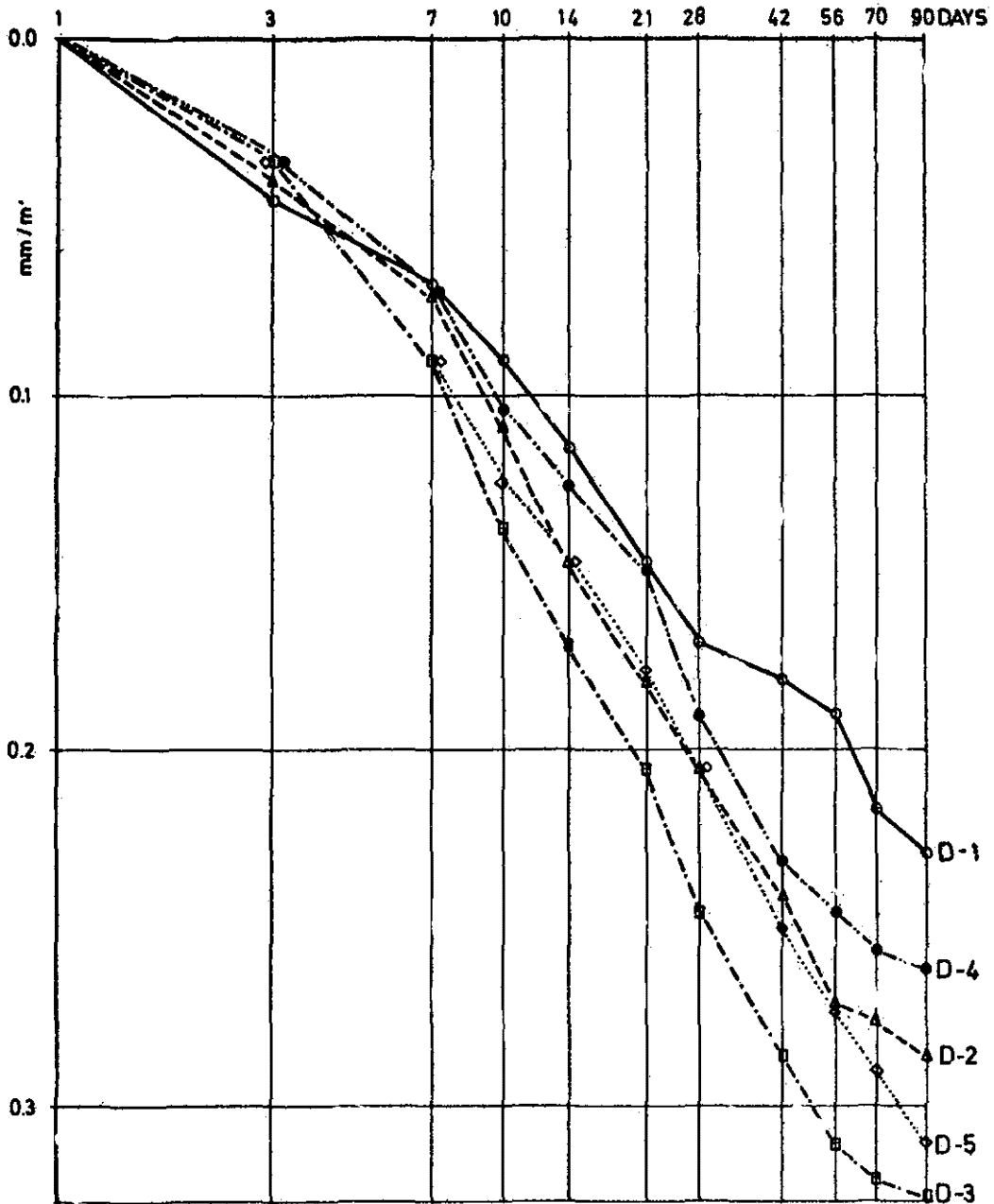


Figure 42. Cement with limestone addition. Shrinkage of concrete specimens.

- D - 1: control
- D - 2: 5% limestone; surface area - 5800 m²/g
- D - 3: 10% limestone; surface area - 5800 m²/g
- D - 4: 5% limestone; surface area - 9000 m²/g
- D - 5: 10% limestone; surface area - 9000 m²/g

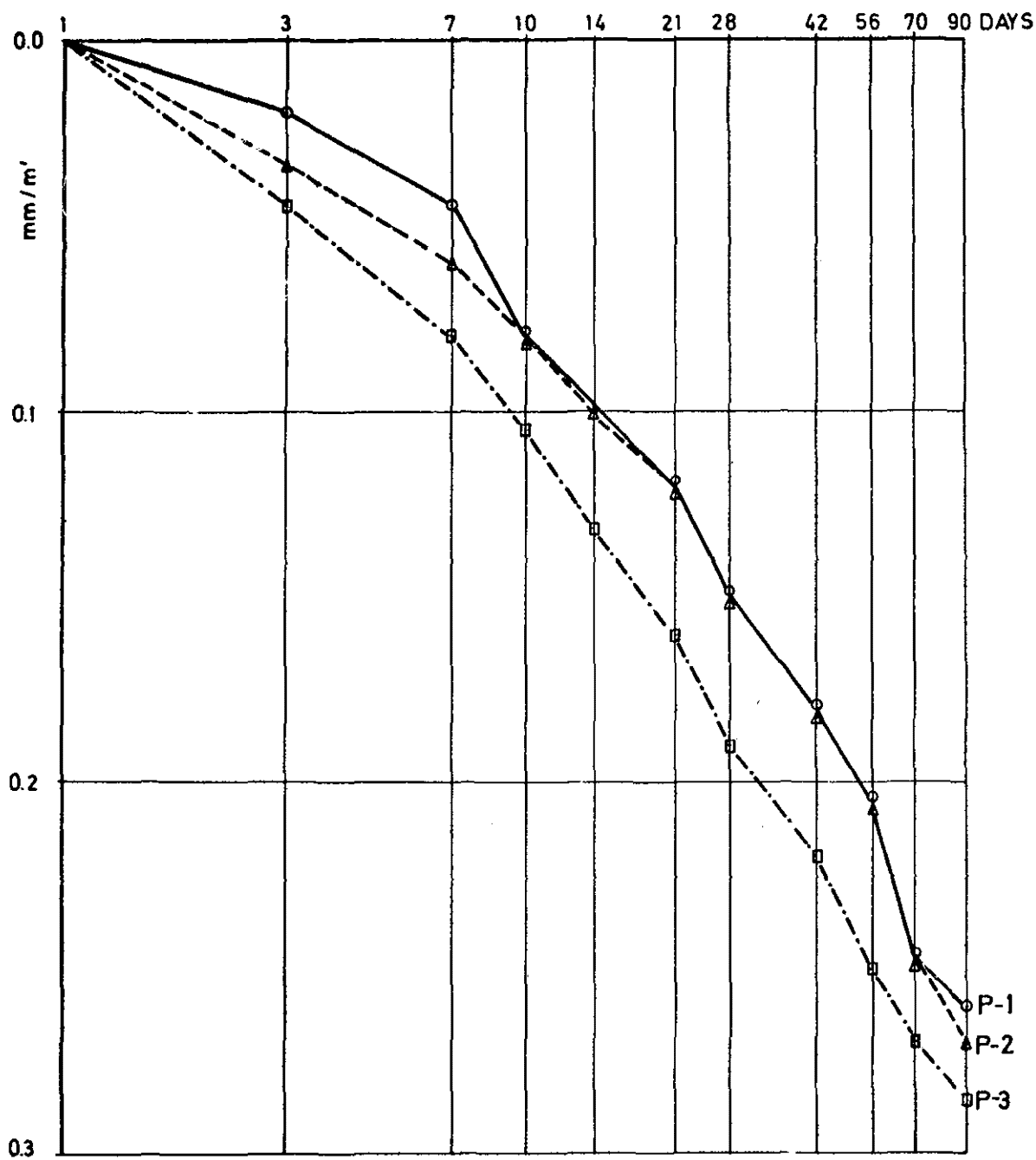


Figure 43. Cement with limestone addition. Shrinkage of concretes.

P-1: control (clinker plus gypsum)

P-2: 5% limestone

P-3: 10% limestone

III. SOREL CEMENT

A. LITERATURE SURVEY

MgO activity and paste composition

The reaction products in a $\text{MgO-MgCl}_2\text{-H}_2\text{O}$ system are Mg(OH)_2 , $\text{Mg}_3(\text{OH})_5\text{Cl}\cdot 4\text{H}_2\text{O}$ (phase 5) and $\text{Mg}_2(\text{OH})_3\text{Cl}\cdot 4\text{H}_2\text{O}$ (phase 3) depending on the molar ratios. Phase 5 is the predominant reaction product in hardened magnesium oxychloride cement with good mechanical properties. For this phase, the molar ratio of the initial mix must approach $\text{MgO}:\text{MgCl}_2:\text{H}_2\text{O} = 5:1:13$ with a slight excess of MgO and the amount of water as close as possible to the theoretical value required for formation of phase 5 and hydration of the excess MgO into Mg(OH)_2 . With reactants at such concentrations, the reaction products will be phase 5 and some Mg(OH)_2 . The reaction products in magnesium oxychloride pastes have recently been discussed (37) and the early reaction products are reported (37) to depend on the reactivity of MgO. This influences the reaction rate and products thus affecting the development of strengths as well.

The reactivity of MgO depends on the temperature of calcination. The required reaction products in the $\text{MgO-MgCl}_2\text{-H}_2\text{O}$ system can be reproduced only by using MgO of equal reactivity. Thus the initial mix for phase 5 and water in excess will give Mg(OH)_2 as the first reaction product if a very reactive MgO has been used although going by the phase diagram $\text{MgO-MgCl}_2\text{-H}_2\text{O}$ (38) a mixture of phase 5 and Mg(OH)_2 may be expected. To compare the actual reaction products with those expected according to the phase diagram, samples must be cured in closed containers to avoid water evaporation and phase transformation, brought about by CO_2 from the air.

The findings of this work provide additional information and explanation regarding the relationship between MgO properties and the observed reaction products.

Strength development in phases 5 and 3

The storing of the reaction samples in closed containers essentially simulates the curing conditions in the interior of cement mortars with attendant expectations of similarity of reaction products. Since Sorel cement is mostly used for

flooring and the applied magnesium oxychloride layers are thin with extensive surface areas exposed to atmospheric CO_2 and humidity, it is logical to study and examine air-cured samples. The samples tested in the present work were therefore air-cured and their surface to volume ratio was similar to that of floor layers made in Sorel cement and air-cured.

Sorel cement exposed to air for a long period of time and then temporarily to water will have phases that cannot form in a protected $\text{MgO-MgCl}_2\text{-H}_2\text{O}$ system. Among such phases are $\text{Mg}_2(\text{OH})\text{ClCO}_3\cdot 3\text{H}_2\text{O}$ and $\text{Mg}_5(\text{OH})_2(\text{CO}_3)_4\cdot 4\text{H}_2\text{O}$. It has been established that $\text{Mg}_2(\text{OH})\text{ClCO}_3\cdot 3\text{H}_2\text{O}$ transforms faster from phase 3 than from phase 5 if both phases are exposed to air under the same conditions (39,40). Basic magnesium carbonate $\text{Mg}_5(\text{OH})_2(\text{CO}_3)_4\cdot 4\text{H}_2\text{O}$ was found together with $\text{Mg}_2(\text{OH})\text{ClCO}_3\cdot 3\text{H}_2\text{O}$ in old hardened Sorel cements which had been exposed to atmospheric CO_2 and then temporarily to water (38,41,42). The reason for this is that $\text{Mg}_2(\text{OH})\text{ClCO}_3\cdot 3\text{H}_2\text{O}$ which is unstable in the presence of CO_2 and water, loses the chloride ion and transforms into a more basic hydroxocarbonate hydrate (43), $\text{Mg}_5(\text{OH})_2(\text{CO}_3)_4\cdot 4\text{H}_2\text{O}$.

The reaction products in air-cured samples of mixes containing water in excess of the theoretically required value for phases 5 and 3 have recently been reported (37). In the present study experiments were carried out on 5:1:13 and 3:1:11 mixes resulting in products corresponding exactly to phases 5 and 3.

Effectiveness of phosphates on the water resistance of hardened Sorel cement

Water resistance of magnesium oxychloride cements can be improved by various admixtures such as phosphoric acid, melamine and urea formaldehyde resin (44) or inorganic phosphates such as $\text{ZnHPO}_4\cdot \text{H}_2\text{O}$ and $\text{AlH}_3(\text{PO}_4)_2\cdot 3\text{H}_2\text{O}$ and phosphate waste products (45). It has been reported that the early strength is slightly lower when phosphate is added, but aging samples with phosphate have more constant strengths than those without admixtures.

Phosphates significantly ameliorate the water resistance of hardened Sorel cement. If stored in water, samples without phosphate disintegrate within 3 to 4 weeks, whereas samples with phosphate admixtures lose strength gradually.

The question still remains as to the various effects of soluble and insoluble phosphates on the water resistance of hardened Sorel cement. Two phosphates were tested: the soluble $\text{Ca}(\text{H}_2\text{PO}_4)_2 \cdot \text{H}_2\text{O}$ and the practically insoluble $\text{Ca}_5(\text{PO}_4)_3(\text{OH})$.

B. EXPERIMENTAL DATA

Materials

Reagent grade chemicals used for the preparation of pastes:

$\text{Mg}_5(\text{OH})_2(\text{CO}_3)_4 \cdot 4\text{H}_2\text{O}$, Kemika, Zagreb, Yugoslavia;
 $\text{MgCl}_2 \cdot 6\text{H}_2\text{O}$, E. Merck AG. Darmstadt, West Germany;
 $\text{Ca}(\text{H}_2\text{PO}_4)_2 \cdot \text{H}_2\text{O}$, Hopkin Williams, England;
 $\text{Ca}_5(\text{PO}_4)_3(\text{OH})$, Kemika, Zagreb, Yugoslavia;

Materials for the preparation of mortars were commercial flooring products:

-calcined magnesite containing 83% MgO and 17% impurities (magnesium silicates with less than 2% free CaO);

-quartz sand (95% SiO_2).

Magnesium oxide for paste preparation was obtained by calcination of basic magnesium carbonate $\text{Mg}_5(\text{OH})_2(\text{CO}_3)_4 \cdot 4\text{H}_2\text{O}$ in an electric furnace with a homogeneous temperature field (IRYD-1, BTU Engin, Corp. North Billerica, Mass.) for 6 hours at 600, 800 and 1000°C respectively. The specimens are referred to as MgO_{600} , MgO_{800} , and MgO_{1000} . They were examined by X-ray diffraction and no traces of basic magnesium carbonate or compounds other than MgO were observed. After preparation, the calcined MgO was kept in sealed plastic bottles.

As previously mentioned the reactivity of magnesium oxide depends on the temperature of calcination and is characterized by the specific surface and the size of the crystallites. Data on the specific surface and crystallite size of MgO obtained at different temperatures were reported earlier (37).

The solution of magnesium chloride was prepared by dissolving $\text{MgCl}_2 \cdot 6\text{H}_2\text{O}$ in distilled water. The concentration of the chloride ion (Cl^-) was measured by potentiometric titration with an AgNO_3 standard solution.

Preparation of specimens

Sorel cement paste samples were prepared at various $\text{MgO}:\text{MgCl}_2:\text{H}_2\text{O}$ molar ratios with the addition of phosphate or without admixture. The ingredients were mixed by hand in a bowl.

To compare the reaction products with the $\text{MgO}-\text{MgCl}_2-\text{H}_2\text{O}$ phase diagram (38), mixes were cast into cylindrical cups (0.5 cm diameter, 2 cm height) and cured at room temperature in sealed cups to avoid water evaporation. Mixes 4:1:22 and 3:1:21 with MgO_{1000} gave a very thin slurry with sharp segregation between solids and liquid, the solids settling rapidly.

Mixes 5:1:13 and 3:1:11 (some with phosphates added) served to determine the reaction products and strength development and to examine the improvement of water resistance. Specimens were cast and stored in molds (1x1x4 cm) for 24 hours, then removed from the forms if rigid enough or kept for 48 hours and then air-cured or water-cured at room temperature.

Prior to past preparation, phosphates were homogeneously mixed with MgO powder, the quantity being 15% (wt.) of the added MgO . Two phosphates were used: soluble $\text{Ca}(\text{H}_2\text{PO}_4)_2 \cdot \text{H}_2\text{O}$ (solubility 18 g in 1 liter of cold water) and insoluble $\text{Ca}_5(\text{PO}_4)_3(\text{OH})$.*

Mortars were made from a mixture of magnesium oxide and quartz sand homogeneously mixed by hand either with or without calcium phosphate, with the addition of 15% (wt.) of selected MgO . Weight ratio of $\text{MgO}:\text{filler}$ was 1:2 with the quartz sand, taking into account as fillers the added phosphate and impurities in the magnesium oxide (17%).

*(For practical purposes the term soluble is often used when the solubility of a substance exceeds 10 g of solute per 1 liter of solution).

Four kinds of mixes of $MgO:MgCl_2:H_2O$ were prepared:

- (1) mix 5:1:13 without phosphate,
- (2) mix 5:1:13 with 15% phosphate,
- (3) mix 3:1:11 without phosphate,
- (4) mix 3:1:11 with 15% phosphate.

The $MgCl_2$ solution was obtained by dissolving $MgCl_2 \cdot 6H_2O$ in sufficient water to produce the desired ratios for the 5:1:13 and 3:1:11 mixes. The $MgCl_2$ and water contents were controlled by determining the relative density of the $MgCl_2$ solution. Mortars were mixed by hand and then compacted for three minutes by vibration in 4x4x16 cm molds on a vibrating table (3000 vibrations per minute, vibration range 0.5 ± 0.1 mm). After 24 hours the molds were removed and the specimens placed in an air-conditioned room at $20 \pm 2^\circ C$ with 60% relative humidity. After 28 days some specimens with phosphate addition were stored in water ($20 \pm 2^\circ C$) and kept there until testing.

Investigative methods

The reaction products were examined by X-ray diffraction on a Philips diffractometer (Philips N. V., Eindhoven, Holland) and a proportional counter. The phases were determined either by semiquantitative analysis (comparing the intensities of diffraction maxima) or by a quantitative method based on the proportionality between the ratio of weight fractions of two phases in a mixture and the ratio of the integrated intensities of their diffraction peaks. The proportionality constants for the phases present in Sorel cement were calculated using quartz as an internal standard. The error in determining the weight fractions of the phases was approximately 2%. The method used has been described by several authors (46 to 49).

Compressive strength was measured on air-cured and/or water-cured samples and the mean values of three measurements are graphically presented in Figures 46 and 53 (pages 110 and 120).

It should be noted that pastes with MgO_{600} had a strong shrinkage and were easily removed from their forms 24 hours after casting, while those with MgO_{800} and MgO_{1000} exhibited expansion thus making the removal difficult. Some samples prepared as a 5:1:13 mix with MgO_{600} particularly those with additions of $Ca_5(PO_4)_3(OH)$, had visible surface cracks a month after preparation.

The air-cured samples prepared from a 3:1:11 mix with MgO_{600} with either an addition of insoluble phosphate or without admixture were deformed at the age of one or two weeks. The upper layer consisted of 51% phase 5, ($5 MgO \cdot MgCl_2 \cdot 8H_2O$ or $Mg_3(OH)_5Cl \cdot 1.4H_2O$), and 49% phase 3, ($3 MgO \cdot MgCl_2 \cdot 8H_2O$) or $Mg_2(OH)_3Cl \cdot 1.4H_2O$), whereas the underlying part had 11% phase 5, 86% phase 3 and 3% $Mg_2(OH)ClCO_3 \cdot 3H_2O$.

C. RESULTS AND DISCUSSION

MgO activity and paste composition

Samples cured in closed containers were used to investigate the influence of MgO activity on paste composition and also to compare the reaction products with those on the phase diagram. Some preliminary data on the subject have recently been published (37) and the results presented in this work (Table 22) offer additional information, as different ratios of reactants were used. Moreover, the reaction products have been determined by quantitative X-ray analysis over a period of one year of aging.

Some general conclusions about the reactivity of MgO can be inferred from Table 22. The very reactive MgO_{600} rapidly disappears from the paste. In pastes with a 3:1:11 mix with the lesser reactive MgO_{1000} , the reaction product will be phase 3, whereas a content of the very reactive MgO_{600} will give phase 5. When pastes are prepared to give phase 5 or a mixture of phase 5 and $\text{Mg}(\text{OH})_2$, the less active MgO_{1000} will yield the expected reaction product(s) but if the very active MgO_{600} is used, $\text{Mg}(\text{OH})_2$ will predominate or come as the only reaction product.

Additional conclusions can be drawn if we consider the reaction products in pastes regardless of the MgO used (very active MgO_{600} or insufficiently active MgO_{1000}). Subject to the concentration of the magnesium chloride solution and the content of magnesium oxide in the initial mix, one of the following phases will form as reaction product: $\text{Mg}(\text{OH})_2$, phase 5, phase 3 or their mixtures consisting of two or all three phases in all possible combinations.

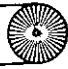
Phase 3 or a mixture of phases 3 and 5 will crystallize at a higher MgCl_2 concentration or a lower MgO content. At a higher MgO content or lower MgCl_2 concentration, the crystalline reaction product will be $\text{Mg}(\text{OH})_2$, a mixture of phase 5 and $\text{Mg}(\text{OH})_2$ or phase 5 alone.

These observations together with the data published in the literature help to interpret the role of MgO activity in the formation and development of crystalline reaction products in hardened pastes. The chemical formula and

Table 22. Crystalline reaction products in magnesium oxychloride pastes
(cured in closed containers)

Calcination temp. of MgO (°C)	Mix composition		PHASE COMPOSITION (wt. %)				
	MgO : MgCl ₂ : H ₂ O molar ratios	weight percentage	6 hours	1 day	21 days	6 months	1 year
600	8 : 1 : 26	36 : 11 : 58	-	Mg(OH) ₂ (100)	Mg(OH) ₂ (100)	Mg(OH) ₂ (89) Phase 5 ² (7) Phase 3 (4)	-
1000			-	MgO (19) Mg(OH) ₂ (11) Phase 5 ² (70)	Mg(OH) ₂ (47) Phase 5 ² (53)	Mg(OH) ₂ (48) Phase 5 ² (52)	-
600	5 : 1 : 23	28 : 14 : 58	Mg(OH) ₂ (100)	Mg(OH) ₂ (100)	Mg(OH) ₂ (100)	Mg(OH) ₂ (78) Phase 3 ² (22)	Mg(OH) ₂ (58) Phase 3 ² (42)
1000			MgO (60) Phase 5 (40)	MgO (1) Mg(OH) ₂ (39) Phase 5 (60)	Mg(OH) ₂ (58) Phase 5 ² (42)	Mg(OH) ₂ (52) Phase 5 ² (48)	Mg(OH) ₂ (40) Phase 5 ² (43) Phase 3 (17)
600	4 : 1 : 22	25 : 14 : 61	-	Mg(OH) ₂ (73) Phase 5 (27)	Mg(OH) ₂ (61) Phase 5 (39)	Mg(OH) ₂ (53) Phase 5 (47) Phase 3 (8)	-
1000			-	MgO (19) Phase 5 (81)	Mg(OH) ₂ (11) Phase 5 (89)	Mg(OH) ₂ (18) Phase 5 (82)	-
600	3 : 1 : 21	20 : 16 : 64	Mg(OH) ₂ (65) Phase 5 ² (35)	Mg(OH) ₂ (68) Phase 5 ² (32)	Mg(OH) ₂ (67) Phase 5 ² (33)	Phase 5 (11) Phase 3 (81)	-
1000			MgO (55) Phase 5 (45)	MgO (x) Mg(OH) ₂ (23) Phase 5 (77)	Mg(OH) ₂ (26) Phase 5 ² (74)	Mg(OH) ₂ (18) Phase 5 (69) Phase 3 (13)	-
600	8 : 1 : 16	46 : 13 : 41	-	MgO (13) Mg(OH) ₂ (x) Phase 5 (87)	MgO (7) Mg(OH) ₂ (2) Phase 5 (91)	Mg(OH) ₂ (20) Phase 5 ² (80)	-
1000			-	MgO (16) Mg(OH) ₂ (8) Phase 5 ² (76)	MgO (x) Mg(OH) ₂ (23) Phase 5 (77)	Mg(OH) ₂ (15) Phase 5 ² (85)	-
600	5 : 1 : 15	35 : 17 : 48	-	Mg(OH) ₂ (x) Phase 5 (100)	Mg(OH) ₂ (10) Phase 5 ² (90)	-	-
1000			-	MgO (4) Phase 5 (96)	Mg(OH) ₂ (x) Phase 5 ² (100)	-	-
600	5 : 1 : 13	38 : 18 : 44	MgO (4) Phase 5 (96)	Phase 5 (100)	Phase 5 (100)	Phase 5 (100)	Phase 5 (100)
1000			MgO (64) Phase 5 (36)	MgO (16) Phase 5 (84)	Phase 5 (100)	Phase 5 (100)	Phase 5 (100)
600	4 : 1 : 12	34 : 20 : 46	-	Phase 5 (100)	Phase 5 (100)	Phase 5 (68) Phase 3 (32)	-
1000			-	MgO (23) Phase 3 (77)	MgO (4) Phase 5 (21) Phase 3 (75)	MgO (2) Phase 5 (18) Phase 3 (80)	-
600	3 : 1 : 11	29 : 23 : 48	MgO (7) Phase 5 (93)	Phase 5 (100)	Phase 5 (11) Phase 3 (89)	Phase 3 (100)	Phase 3 (100)
1000			MgO (100)	MgO (7) Phase 3 (93)	Phase 3 (100)	Phase 3 (100)	Phase 3 (100)

(x) - not determined, present in very small quantity

Reproduced from
best available copy. 

crystal structure of MgO correspond to those of the mineral periclase (50) which has but one modification (51). It can therefore be inferred that regardless of the temperature at which it has been obtained, the MgO will always react chemically in the same way and give the same reaction products. However, if obtained at higher temperatures (1000°C) or calcined for a longer time the MgO will have a smaller specific surface (37), a larger mean crystallite size (37,50) and a slightly smaller unit cell (50) than the MgO formed at a lower temperature (600° C) which is distinguished by a larger specific surface and a smaller crystallite size. These differences make the MgO₁₀₀₀ explicitly less active than MgO₆₀₀ and it consequently reacts very slowly with other substances. Regardless of its activity, the solubility of MgO is better in MgCl₂ solution than in water (52), increasing with higher concentrations of MgCl₂ (53,54,55). It is evident from Table 22 that the active MgO in pastes disappears faster than the insufficiently active one, because it dissolves more rapidly and in larger quantities in MgCl₂ solutions. Since the dissolved MgO reacts chemically with the MgCl₂ in solution, the crystalline product will be either Mg(OH)₂, phase 5 or phase 3 and/or a mixture of two or three phases depending on the concentrations of both MgO and MgCl₂ .

At very high MgCl₂ concentrations even MgCl₂.6H₂O will form. The fact is that Mg(OH)₂ crystallizes from MgCl₂ solution with concentrations ranging between 1.25 and 1.5 mol dm⁻³ or lower (54,55,56) but it can also crystallize from solutions with concentrations up to 2.5 mol dm⁻³ (55). It has been reported that Mg(OH)₂ will be the reaction product when a more active MgO is dissolved in 1.5 mol dm⁻³ MgCl₂ solution, while phase 5 will crystallize if the MgO is less active (57). Therefore, the crystallization of a particular phase does not depend exclusively upon the MgCl₂ concentration but also on the concentration of the MgO dissolved in MgCl₂ solution. This has been confirmed in other cases too; thus the first reaction product in 2.5 mol dm⁻³ MgCl₂ solution will be phase 5 provided that the MgO concentration amounts to 5 g/dm⁻³; at lower concentrations phase 3 will appear. When phase 5 is desired to be the first reaction product, the concentration of MgO should be 25 g/dm⁻³ in a 4.6 mol dm⁻³ of MgCl₂ solution (55).

The results of the present work (Table 22) are in agreement with the data mentioned above and help to explain the formation and development of reaction products in the $\text{MgO-MgCl}_2\text{-H}_2\text{O}$ system as well as the role of MgO reactivity on the rate of reaction and formation of products. The cementitious phases in magnesium oxychloride pastes are formed as follows: first MgO dissolves when mixed with the MgCl_2 solution and once the required saturation has been attained, a magnesium oxychloride phase crystallizes. Thus with an appropriate initial mix for phase 3 formation (molar ratio $\text{MgO:MgCl}_2\text{:H}_2\text{O} = 3:1:11$) the final reaction product will be phase 3, as indicated by the phase diagram. With a more active MgO which dissolves more rapidly (attaining higher concentrations in MgCl_2 solution than required for the crystallization of a particular phase, say phase 3), the early reaction product will be a more basic phase, e.g., phase 5. Under such circumstances the unreacted MgCl_2 in the paste will make phase 5 transform into phase 3 as the final reaction product. The crystallization will begin with one of the following phases: Mg(OH)_2 , phase 5 or phase 3 depending on the concentration of the magnesium chloride solution and that of the dissolved MgO. At higher MgCl_2 concentrations the first to crystallize will be phase 3 or a mixture of phases 3 and 5. At lower MgCl_2 concentrations or higher MgO contents it will be phase 5 or a mixture of phase 5 and Mg(OH)_2 . A highly active MgO has the same effects on the early reaction products as a higher content of MgO or a lower concentration of MgCl_2 .

The water content in the reaction mix is closely connected with the MgCl_2 concentration and should not be neglected. With water in excess of the theoretical value required for a particular phase or combination of phases, the MgCl_2 concentration will be lower and the reaction product(s) will form in conformity with the phase diagram. It should be noted that here, too, an active MgO can influence the development of the first reaction products; thus if MgO_{600} is used in pastes with 5:1:23 mix, the first reaction product will be Mg(OH)_2 instead of a combination of phase 5 and Mg(OH)_2 as expected from the phase diagram. In this case, the unreacted MgCl_2 in the paste will provoke the transformation of Mg(OH)_2 into one of the magnesium oxychloride phases, generally phase 3, depending on the concentration of the reactants in the solution. Since Mg(OH)_2 does not dissolve quickly in MgCl_2 solutions, the transformation will progress slowly.

The final reaction products are formed when all the reactants involved in the reaction are balanced out in quantities required for the product and when they have completely reacted and disappeared from the system. The reaction products are then stable unless attacked by water or CO_2 . Here, too, the activity of MgO must be taken into account because a very active MgO can influence the reaction rate, like in the 5:1:13 mix (Table 22), or the formation of the early reaction products which differ from the final products, as in the case of the 3:1:11 mix where after a few hours a very active MgO yielded phase 5 instead of phase 3. In addition to phase 5 there will also be an excess of unreacted MgCl_2 solution and since phase 5 is not stable under such conditions, it will transform into phase 3, the process of transformation being rather slow. Data from Table 22 shows that after 21 days the paste still contained 11% of phase 5. The transformation terminated at later ages and after 6 months there was but one reaction product present, i.e., phase 3.

This seems to contradict the statement that very active MgO influences the rate of reaction; the fact of the matter is that a very active MgO has higher solubility in MgCl_2 solution and is therefore decisive for the formation of the early reaction product, which may differ from the final one. Since every phase transformation in hardened cement lowers its strength, it should be recollected that the reaction products in the system $\text{MgO-MgCl}_2\text{-H}_2\text{O}$ depend both on the molar ratio and on the reactivity of MgO.

The results presented on the influence of calcining temperature on the activity of MgO and of the MgO on the reaction products refer to MgO prepared from basic magnesium carbonate and cannot automatically be applied to the MgO obtained from commercially exploited rocks.

Strength development in phases 5 and 3

Reaction products in air-cured pastes from 5:1:13 mix (Fig.44) and 3:1:11 mix (Fig. 45) were investigated over a period of one year. Phase 5 was the only reaction product in pastes with 5:1:13 mix and it remained stable because all

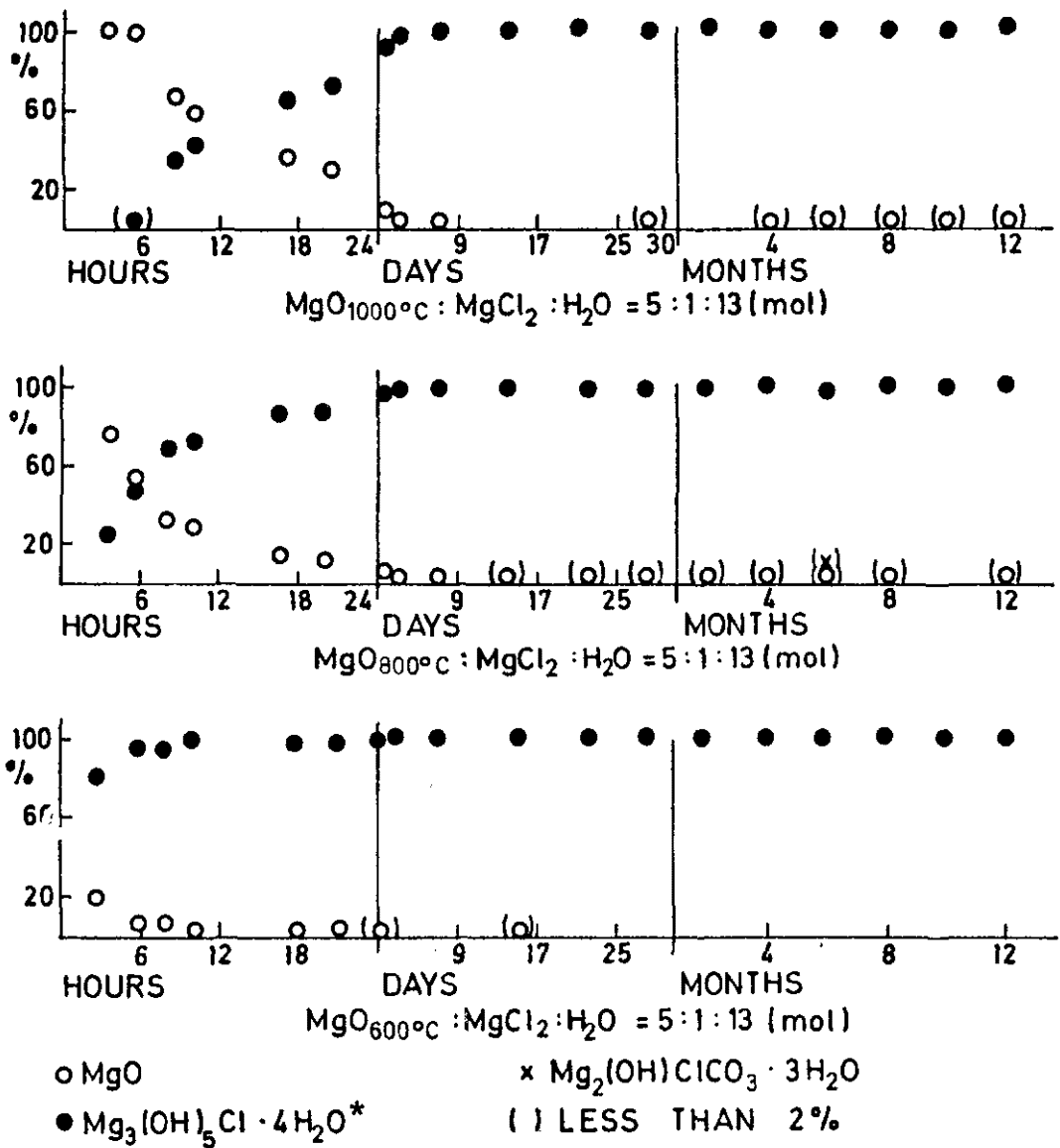


Figure 44. Reaction products in Sorel cement pastes from mixes expected to give phase 5.

* Equivalent to $5 \text{ Mg}(\text{OH})_2 \cdot \text{MgCl}_2 \cdot 8\text{H}_2\text{O}$.

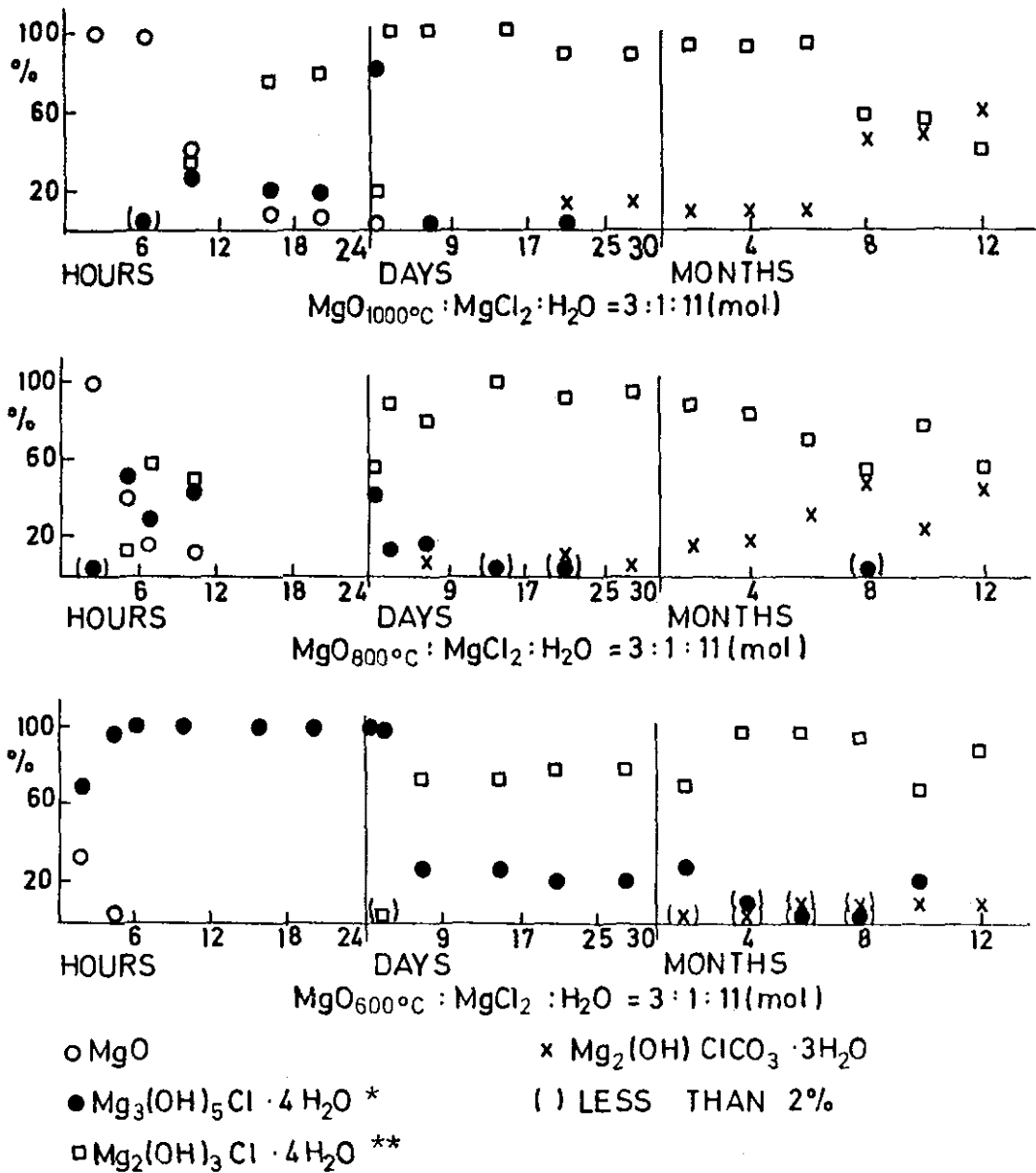


Figure 45. Reaction products in Sorel cement pastes from mixes expected to give phase 3.

* Equivalent to 5 Mg(OH)₂ · MgCl₂ · 8H₂O.
 ** Equivalent to 3 Mg(OH)₂ · MgCl₂ · 8H₂O.

the reactants were in quantities required for its formation. Phase 5 was resistant to the atmospheric CO_2 as well, since only traces of $\text{Mg}_2(\text{OH})\text{ClCO}_3 \cdot 3\text{H}_2\text{O}$ were detected in one sample at later ages. This is in agreement with literature data (39,40).

In pastes where water was in excess of the value required for phase 5 and where the reaction product was a mixture of $\text{Mg}(\text{OH})_2$ and phase 5, $\text{Mg}_2(\text{OH})\text{ClCO}_3 \cdot 3\text{H}_2\text{O}$ crystallized earlier, i.e. after one month (37) and in a larger proportion. This is confirmed by data in Table 23 showing the reaction products in pastes with two 5:1:23 mixes containing MgO of different reactivities.

The development of crystalline reaction products in pastes with 3:1:11 mix is presented in Figure 45. Due to the higher solubility in the more concentrated MgCl_2 solutions, the MgO disappeared more rapidly from the system than in the previous case. Though all the reactants were in prescribed quantities for the formation of phase 3, it was phase 5 that crystallized as the first reaction product in all of the study samples, even in those prepared with MgO_{1000} . Under such conditions and with an excess of unreacted MgCl_2 in the liquid, phase 5 was not stable and transformed eventually into phase 3.

In pastes containing active MgO_{600} phase 5 was present in a larger proportion than in pastes prepared with the insufficiently active MgO_{1000} for reasons already explained. Phase 3 was the first reaction product in pastes prepared from the 3:1:11 mix with MgO_{1000} and cured in a closed container (Table 22). It is not yet fully understood why the early reaction products in samples cured in sealed bottles are different from those in the air-cured samples. The formation and development of phases in pastes with the 3:1:11 mix are more complex than in those with the 5:1:13 mix. If MgO_{600} is used in combination with the 3:1:11 mix, phase 5 will develop faster and in larger quantities and will remain unchanged much longer than in pastes prepared with MgO_{1000} . It may therefore be inferred that in pastes with MgO_{600} , phase 3 develops only by transformation from phase 5. This conclusion should not be generalized because 3:1:11 pastes prepared with the less active MgO_{1000} have phase 3 as

Table 23. Crystalline reaction products in air-cured
Sorel cement pastes from 5 : 1 : 23

Calcination temp. of MgO (°C)	PHASE COMPOSITION (wt. %)	
	1 day	1 month
1000	Mg(OH) ₂ (14) phase 5 (86)	Mg(OH) ₂ (21) phase 5 (66) Mg ₂ (OH)ClCO ₃ ·3H ₂ O (13)
600	Mg(OH) ₂ (100)	Mg(OH) ₂ (100) Mg ₂ (OH)ClCO ₃ ·3H ₂ O (x)

(x) detected, present in very small quantity

the only reaction product (Table 22) when cured in closed containers. Since MgO_{1000} dissolved very slowly in MgCl_2 solution, the low concentrations of MgO allow the formation of the less basic phase 3 as the only reaction product. In air-cured samples, the humidity in the air probably contributes to a faster solubility of MgO in the MgCl_2 solution.

The development of $\text{Mg}_2(\text{OH})\text{ClCO}_3 \cdot 3\text{H}_2\text{O}$ was more prevalent in pastes with the 3:1:11 mix than in those with the 5:1:13 mix, which is in conformity with literature data (39).

Although strength tests on neat cement pastes do not furnish reliable indications on the quality of cements, they were applied in this study for a number of reasons, one of them being the limited quantity of MgO obtained by calcination from chemicals (reagent grade) in a furnace having a homogeneous temperature field. The pastes were originally prepared for the study of reaction products and there was but little additional work needed to mold specimens and test their compressive strength. The results of the testing varied considerably and are not presented. They nevertheless indicate that both phases have binding properties and that strengths develop faster and attain higher values in pastes with the 5:1:13 mix where phase 5 is the only reaction product than in pastes from the 3:1:11 mix with phase 5 forming at the beginning and then changing into phase 3.

Distinctive cementitious properties of phases 5 and 3 were studied by precise testing of strength development in air-cured mortars of $\text{MgO}:\text{MgCl}_2:\text{H}_2\text{O}$ molar ratio 5:1:13 and 3:1:11. The results are presented graphically in Figure 46.

Both phases have binding properties but strength develops faster and reaches higher values in mortars from the 5:1:13 mix with phase 5 as the predominant reaction product. Mortars with the 5:1:13 mix attain about 80% of their maximal strength at a day's aging, whereas those from 3:1:11 mix attain maximal strength at a month's aging, subsequently losing it very rapidly. Table 24 shows the reaction products of a 3:1:11 mix (expected to form phase 3) and a 5:1:13 mix (expected to give phase 5). In a 3:1:11 mix the MgO disappears from the system faster than in a 5:1:13 mix; this holds for the paste samples too. The reaction

Table 24. Initial mix and phase composition in Sorel cement mortars with MgO₈₀₀

Sample	Mix composition						Phase composition (qualitative analyses) (wt. %)					
	MgO:MgCl ₂ : :H ₂ O (mol. ratios)	Calc. MgCO ₃ * (wt.%)	Quartz (wt.%)	Phosph.+ (wt.%)	MgCl ₂ · 6H ₂ O (wt.%)	Water (wt.%)	1 day	3 days	7 days	14 days	21 days	30 days
D-T5	5:1:13	26.0	35.5	3.2	21.8	13.5	SiO ₂ Phase 5 MgO Phosph.+	SiO ₂ Phase 5 MgO Phosph.+	- MgO Phosph.+	SiO ₂ Phase 5	- MgO Phosph.+	SiO ₂ Phase 5 MgO Phosph.+
D-5	5:1:13	26.0	38.7	-	21.8	13.5	SiO ₂ Phase 5 MgO	SiO ₂ Phase 5 MgO	SiO ₂ Phase 5 MgO	SiO ₂ Phase 5 MgO	SiO ₂ Phase 5 MgO	SiO ₂ Phase 5 MgO
D-T3	3:1:11	22.2	30.4	2.6	31.1	13.7	SiO ₂ Phase 5 MgO Phase 3 Phosph.	SiO ₂ Phase 5 Phase 3 MgO Phosph.	- Phase 5 MgO	SiO ₂ Phase 3 Phase 5 MgO	- Phase 5 Phosph.	SiO ₂ Phase 3 Phase 5 Phosph.
D-3	3:1:11	22.2	33.1	-	31.0	13.7	SiO ₂ Phase 5 MgO Phase 3	SiO ₂ Phase 5 Phase 3 MgO	SiO ₂ Phase 3 Phase 5 MgO	SiO ₂ Phase 3 Phase 5 MgO	SiO ₂ Phase 3 Phase 5 MgO	SiO ₂ Phase 3 Phase 5 MgO

* Calcined magnesite contains 83% MgO

+ Ca(H₂PO₄)₂·H₂O

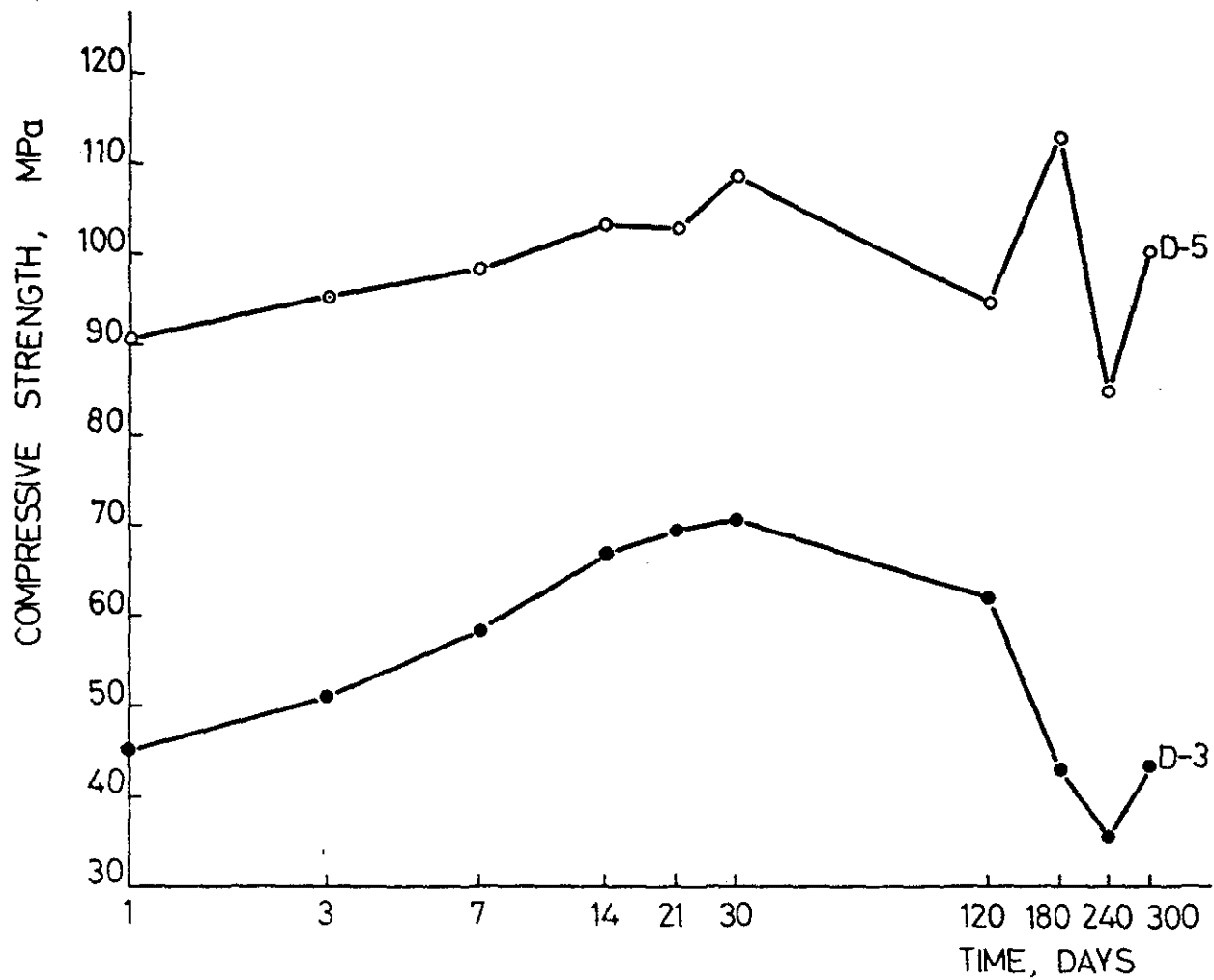


Figure 46. Compressive strengths in Sorel cement mortars from 5 : 1 : 13 (sample D-5) and 3 : 1 : 11 (sample D-3) mixes

products formed in the interim between one day and one month in the 3:1:11 mix were phases 3 and 5 with some unreacted MgO and quartz coming from the filler. Although unreacted $MgCl_2$ was expected in the liquid phase, it was not discernible by x-ray diffraction. It is logical that under such circumstances in the presence of unreacted $MgCl_2$ phase 5 transformed into phase 3 with an expressed strength decrease. Therefore, the 6 months old mortar samples had approximately the same strength as the 1 day old specimens. Cracks were visible on the surface of these samples as well as on samples tested at later ages. It follows that mixes with a molar ratio $MgO:MgCl_2 = 3$ and a water content close to the theoretical value for phase 3 are not suitable for floorings because of their very low strength as compared to that of the 5:1:13 mixes. The release of corrosive $MgCl_2$ solution in mortars with the 3:1:11 mix is more pronounced than in those with the 5:1:13 mix, since unreacted $MgCl_2$ is present in excess both during the formation of phase 5 and its transformation into phase 3.

Effects of phosphates on water resistance of hardened cement

Reaction products which formed in air-cured cement pastes from the 5:1:13 and 3:1:11 mixes with additions of 15% phosphate are presented in Figures 47-50. There was no change in the crystallization rate or the quantity of phase 5 formed in samples prepared from the 5:1:13 mix with MgO of identical activity due to additions of soluble or insoluble phosphates (Figs. 47 and 48).

In pastes where phase 3 was expected as the final product (Figs. 49 and 50), added phosphate retarded the transformation of phase 5 into phase 3 by inhibiting the action of the unreacted $MgCl_2$ solution. In samples prepared with MgO of equal activity, the soluble phosphate was a more effective retarder than the insoluble one.

The effects on water resistance of soluble and insoluble phosphate were investigated by storing the treated hardened cement pastes in water. The experiments involved using MgO_{800} because its activity corresponded to that of MgO in the preparation of mortar samples. The reaction products which formed when 1 - day hardened pastes were stored in water are graphically presented in Figure 51 and 52. Figure 51 refers to the initial raw mix (5:1:13) with completely (100%) crystallized phase 5 at the moment of immersion. Within 9 days phase 5

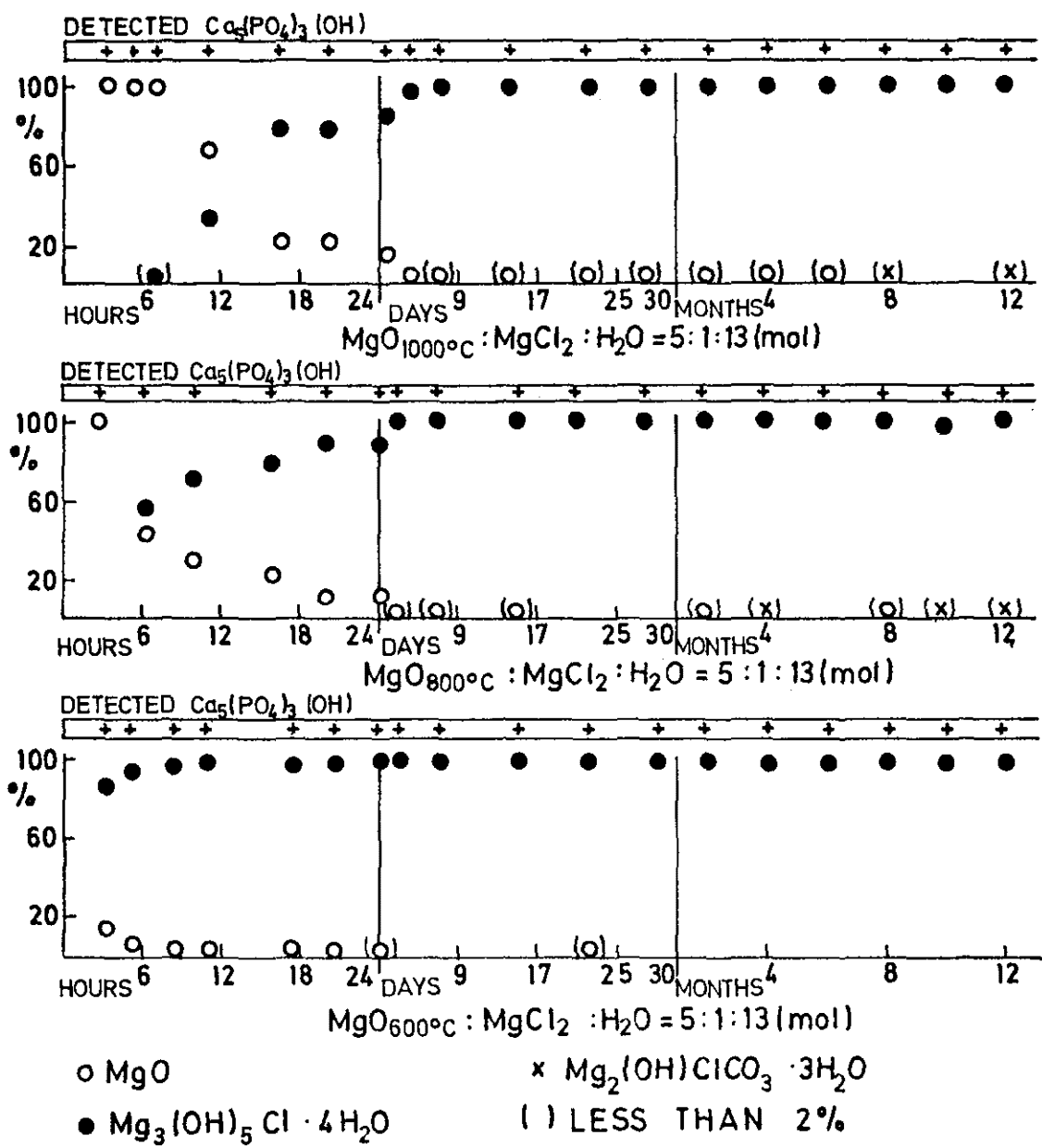


Figure 47. Sorel cement with $\text{Ca}_5(\text{PO}_4)_3(\text{OH})$ addition: Reaction products in pastes from mixes expected to give phase 5.

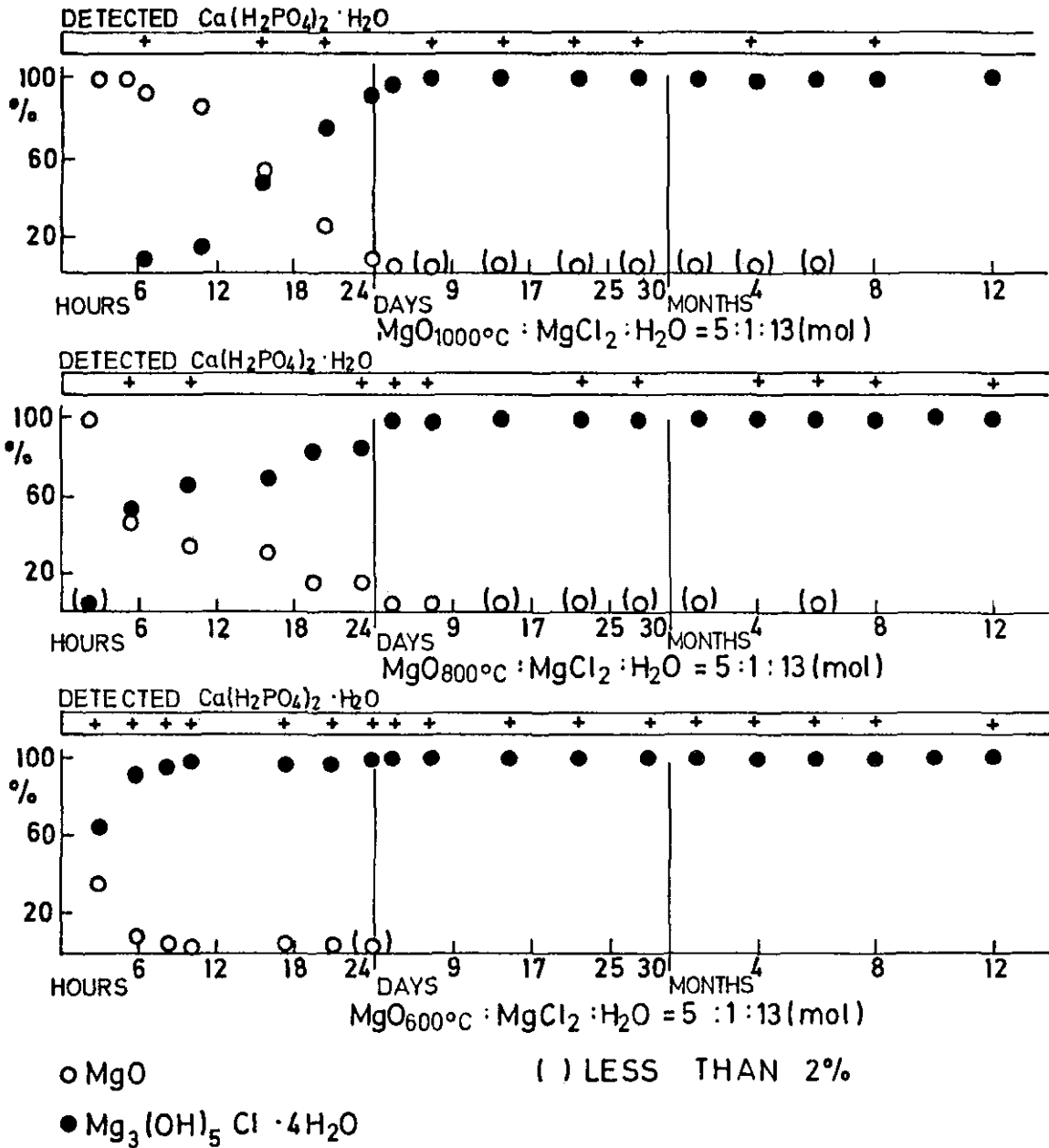


Figure 48. Sorel cement with $\text{Ca}(\text{H}_2\text{PO}_4)_2 \cdot \text{H}_2\text{O}$ addition: Reaction products in pastes from mixes expected to give phase 5.

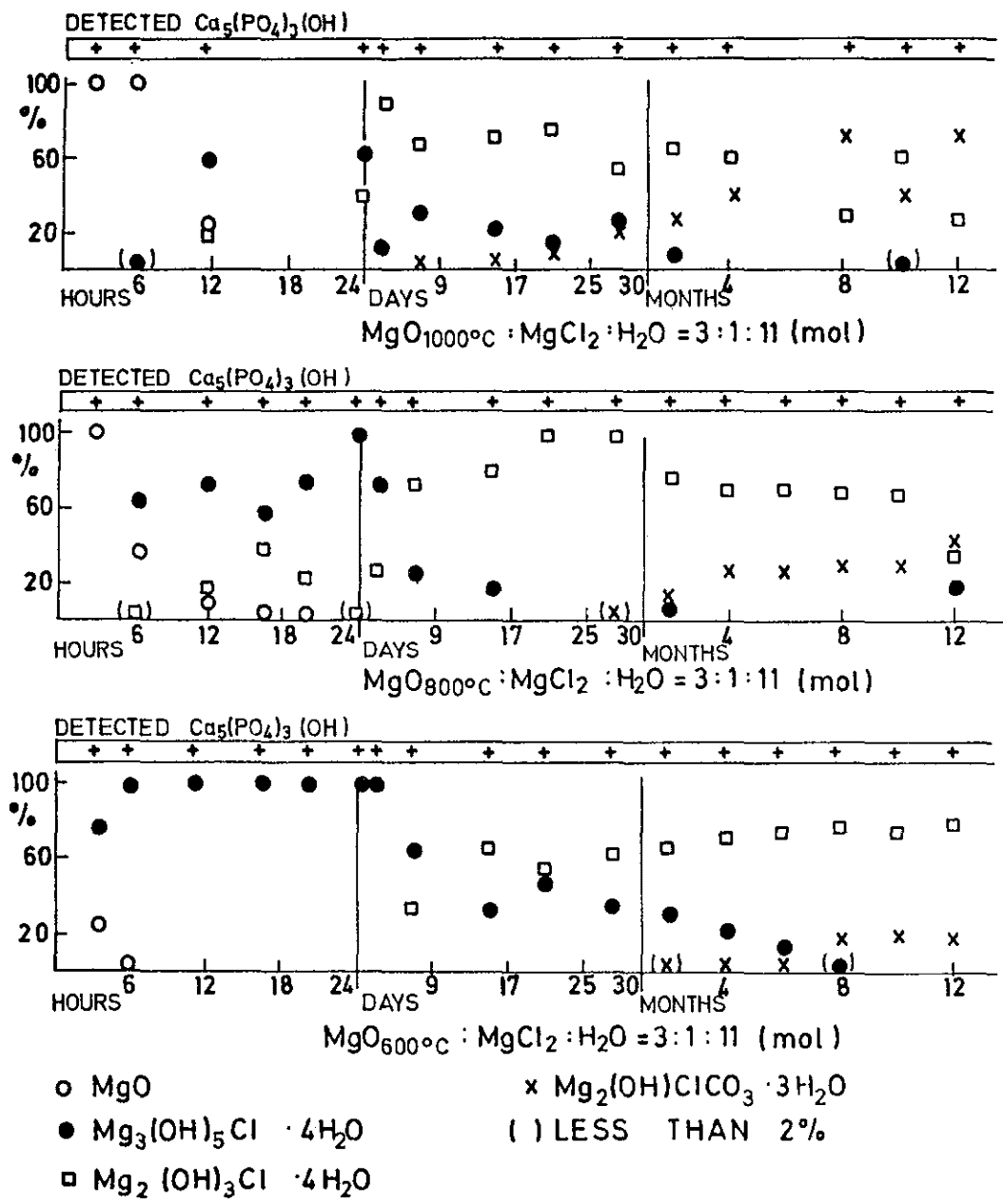


Figure 49. Sorel cement with $\text{Ca}_5(\text{PO}_4)_3(\text{OH})$ addition: Reaction products in pastes from mixes expected to give phase 3

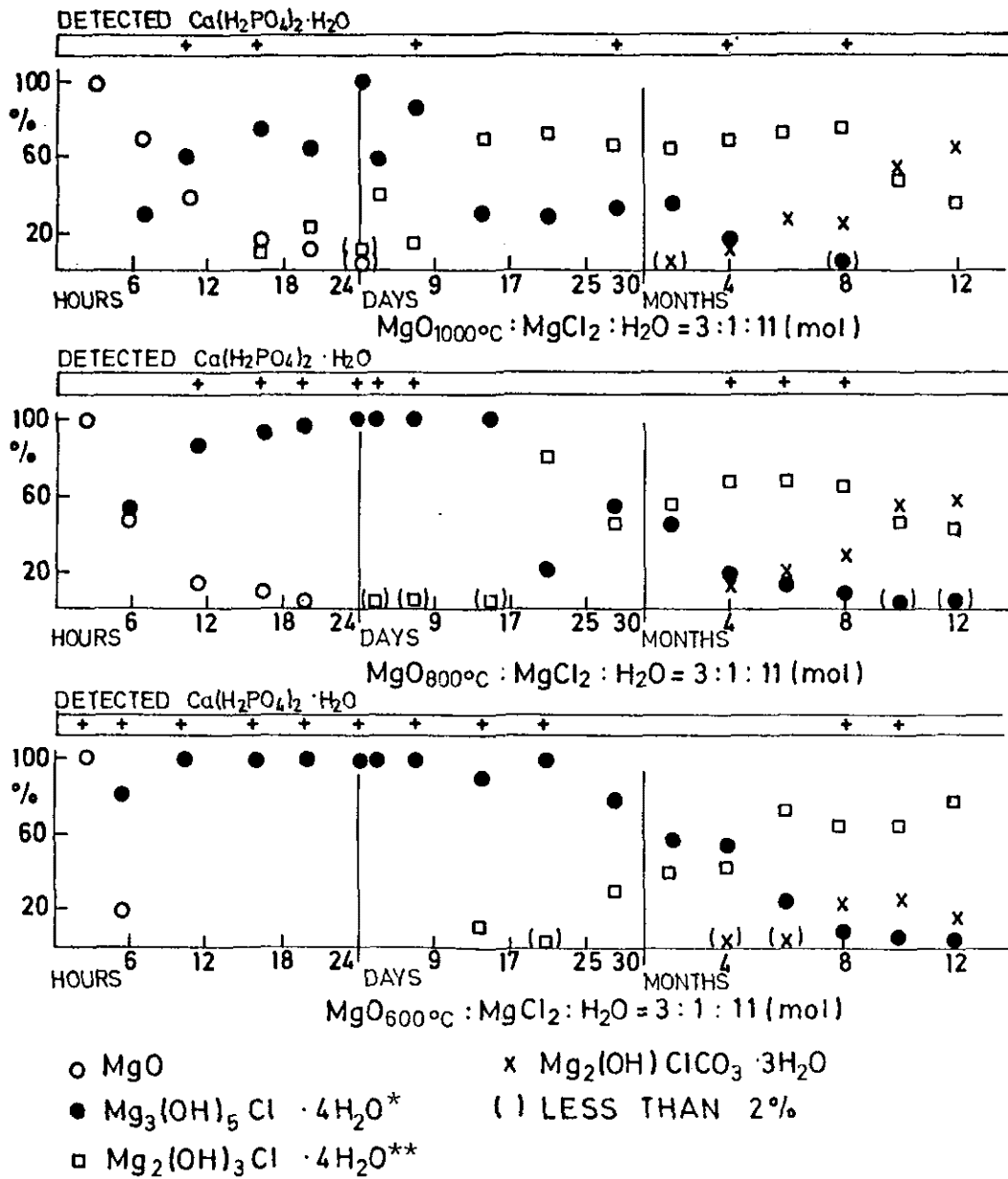


Figure 50. Sorel cement with $\text{Ca}(\text{H}_2\text{PO}_4)_2 \cdot \text{H}_2\text{O}$ addition: Reaction products in pastes from mixes expected to give phase 3.

* phase 5.
** phase 3.

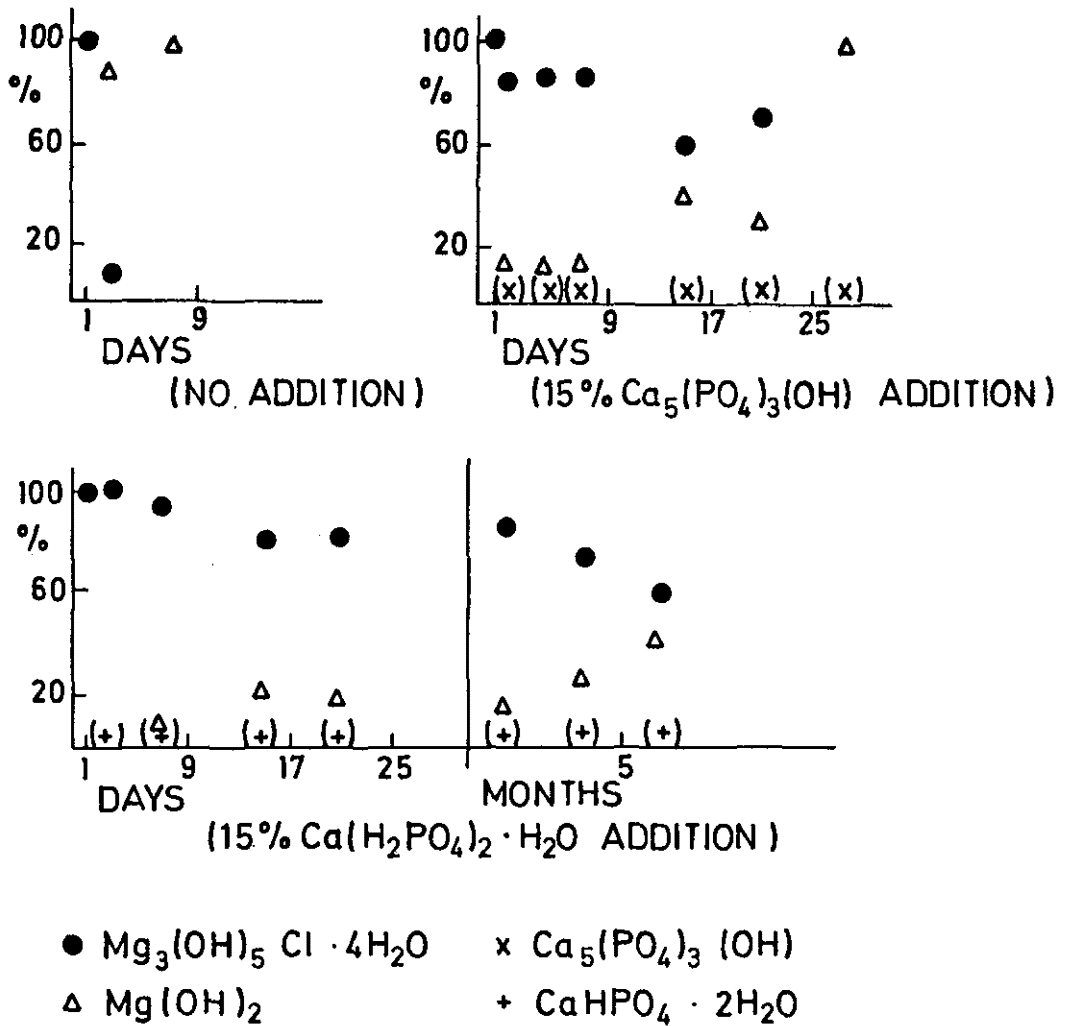


Figure 51. Sorel cement with phosphate addition (5 : 1 : 13 mix with MgO₈₀₀): Phases in hardened pastes stored in water.

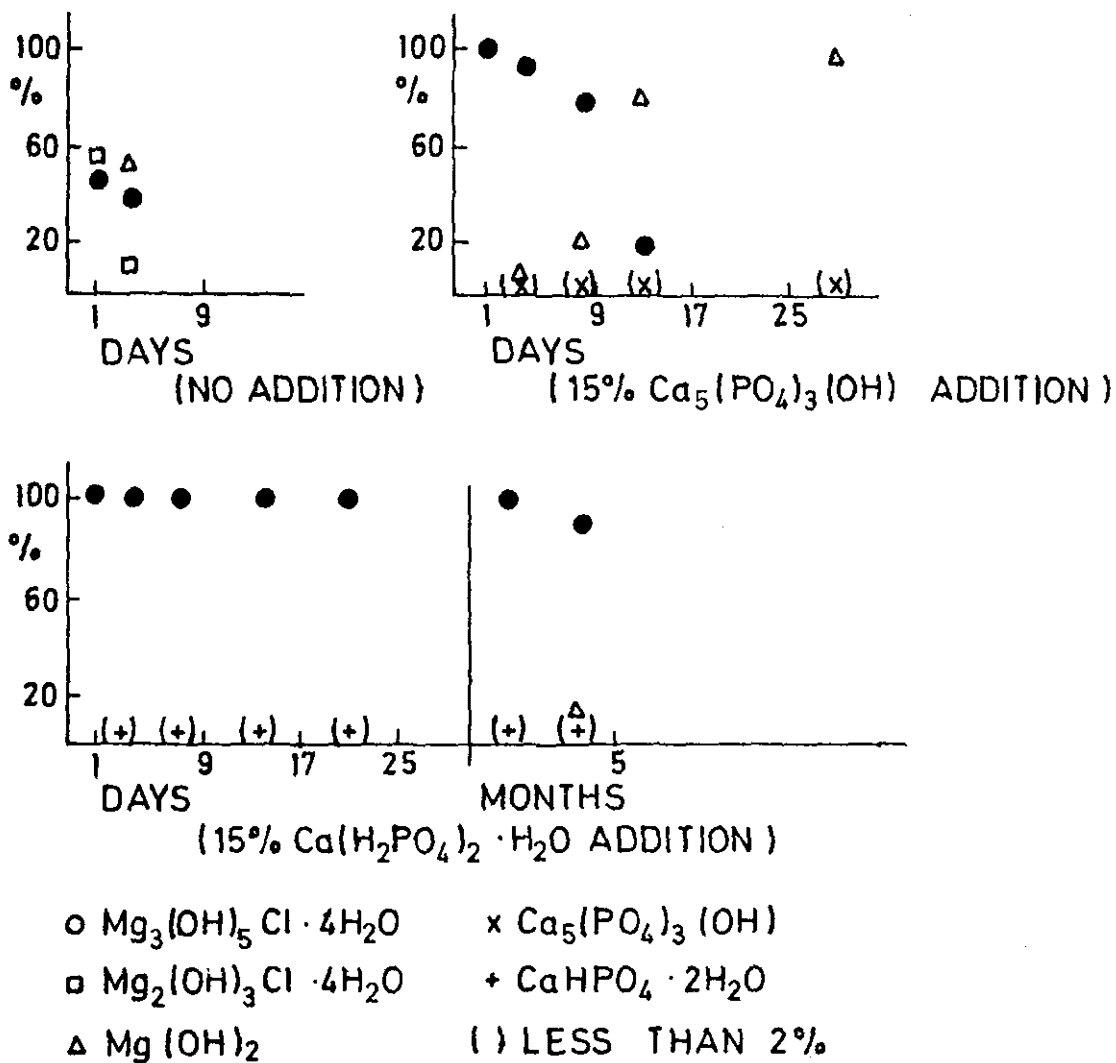


Figure 52. Sorel cement with phosphate addition (3:1:11 mix with MgO_{800}): Phases in hardened pastes stored in water.

transformed completely into $\text{Mg}(\text{OH})_2$ when the pastes had no phosphate additions. In pastes containing 15% $\text{Ca}_5(\text{PO}_4)_3(\text{OH})$, the transformation was slower and took approximately one month, whereas in pastes with 15% $\text{Ca}(\text{H}_2\text{PO}_4)_2 \cdot \text{H}_2\text{O}$ it was considerably retarded and after 6 months only half of phase 5 was transformed into $\text{Mg}(\text{OH})_2$. It should be noted that during the hydration process the soluble phosphate calcium dihydrogenphosphate $\text{Ca}(\text{H}_2\text{PO}_4)_2 \cdot \text{H}_2\text{O}$, changed into the less soluble $\text{CaHPO}_4 \cdot 2\text{H}_2\text{O}$, calcium hydrogen phosphate, the solubility being 0.32 g/dm^{-3} in cold water: $\text{CaHPO}_4 \cdot 2\text{H}_2\text{O}$ was detected by x-ray diffraction analysis, with no traces of any other phosphate compound. It was concluded that phosphates did not participate in any chemical reactions.

Figure 52 shows the reaction products in 1-day old hardened pastes from 3:1:11 mixes prior to water storage. A mixture of phases 5 and 3 already formed before the immersion of the samples after which both phase 5 and 3 rapidly transformed into $\text{Mg}(\text{OH})_2$. At the moment of immersion phase 5 predominated in pastes prepared with 15% phosphate additions. It transformed more slowly than in samples without phosphate. The experiment confirmed that the soluble phosphate is more effective than the insoluble one in improving the water resistance of phase 5. Soluble phosphate $\text{Ca}(\text{H}_2\text{PO}_4)_2 \cdot \text{H}_2\text{O}$, calcium dihydrogenphosphate transformed during hydration into the less soluble $\text{CaHPO}_4 \cdot 2\text{H}_2\text{O}$, calcium hydrogen phosphate.

Compressive strengths were also obtained on the samples used for phase analyses. The results are not reported because of their large variabilities. However, they support the conclusion that the addition of $\text{Ca}_5(\text{PO}_4)_3(\text{OH})$ or $\text{Ca}(\text{H}_2\text{PO}_4)_2 \cdot \text{H}_2\text{O}$ ameliorates the resistance of Sorel cements against water attack and that the soluble $\text{Ca}(\text{H}_2\text{PO}_4)_2 \cdot \text{H}_2\text{O}$ is more effective in this respect.

Improved water resistance can probably be attributed to the adsorption of phosphates on the crystals of magnesium oxychloride hydrates. Phosphates adsorb on the crystals of phase 5, surrounding and protecting them against water attack. In Sorel cement, phosphates act similarly to phosphogypsum in the hydration process of Portland cement. Phosphate impurities from phosphogypsum retard the setting of Portland cement but do not affect the strength at later ages. Murakami (58) explained the retarding mechanism as follows: phosphoric

compounds deposit on cement particles, surrounding them and impeding hydration. The likelihood that the same mechanism applies to Sorel cement is supported by the fact that phase 5 and insoluble phosphate were the only compounds detected in the hardened cement when insoluble phosphate was added to the initial mix. The soluble phosphate, on the other hand dissolves in the paste and passes into the less soluble state which crystallizes on the particles of the reaction products. Precipitated phosphates protect the crystals of magnesium oxychloride hydrates against water attack. Phosphates also precipitate in voids and pores thus shielding the most sensitive areas in the hardened cement. This is most likely the reason why soluble phosphates are more effective than insoluble ones.

Further data was obtained relevant to the effect of soluble phosphate on the strength development of cement mortars with predominantly phase 5 (5:1:13 mix) and those with the initial mix formulated for phase 3 (3:1:11) where a mixture of phases 5 and 3 formed instead. The results are presented in Figure 53. The effects of phosphate on strength development in mortars with phase 5 in prevalence differed from those in mortars where phase 3 was expected to be the final product. In mortars with predominantly phase 5, the early strength development was slightly lowered by phosphate addition, but with aging the strength of the samples containing phosphates was higher and more constant than in samples without admixture (Fig. 46). The first and only reaction product that formed in these mortars was phase 5 (Table 24). It is worth noting that mortar D-T5 still had unreacted MgO at the age of one month.

A slower strength development was observed in air-cured mortars (3:1:11 mix) where phase 3 was expected as the final reaction product. At early aging, samples with soluble phosphate had a similar strength development (Fig. 53) to mortars without phosphate (Fig. 46), but from one month's aging onwards their strength did not decrease as in samples without phosphates; on the contrary strengths continued to increase. A mixture of phases 5 and 3 was the first reaction product and the unreacted portion of MgO disappeared faster than in mortars from 5:1:13 mix.

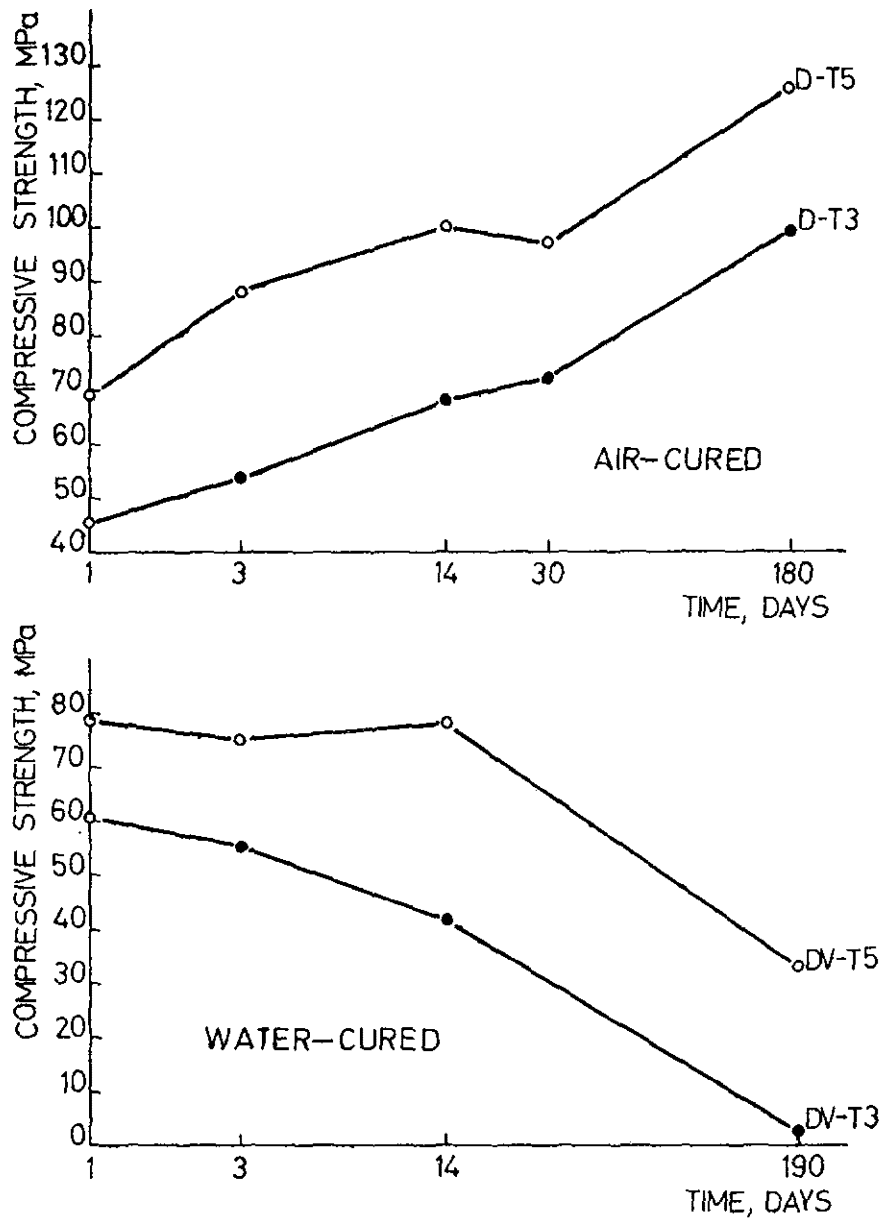


Figure 53. Compressive strengths in Sorel cement mortars with $\text{Ca}(\text{H}_2\text{PO}_4)_2 \cdot \text{H}_2\text{O}$ addition. Samples D-T5 and DV-T5 prepared from 5:1:13 mix and samples D-T3 and DV-T3 from 3:1:13 mix. Water cured samples were first air cured for 28 days, then stored in water.

Some of the above study samples were stored in water at 28 days of aging. Figure 53 shows that with the same content of phosphate (15% wt. of MgO used) the samples with the 5:1:13 mix are much more water resistant than those from the 3:1:11 mix.

It should be noted that the unreacted MgO existing in specimens from the 5:1:13 mix at the moment of immersion (28 days) may cause a faster decrease of strength in water-cured mortars. This will not happen if MgO has quickly transformed into phase 5 or $Mg(OH)_2$. It is known from experience that an initial mixture for magnesium oxychloride cement as flooring material should be close to the molar ratio $MgO:MgCl_2:H_2O = 5:1:13$ with some excess of MgO, and the amount of water as close as possible to the theoretical value for complete reaction of MgO with $MgCl_2$ solution into phase 5 and excess of MgO into $Mg(OH)_2$. With these concentrations of reactants, the reaction products will be phase 5 (major reaction product) and some $Mg(OH)_2$. Such an initial raw mix with phosphate addition would perhaps be more water resistant than the mortars investigated with the initial raw mix of exactly 5:1:13 where no $Mg(OH)_2$ can form. The role of $Mg(OH)_2$ in strength development has not been fully explained yet.

D. CONCLUSIONS

The reaction products in the $MgO-MgCl_2-H_2O$ system do not depend exclusively on the molar ratio of reactants but on the activity of MgO as well. Very active MgO dissolves more rapidly in $MgCl_2$ solution and influences the formation of early reaction product(s) which may differ from the final product(s). The decrease in strength is brought about by the transformation of early reaction products into the final ones.

Strengths develop faster and achieve higher values in samples from the 5:1:13 mix (with phase 5 as the only reaction product) than in those from the 3:1:13 mix where phase 5 and 3 coexist at the beginning and phase 5 eventually passes into phase 3.

Cement resistance against water attack is improved by phosphate additions, with soluble phosphate being more effective. If the level of phosphate is identical, mortars from the 5:1:13 mix will exhibit a better resistance to water attack than those made from the 3:1:11 mix.

IV. CONCLUSIONS

PORTLAND CEMENT

Stabilizers and clinker activity

Barium sulfate, $BaSO_4$, calcium phosphate tribasic, $Ca_5(PO_4)_3(OH)$ and vanadium oxide, V_2O_5 all stabilize the β -, α' - and/or α -modification of dicalcium silicate, C_2S depending on the level of the stabilizer added to the raw mix. The α -polymorph being stable only at very high levels was excluded from the present work.

The crystal growth of C_2S is affected differently by different stabilizers; thus, with V_2O_5 the grain size is approximately $50\mu m$, with $BaSO_4$ from 20 to $30\mu m$ and with $Ca_5(PO_4)_3(OH)$ only 5-15 μm .

Stabilized α' -belites have a faster strength development than β - C_2S in the first month of hydration. Mortar tests have shown that the development of strength is affected differently by various types of stabilizers. Belites doped with phosphate develop strengths very slowly and at levels that are inferior to those for $BaSO_4$ -stabilized belites in the first month of hydration. Dicalcium silicates doped with V_2O_5 have a development of strength similar to that of $Ca_5(PO_4)_3(OH)$ -stabilized C_2S according to tests on cement pastes.

More Ba atoms than SO_4 groups are incorporated in $BaSO_4$ -stabilized belites since $BaSO_4$ decomposes during the formation of the solid solution and a part of the sulphate evaporates as sulphur trioxide, SO_3 .

$BaSO_4$ doped belite clinkers with some alite have higher strengths than belites of a similar composition but without $BaSO_4$ addition. With an increased percentage of $BaSO_4$ in the raw mix, the content of alite in the clinker will be smaller and that of belite higher with CaO in excess of the quantity required for C_2S , calcium oxide having entered into C_2S solid solution together with other impurities such as Ba, Al, Fe atoms and SO_4 groups.

A method was developed to determine the polymorphous modifications of C_2S by optical microscopy in reflected light. The distribution of the stabilizers in C_2S solid solution was not homogeneous as deduced from differential thermal curves for $\alpha'_H \rightarrow \alpha$ -conversion and identified in optical microscope by visual observations of the effect brought about by $\alpha' \rightarrow \alpha$ - C_2S phase transition.

Effects of carbonation on the hydration process

The release of CO_2 during the decomposition of diethyl pyrocarbonate added to cement, sand, and water mix did not accelerate the strength development as expected.

Cement with limestone addition

Tests have shown that limestone additions (5 or 10%) do not accelerate strength development in Portland cement mortars and concretes.

SOREL CEMENT

The reaction products of the $MgO-MgCl_2-H_2O$ system are dependent not only on the proportion of reactants but also on the MgO activity. Very active MgO dissolves more rapidly in $MgCl_2$ solution and speeds the formation of the early reaction product(s) which may differ from the final product(s). When the early reaction products differ from the final ones, a decrease in strength results due to the early reaction products changing into the final ones in the process of hardening.

Strength develops faster and is greater in samples from the 5:1:13 mix where phase 5 is the only reaction product, than in those from the 3:1:11 mix, where phase 5 and 3 are coexistent at the beginning of the reaction, with a subsequent transformation of phase 5 into phase 3.

Phosphate addition improves the water resistance of Sorel cement, soluble phosphates being more effective in this respect. At an identical level of phosphates, the mortars from the 5:1:13 mix exhibit a better resistance to water than those made from the 3:1:11 mix.

V. RECOMMENDATIONS

Energy consumption in the manufacture of Portland cement has become quite a problem, particularly for those cement producers who use oil and/or gas as fuel since their prices are continuously increasing. The energy consumption has been considerably reduced by changing from a wet to a dry process utilizing kilns with preheaters, yet changes in the technological process and kiln design are not the only means of saving energy.

Energy saving can be achieved also by changing the raw meal composition or by the use of additives. A prime consideration is that much of the heat needed for clinker manufacture goes for the decarbonation process, i.e. for the formation of calcium oxide (CaO) from calcium carbonate ($CaCO_3$). The formulae of alite (C_3S) and belite (C_2S) clearly indicate that there is more calcium oxide in the tricalcium than in the dicalcium silicate, hence more energy is required for the formation of alite than of belite.

An important item in the total heat balance is the loss of heat by radiation through the kiln shell, this being proportional to the fourth power of the absolute temperature. In the sintering zone of a rotary kiln the usual temperatures for alite clinkers are $1450 \pm 50^{\circ}\text{C}$, so energy could be saved by manufacturing belite clinkers which have lower sintering temperatures or by using mineralizers which accelerate the sintering process allowing alite clinkers to start forming at approximately 1300°C .

Energy could thus be saved by manufacturing cement clinkers at lower temperatures and by using raw materials with less calcium carbonate than required for alite clinkers. For this reason belite cements, i.e. cements with low alite content are arousing more and more interest. They are also interesting because less calcium hydroxide ($\text{Ca}(\text{OH})_2$) forms in the process of hydration and the heat development is lower than in cements rich with alite. However, it should be noted that such cements have much lower initial strengths (after 1, 3, and 7 days) than Portland cements with a high alite content, but the final strengths of belite cements will be identical to those of alite cements or even better.

The present investigation has demonstrated that BaSO_4 doped belite clinkers with up to 35% of alite have greater strengths than clinkers of similar composition without BaSO_4 .

Since stabilized belite clinkers are of interest, we propose that the program for the second phase be focused on the determination of the optimal amount of stabilizers and the belite:alite ratio for energy saving and the development of strengths in cement mortars and concretes. White cement should also be included in the investigation because the results obtained with additions of BaSO_4 suggest the possibility of substituting cheaper quartz sand for the expensive kaolin. Clinkers demonstrating the best results in laboratory testing would be prepared on a pilot plant scale provided there are funds for such. The behavior of cement would also be studied under accelerated curing conditions (low-pressure and high-pressure steam curing) and compared with that of the normally cured specimens.

REFERENCES

- (1) M. Regourd and A. Guinier, "The crystal chemistry of the constituents of Portland cement clinker," Proc. 6th Int. Congress Chem. Cem., Moscow, 1974, Vol. 1. pp. 25-51 (Strovizdat, Moscow, 1976, Russ.ed.).
- (2) I. M. Pritts and K. E. Daugherty, "The effect of stabilizing agents on the hydration rate of β - C_2S ," Cem. Concr. Res., (6) 783-796 (1976).
- (3) W. A. Klemm and R. L. Berger Accelerated curing of cementitious systems by carbon dioxide. II. Hydraulic calcium silicates and aluminates Cem. Concr. Res., 2 (6) 647-652 (1972).
- (4) J. F. Young, R. L. Berger and J. Breese, "Accelerated curing of compacted calcium silicate mortars on exposure to CO_2 ," J. Am. Ceram. Soc., 57 (9) 394-397 (1974).
- (5) J. H. Welch and W. Gutt, "The effect of minor components on the hydraulicity of the calcium silicates," Proc. 4th Int. Symp. Chem. Cem., Washington, 1960, Vol. 1., pp. 59-68 (U.S. Depart. of Commerce, 1962).
- (6) K. Suzuki and G. Yamaguchi, "A structural study on α' - Ca_2SiO_4 ," Proc. 5th Int. Symp. Chem. Cem., Tokyo, 1968, Vol. 1. pp. 67-72 (Cement Assoc. of Japan, Tokyo, 1969).
- (7) W. Kurdowski, "Influence of minor components on hydraulic activity of Portland cement clinker," Proc. 6th Int. Congress Chem. Cem., Moscow, 1974, Vol. 1. pp. 203-207 (Stroyizdat, Moscow 1976, Russ. ed.).
- (8) W. Lerch and R. H. Bogue, "Revised procedure for the determination of uncombined lime in Portland cement," Ind. Eng. Chem. Anal. Ed. , 2 (3) 296-298 (1930).

- (9) S. Takashima, "Systematic dissolution of calcium silicate in commercial Portland cement by organic acid solution," Rev. 12th Gen. Meeting, Tokyo, 1958, pp. 12-13. (Japan Cement Engin. Assoc., Tokyo, 1959).
- (10) J. Schwartz, "The aluminoferritic phase of Portland cement clinkers (in French), Rev. Mater. Constr. Trav. Publics, No. 669-670, 159-172 (1971).
- (11) N. I. Fateeva and V. K. Kozlova, "Determination of calcium in clinker and cement," (in Russ.) Tsement, 32 (4) 13-14 (1966).
- (12) T. Gacesa, I. Jelenic and V. Carin, "Alkalies and sulphate distribution in Portland cement clinker and its effect on the hydration process," (in Croat.) Cement (Zagreb), 18 (4) 190-199 (1975).
- (13) S. Takashima and K. Higaki, "Dissolution and determination of glass phase in portland cement by the picric acid methanol method," Rev. 23rd Gen. Meeting, Tokyo, 1969, pp. 47-50 (Cement Assoc. of Japan, Tokyo, 1970).
- (14) H. Lehmann, K. Niesel and P. Thormann, "Stability fields of the polymorphic forms of dicalcium silicate," (in Germ.) Tonind. Ztg., 93 (6) 197-209 (1969).
- (15) G. Yamaguchi and S. Takagi, "The analysis of Portland cement clinker," Proc. 5th Int. Symp. Chem. Cem., Tokyo, 1968, Vol. 1. pp. 181-218 (Cement Assoc. of Japan, Tokyo, 1969).
- (16) Y. Ono, S. Kawamura and Y. Soda, "Microscopic observation of alite and belite and hydraulic strength of cement," Proc. 5th Int. Symp. Chem. Cem., Tokyo, 1968, Vol. 1. pp. 275-284 (Cement Assoc. of Japan, Tokyo, 1969).
- (17) S. Chromy, "The inversion of the β - γ modifications of dicalcium silicate," Zem.-Kalk-Gips, 23 (8) 382-389 (1970).

- (18) Y. Ono, "Microscopic analysis of clinker," Section B in Microscopy of clinker and cement (Portland Cement Assoc., Skokie, Ill., 1975).
- (19) M. Y. Bikbau, "On hydration activity of silicates," 6th Int. Congress Chem. Cem., Moscow, 1974 (Suppl. Paper 11/1-6).
- (20) L. E. Copeland and D. L. Kantro, "Hydration of Portland cement," Proc. 5th Int. Symp. Chem. Cem., Tokyo, 1968, Vol. 11. pp. 387-420 (Cement Assoc. of Japan, Tokyo, 1969).
- (21) F. Massazza and M. Pezzuoli, "Influence of strontium on the clinker mineralogical composition," 6th Int. Congress Chem. Cem., Moscow, 1974 and II Cemento, 71 (4) 167-175 (1974).
- (22) I. Jawed and J. Skalny, "Alkalies in cement: A review. I. Forms of alkalies and their effect on clinker formation," Cem. Concr. Res., 7 (6) 719-730 (1977).
- (23) P. K. Mehta and J. R. Brady, "Utilization of phosphogypsum in Portland cement industry," Cem. Concr. Res., 7 (5) 537-543 (1977).
- (24) S. Chromy, "High-temperature microphotometry and microdilatomety," (in Czech) Silikaty, No. 2, 105-124 (1974).
- (25) M. Sittig, "Toxic metals, pollution control and worker protection," pp. 4 (Noyes Data Corp., Park Ridge, New Jersey, 1976).
- (26) H. Saalfeld, "Contribution to the crystal chemistry of C_2S ," Ber. Deut. Keram. Ges., 44 (6) 279-283 (1967).
- (27) H. Saalfeld, "Stabilization of Verneuil boules consisting of Ca_2SiO_4 by $Ca_3(PO_4)_2$ and V_2O_5 ," Ber. Deut. Keram. Ges., 48 (10) 435-440 (1971).

- (28) V. I. Korneyev, "Composition zones of silicate phases in Portland cement clinker," Proc. 6th Int. Congress Chem. Cem., Moscow, 1974, Vol. 1. pp. 71-76 (Stroyizdat, Moscow, 1976, Russ. ed.).
- (29) G. E. Bessey, "Calcium aluminate and calcium silicate hydrate," Proc. Symp. Chem. Cem., Stockholm, 1938, pp. 178-215 (Ingeniorsvetenskapsakademien, Stockholm).
- (30) P. Seligmann and N. R. Greening, "The State of hydration of calcium sulfate in cement," Proc. 4th Int. Symp. Chem. Cem., Washington, 1960, Vol. 1. pp. 408-410 (U.S. Dept. of Commerce, Washington, 1962).
- (31) R. F. Feldman, V. S. Ramachandran and J. P. Sereda, "Influence of CaCO_3 on the hydration of $3\text{CaO}\cdot\text{Al}_2\text{O}_3$," J. Am. Ceram. Soc., 48 (1) 25-30 (1965).
- (32) E. Spohn and W. Lieber, "Reactions between calcium carbonate and Portland cement," contributions to the systems $\text{C}_3\text{A}-\text{CaCO}_3-\text{H}_2\text{O}$ and $\text{C}_4\text{AF}-\text{CaCO}_3-\text{H}_2\text{O}$ (in Ger.) Zem.-Kalk-Gips, 18 (9) 483-485 (1965).
- (33) F. M. Lea, "The chemistry of cement and concrete," p. 537 (Edward Arnold Ltd., 3rd ed., Glasgow, 1970).
- (34) I. Soroka and N. Stern, "Calcareous fillers and the compressive strength of portland cement," Cem. Concr. Res., 6 (3) 367-376 (1976).
- (35) I. Soroka and N. Setter, "The effect of fillers on strength of cement mortars," Cem. Concr. Res., 7 (4) 449-456 (1977).
- (36) G. S. Bobrowski, J. L. Wilson and K. E. Daugherty, "Limestone substitutes for gypsum as a cement ingredient," Rock Prod., 80 (2) 64-67 (1977).
- (37) B. Matkovic, S. Popovic, V. Rogic, T. Zunic and J. F. Young, "Reaction products in Sorel cement pastes," System $\text{MgO}-\text{MgCl}_2-\text{H}_2\text{O}$, J. Am. Ceram. Soc., 60 (11-12) 504-507 (1977).

- (38) C. A. Sorrell and C. R. Armstrong, "Reactions and equilibria in magnesium oxychloride cements," J. Am. Ceram. Soc. 59 (1-2) 51-54 (1976).
- (39) L. Walter-Levy and P. M. de Wolff, "The study of Sorel cement (in French)," Compt. rend., 229, 1077-1079 (1949).
- (40) W. F. Cole and T. Demediuk, "X-ray, thermal, and dehydration studies on magnesium oxychlorides," Aust. J. Chem., 8 (2) 234-251 (1955).
- (41) J. W. Meuser-Bourgognion and P. M. de Wolff, "Magnesium oxychloride floors 1. & 11," (in Ger.) Schweiz. Arch. angew. Wiss. u. Tech., 21, 199-203, 241-250 (1955).
- (42) V. Rogic and B. Matkovic, "Phases in magnesium oxychloride cement," (in Croat.) Cement (Zagreb), 16 (2) 61-69 (1972).
- (43) L. Walter-Levy, P. M. de Wolf and I. Soleilhavoup, "The setting of the salt $MgCl_2 \cdot 2MgCO_3 \cdot Mg(OH)_2 \cdot 6H_2O$," (in French) Compt. rend., 236, 2069-2071 (1953).
- (44) B. Matkovic and V. Rogic, "Modified magnesium oxychloride cement," 6th Int. Congress Chem. Cem., Moscow, 1974 (Suppl. Paper III/III-5).
- (45) B. Matkovic, V. Rogic and F. Kaluza, "The possibility of waste phosphate addition to Sorel cement (in Croat.)," Kem. Ind. (Zagreb), 25 (11) 610-624 (1976).
- (46) L. E. Copeland and R. H. Bragg, "Quantitative X-ray diffraction analysis," Anal. Chem. 30, 196-201 (1958).
- (47) A. Bezjak and I. Jelenic, "The application of the doping method in quantitative X-ray diffraction analysis," Croat. Chem. Acta, 43, 193-198 (1971).

- (48) F. H. Chung, "Quantitative interpretation of X-ray diffraction patterns of mixtures. I. Matrix-flushing method for quantitative multicomponent analyses. II. Adiabatic principle of X-ray diffraction analysis of mixtures. III. Simultaneous determination of a set of reference intensities," J. Appl. Cryst. 7 (7) 519-525 & 526-531 (1974)
J. Appl. Cryst. 8 (1) 17-19 (1975).
- (49) S. Popovic and T. Zunic, "New method for quantitative phase analysis of mineral ores (in Croat.)," Proc. Symp. Methods Geol. Investigations (Zbornik), Opatija 1976, pp. 335-340.
- (50) W. R. Eubank, "Calcination studies of magnesium oxides," J. Am. Ceram. Soc., 34 (8) 225-229 (1951).
- (51) V. S. Ramachandran, K. P. Kacker and M. Rai, "Chloromagnesian cement prepared from calcined dolomite (in Russ.)," Zh. Prikl. Khim., 40 (8) 1687-1695 (1967).
- (52) P. P. Budnikov and H. S. Vorob'ev, "Rate of hydration of magnesium oxide fired at different temperatures," Zh. Prikl. Khim., 32, 253-258 (1959).
- (53) T. Demediuk, W. F. Cole and H. V. Hueber, "Studies on magnesium and calcium oxychlorides" Aust. J. Chem., 8 (2) 215-233 (1955).
- (54) E. S. Newman, "A study of the system magnesium oxide-magnesium chloride," J. Res. Nat. Bureau Standards, Washington, 54 (6) 347-355 (1955)
- (55) B. I. Smirnov, E. S. Solov'eva and E. E. Segalova, "Chemical reaction of magnesium oxide with magnesium chloride solutions of various concentrations," (in Russ.) Zh. Prikl. Khim., 40 (3) 505-515 (1967)
- (56) C. R. Bury and F. R. H. Davies, "The system magnesium oxide-magnesium chloride-water," J. Chem. Soc. (London), 135, 2008-2015 (1932).

- (57) W. Feitknecht and F. Held, "Hydroxy salts of bivalent metals. XXV. Hydroxy chlorides of magnesium," *Helv. Chim. Acta*, 27, 1480-1495 (1944).
- (58) K. Murakami, "Utilization of chemical gypsum for Portland cement," *Proc. 5th Int. Symp. Chem. Cem.*, Tokyo, 1968, Vol. IV, pp. 457-510 (Cement Assoc. of Japan, Tokyo, 1969).

FEDERALLY COORDINATED PROGRAM (FCP) OF HIGHWAY RESEARCH AND DEVELOPMENT

The Offices of Research and Development (R&D) of the Federal Highway Administration (FHWA) are responsible for a broad program of staff and contract research and development and a Federal-aid program, conducted by or through the State highway transportation agencies, that includes the Highway Planning and Research (HP&R) program and the National Cooperative Highway Research Program (NCHRP) managed by the Transportation Research Board. The FCP is a carefully selected group of projects that uses research and development resources to obtain timely solutions to urgent national highway engineering problems.*

The diagonal double stripe on the cover of this report represents a highway and is color-coded to identify the FCP category that the report falls under. A red stripe is used for category 1, dark blue for category 2, light blue for category 3, brown for category 4, gray for category 5, green for categories 6 and 7, and an orange stripe identifies category 0.

FCP Category Descriptions

1. Improved Highway Design and Operation for Safety

Safety R&D addresses problems associated with the responsibilities of the FHWA under the Highway Safety Act and includes investigation of appropriate design standards, roadside hardware, signing, and physical and scientific data for the formulation of improved safety regulations.

2. Reduction of Traffic Congestion, and Improved Operational Efficiency

Traffic R&D is concerned with increasing the operational efficiency of existing highways by advancing technology, by improving designs for existing as well as new facilities, and by balancing the demand-capacity relationship through traffic management techniques such as bus and carpool preferential treatment, motorist information, and rerouting of traffic.

3. Environmental Considerations in Highway Design, Location, Construction, and Operation

Environmental R&D is directed toward identifying and evaluating highway elements that affect

the quality of the human environment. The goals are reduction of adverse highway and traffic impacts, and protection and enhancement of the environment.

4. Improved Materials Utilization and Durability

Materials R&D is concerned with expanding the knowledge and technology of materials properties, using available natural materials, improving structural foundation materials, recycling highway materials, converting industrial wastes into useful highway products, developing extender or substitute materials for those in short supply, and developing more rapid and reliable testing procedures. The goals are lower highway construction costs and extended maintenance-free operation.

5. Improved Design to Reduce Costs, Extend Life Expectancy, and Insure Structural Safety

Structural R&D is concerned with furthering the latest technological advances in structural and hydraulic designs, fabrication processes, and construction techniques to provide safe, efficient highways at reasonable costs.

6. Improved Technology for Highway Construction

This category is concerned with the research, development, and implementation of highway construction technology to increase productivity, reduce energy consumption, conserve dwindling resources, and reduce costs while improving the quality and methods of construction.

7. Improved Technology for Highway Maintenance

This category addresses problems in preserving the Nation's highways and includes activities in physical maintenance, traffic services, management, and equipment. The goal is to maximize operational efficiency and safety to the traveling public while conserving resources.

0. Other New Studies

This category, not included in the seven-volume official statement of the FCP, is concerned with HP&R and NCHRP studies not specifically related to FCP projects. These studies involve R&D support of other FHWA program office research.

* The complete seven-volume official statement of the FCP is available from the National Technical Information Service, Springfield, Va. 22161. Single copies of the introductory volume are available without charge from Program Analysis (HRD-3), Offices of Research and Development, Federal Highway Administration, Washington, D.C. 20590.

